STRUCTURAL SYSTEMS

RESEARCH PROJECT

Report No.
TR-06/01

SUBASSEMBLAGE TESTING OF COREBRACE BUCKLING-RESTRAINED BRACES (G SERIES)

by

JAMES NEWELL

CHIA-MING UANG

GIANMARIO BENZONI

Final Report to CoreBrace, LLC.

January 2006

Department of Structural Engineering
University of California, San Diego
La Jolla, California 92093-0085

University of California, San Diego
Department of Structural Engineering
Structural Systems Research Project

Report No. TR-06/01

SUBASSEMBLAGE TESTING OF COREBRACE BUCKLING-RESTRAINED BRACES (G SERIES)

by

James Newell
Graduate Student Researcher

Chia-Ming Uang
Professor of Structural Engineering

Gianmario Benzoni
Research Scientist

Final Report to CoreBrace, LLC

Department of Structural Engineering
University of California, San Diego
La Jolla, California 92093-0085

January 2006

ABSTRACT

Subassemblage testing of four full-scale buckling-restrained braces (BRBs) for CoreBrace was conducted using a shake table facility at the University of California, San Diego. The specimens featured an A36 steel yielding core plate with grout fill in a hollow structural section (HSS) casing. Each specimen was bolted to gusset brackets at each end of the brace. One end of the brace was connected to a strong-wall, and the shake table imposed both longitudinal and transverse displacements to the other end of the brace. Standard Loading Protocol, High-Amplitude Loading Protocol, and Low-Cycle Fatigue Loading Protocol tests were conducted. The Standard Loading Protocol was derived from a combination of the 2005 AISC *Seismic Provisions for Structural Steel Buildings* and 2003 *NEHRP Recommended Provisions for Seismic Regulations for New Buildings and Other Structures* (FEMA 450). The High-Amplitude Loading Protocol imposed deformation demand on the BRB specimens that was significantly greater than that prescribed in the AISC *Seismic Provisions* and FEMA 450.

All specimens preformed well under the Standard Loading Protocol. The steel core plates of Specimens 1G, 2G, and 4G did not fracture during testing. The Specimen 3G core plate fractured on the first $4.3\Delta_{bm}$ tension excursion during the High-Amplitude Loading Protocol. The bolted end connections were able to accommodate an end rotation, resulting from the imposed transverse displacement, of up to 0.031 radians. The hysteretic behavior of the braces was very stable (prior to brace fracture) and a significant amount of energy was dissipated by each specimen. Specimens achieved cumulative inelastic axial deformation values significantly higher than the $200\Delta_{by}$ required by the AISC *Seismic Provisions* for uniaxial brace specimens. All four BRB subassemblage test specimens satisfied the acceptance criteria given in Appendix Section T10 of the 2005 AISC *Seismic Provisions for Structural Steel Buildings* and Section 8.6.3.7.10 of the 2003 *NEHRP Recommended Provisions for Seismic Regulations for New Buildings and Other Structures*.

ACKNOWLEDGEMENTS

Funding for this project was provided by CoreBrace, LLC in West Jordan, Utah. CoreBrace provided test specimens and loading protocols. Technical assistance from the staff at the Seismic Response Modification Device (SRMD) Test Facility at the University of California, San Diego was greatly appreciated.

TABLE OF CONTENTS

LIST OF TABLES

LIST OF FIGURES

LIST OF SYMBOLS

A_{sc} Area of yielding element

E_h Total hysteretic energy dissipated by brace

E_s Young's modulus of elasticity of steel

F_{ya} Actual yield strength of steel core (average of coupon tests)

F_{yn} Nominal yield strength of steel core

L_b Total length of brace

L_y Length of yielding element

P_{max} Maximum brace compressive force

P_{ya} Actual brace yield force, $F_{ya}A_{sc}$

P_{yn} Nominal brace yield force, $F_{yn}A_{sc}$

P_r Resultant axial brace force

R_y Material overstrength factor, F_{ya}/F_{yn}

T_{max} Maximum brace tensile force

β Compression strength adjustment factor, P_{max}/T_{max}

Δ Axial brace deformation

Δ_b Deformation quantity used to control loading of test specimen

Δ_{bm} Value of deformation quanity, Δ_b, corresponding to the design story drift

Δ_{by} Value of deformation quantity, Δ_b, at first significant yield of test specimen

Δ_i^+ Maximum tensile axial deformation for the i^{th} cycle

Δ_i^- Absolute value of the maximum compressive axial deformation for the i^{th} cycle

ε Axial brace strain

η Cumulative inelastic axial deformation capacity

μ_i Inelastic axial deformation of the i^{th} cycle

ω Tension strength adjustment factor, T_{max}/P_{ya}

1. INTRODUCTION

1.1 General

Buckling-restrained braced frames (BRBFs) are becoming a popular seismic force resisting system in the United States (Reina and Normile 1997, Clark et al. 1999, Lopez 2001, Shuhaibar et al. 2002, Sabelli and Aiken 2003). Buckling-restrained braces (BRBs) are designed such that brace buckling is prevented under seismic loading. Provisions for BRBF design and BRB qualifying cyclic testing have been incorporated into the AISC *Seismic Provisions for Structural Steel Buildings* (AISC 2005) and *NEHRP Recommended Provisions for Seismic Regulations for New Buildings and Other Structures* (FEMA 2003). Both these provisions require subassemblage testing to verify the performance of BRBs. The subassemblage testing demonstrates a BRBs ability to accommodate combined axial and rotational deformation demands imposed during a seismic event.

One type of BRB that was developed by CoreBrace, LLC has undergone subassemblage testing at the University of Utah and the University of California, San Diego. Subassemblage testing at the University of Utah was accomplished by applying load with a constant eccentric offset at one end of the BRB (Daniels and Reaveley 2002, Okahashi and Reaveley 2004). Subassemblage testing at the University of California, San Diego was performed by imposing both longitudinal and transverse deformation to the test specimen (Merritt et al. 2003, Newell et al. 2005). Uniaxial BRB testing has also been conducted at the University of Utah (Staker and Reaveley 2002).

1.2 Scope and Objectives

Four full-scale buckling-restrained brace subassemblages were tested at the University of California, San Diego. The objective of this testing program was to evaluate the cyclic performance of these subassemblages based on the acceptance criteria of the AISC *Seismic Provisions* and FEMA 450.

2. TESTING PROGRAM

2.1 Test Specimens

Two pairs of nominally identical buckling-restrained brace (BRB) specimens (four total) were tested. Figure 2.1 shows the overall geometry of test Specimens 1G and 2G, and Figure 2.2 shows Specimens 3G and 4G. Specimens 1G and 2G were composed of a central steel flat core plate (Figure 2.3), which was confined in a grout-filled square HSS. The Specimens 3G and 4G core plates (Figure 2.4) were cruciform in cross section. Table 2.1 provides specimen dimensions and the square HSS size.

2.2 Material Properties

A36 steel, with a nominal yield strength, F_{yn}, of 36 ksi was specified for the core plates, and A500 Grade B steel was specified for the HSS casing. Tensile coupon tests of the core plates were conducted by American Metallurgical Services to determine actual material properties; the results are summarized in Table 2.2. Based on the average measured yield strength (F_{ya}), the values of the material overstrength factor, R_y ($=F_{ya}/F_{yn}$), and the brace yield force, as listed in Table 2.3, were calculated.

The specified 28-day grout-fill compressive strength was 5,000 psi. Table 2.4 provides results for compressive strength testing conducted by CMT Engineering Laboratories for the 4-, 7-, and 28-day cylinder tests. BRB specimens were tested 29 to 34 days after the grout fill was placed.

2.3 End Connections

The ends of each brace were spliced to gusset brackets with A572 Grade 50 steel connection plates that were welded to the BRB core plate and bolted to the gusset brackets with fully-tensioned high-strength A490 bolts. The gusset bracket details are shown in Figure 2.5 and Figure 2.6 shows the specimen end connections. Both the gusset brackets and the BRB connection plates (bolted faying surfaces) were sandblasted to a Class B faying surface (AISC 2001). All bolts in the connection were 1-1/2 in. diameter A490 high-strength structural bolts in double shear. (Specimen 2G used one 1-1/4 in. diameter A490 bolt due to bolt hole misalignment.) Connection plate bolt holes were 1-

9/16 in. diameter and bolt holes in the gusset bracket were 1-11/16 in. diameter. Specimen bolts were tensioned using a hydraulic torque wrench. The hydraulic torque wrench was calibrated with a Skidmore-Wilhelm Bolt Tension Calibrator to assure minimum AISC specified slip-critical connection bolt pretension (AISC 2001)

2.4 Test Setup and Connection Details

A shake table facility, called the Seismic Response Modification Device (SRMD) Test Facility, at the University of California, San Diego was employed to test the brace specimens. The SRMD facility, which has a shake table platen capable of imposing displacement in six degrees of freedom, is shown in Figure 2.7. Figure 2.8 shows one specimen installed in the setup and ready for testing. One end of the specimen was attached to the strong-wall at the west end of the SRMD facility (Figure 2.9). The other end of the brace was attached to the SRMD platen as shown in Figure 2.10. Movement of the shake table platen imposed both longitudinal and transverse deformations to the specimen.

2.5 Loading Protocol

According to the AISC *Seismic Provisions* and FEMA 450, the design of BRBs shall be based upon results from qualifying cyclic tests. Qualifying test results shall consist of at least two successful cyclic tests: one is required to be a test of a brace subassemblage that includes brace connection rotational demands and the other may be either a uniaxial or a subassemblage test. In this testing program all tests were subassemblage tests, including the transverse deformation associated with connection rotational demand.

According to Appendix T of the AISC *Seismic Provisions,* the following loading sequence shall be applied to the test specimen, where the deformation is the steel core axial deformation of the test specimen:

(1) 2 cycles of loading at the deformation corresponding to $\Delta_b=1.0\Delta_{by}$,

(2) 2 cycles of loading at the deformation corresponding to $\Delta_b=0.5\Delta_{bm}$,

(3) 2 cycles of loading at the deformation corresponding to $\Delta_b=1.0\Delta_{bm}$,

(4) 2 cycles of loading at the deformation corresponding to $\Delta_b=1.5\Delta_{bm}$,

(5) 2 cycles of loading at the deformation corresponding to $\Delta_b=2.0\Delta_{bm}$,

(6) Additional complete cycles of loading at the deformation corresponding to $\Delta_b=1.5\Delta_{bm}$ as required for the brace test specimen to achieve a cumulative inelastic axial deformation of at least 200 times the yield deformation.

The above loading sequence requires two quantities: Δ_{by} and Δ_{bm}. Δ_{by} is defined as the axial deformation at first significant yield of the specimen, and Δ_{bm} corresponds to the axial deformation of the specimen at the design story drift. In this testing program Δ_{bm} was assumed to equal $5.0\Delta_{by}$.

According to Section 8.6.3.7.6.3 of FEMA 450, the following loading sequence shall be applied to the test specimen:

(1) 6 cycles of loading at the deformation corresponding to $\Delta_b=1.0\Delta_{by}$,

(2) 4 cycles of loading at the deformation corresponding to $\Delta_b=0.5\Delta_{bm}$,

(3) 4 cycles of loading at the deformation corresponding to $\Delta_b=1.0\Delta_{bm}$,

(4) 2 cycles of loading at the deformation corresponding to $\Delta_b=1.5\Delta_{bm}$,

(5) Additional complete cycles of loading at the deformation corresponding to $\Delta_b=1.0\Delta_{bm}$ as required for the brace test specimen to achieve a cumulative inelastic axial deformation of at least 140 times the yield deformation.

The Standard Loading Protocol developed for this testing program was a combination of the AISC *Seismic Provisions* and FEMA 450 loading sequences. The following loading sequence was applied to the test specimens:

(1) 6 cycles of loading at the deformation corresponding to $\Delta_b=1.0\Delta_{by}$,

(2) 4 cycles of loading at the deformation corresponding to $\Delta_b=0.5\Delta_{bm}$,

(3) 4 cycles of loading at the deformation corresponding to $\Delta_b=1.0\Delta_{bm}$,

(4) 2 cycles of loading at the deformation corresponding to $\Delta_b=1.5\Delta_{bm}$,

(5) 2 cycles of loading at the deformation corresponding to $\Delta_b=2.0\Delta_{bm}$.

For Specimens 1G and 2G a loading sequence for axial deformation, as shown in Figure 2.11(a) and Table 2.5(a), was applied. Additional cycles (AISC *Seismic Provisions* Item 6 and FEMA 450 Item 5) were not required to achieve the target cumulative inelastic axial deformations. An additional High-Amplitude loading sequence was then applied to impose greater deformation demand on the BRB specimens. This

High-Amplitude protocol is shown in Figure 2.12(a) and Table 2.5(b). Finally, 15 cycles of a Low-Cycle Fatigue Protocol, with deformations corresponding to $1.5\Delta_{bm}$ [see Table 2.5(c)], were applied. For Specimens 3G and 4G a similar Standard Loading Protocol [see Figure 2.13(a) and Table 2.5(a)] and High-Amplitude Loading Protocol [see Figure 2.14(a) and Table 2.5(a)] were applied. Note that Specimens 3G and 4G were not subjected to a Low-Cycle Fatigue Loading Protocol.

The calculation of Δ_{by} was based on the deformation expected over the length L_b, which is the overall length of the core plate (see Figure 2.15). To establish the value of Δ_{by}, the following components were considered at the actual yield force level P_{ya}:

(1) deformation of the core plate in the yielding length, L_y (see Figures 2.3, 2.4 and Table 2.1 for L_y), and

(2) deformation of the core plate outside the yielding length. This includes L_t and x on each end of the core plate.

Using the calculated Δ_{by} value for each specimen (see Table 2.3), the shake table displacement protocol was created by adding additional displacement to account for the following:

(1) elastic deformation of the gusset brackets, and

(2) elastic deformation due to flexibility of the end supports and reaction wall at the SRMD facility based on a known total system stiffness of 4,090 kips/in.

Shake table peak input displacements for each cycle are provided in Table 2.6. Input displacements for Specimens 3G and 4G were modified based on the observed bolt slip behavior of Specimens 1G and 2G.

Transverse displacements corresponding to the prescribed axial displacements were calculated based on the specimen brace length, L_b (see Table 2.1), and an assumed brace angle of 60° from horizontal. With this assumption, the corresponding amplitudes for the transverse movement of the shake table were established, as given in Tables 2.5 and 2.6. Transverse displacements for the last High-Amplitude Loading Protocol cycles were modified to limit BRB end rotation to 0.03 radians. Since the loading system is nominally rigid in the transverse direction, no additional transverse displacement, accounting for system flexibility, was added when adapting the prescribed transverse displacements to shake table input transverse displacements. Figures 2.11 to 2.14 show

that the transverse movement is in phase with the longitudinal movement in order to simulate realistic frame action effects at the gusset connections.

2.6 Instrumentation

Four displacement transducers (string potentiometers) labeled *L1* to *L4* in Figure 2.15(a) measured the axial deformation of the brace specimen and gusset brackets. Figure 2.15(b) shows the mounting fixture for these transducers at one end of a specimen. As shown in Figure 2.15(a), the mounting points for the string potentiometers were located at the end of the core plate at each end of the brace for consistency with the Δ_{by} calculation. The longitudinal and transverse displacements of the shake table were also recorded.

The force measured by the load cell in each of the four actuators that drove the shake table was recorded. The resultant force components in both the longitudinal and transverse directions were then computed from these measured forces.

2.7 Data Reduction

Brace Axial Deformation, Δ

In the following chapter, the brace axial deformation, Δ, corresponding to the average of that measured by displacement transducers *L1* and *L2,* in Figure 2.15(a), is reported. The values of axial brace strain reported were calculated as:

$$\varepsilon = \frac{\Delta}{L_y} \tag{2.1}$$

where L_y equals the length of the steel core plate yielding zone. Note that Δ is measured over the length L_b and includes some minor elastic deformation of the core plate outside of the reduced cross section yielding zone length, L_y.

Gusset Bracket Deformation

Bracket deformation measured by displacement transducers *L3* and *L4* corresponds to wall bracket and platen bracket deformation, respectively. These measurements included the bracket deformation, connection plate deformation, and bolt deformation including slippage.

Brace End Rotation

The brace end rotation is computed by dividing the measured table transverse movement by the length L_b shown in Figure 2.15(a).

Resultant Brace Force, P_r

The resultant axial force in the brace, P_r, was calculated as the square root of the sum of the squares of the longitudinal and transverse forces that were recorded.

Tension Strength Adjustment Factor, ω

The AISC *Seismic Provision* defines ω as follows:

$$\omega = \frac{T_{\max}}{P_{ya}} = \frac{T_{\max}}{F_{ya} A_{sc}} \tag{2.2}$$

where F_{ya} = actual yield strength, and A_{sc} = area of the yielding segment of core plate. The variation of ω with respect to the brace axial deformation (Δ) for the Standard, High-Amplitude, and Low-Cycle Fatigue Loading Protocols will be presented. It is noted that the value of ω is dependent on the core plate yield-to-tensile strength ratio. A core plate with a low yield-to-tensile ratio will likely have a higher ω value as compared with a core plate with a higher yield-to-tensile ratio, even if both plates are the same grade of steel.

Compression Strength Adjustment Factor, β

The β value is computed as follows (AISC 2005):

$$\beta = \frac{P_{\max}}{T_{\max}} \tag{2.3}$$

where P_{max} is the maximum compressive force, and T_{max} is the maximum tension force corresponding to a brace deformation of $2.0\Delta_{bm}$. Values of the compression strength adjustment factor, β, at all other axial deformation levels, Δ, are also provided in Chapter 3.

Hysteretic Energy, E_h

The area enclosed by the P_r versus Δ hysteresis loops represents the hysteretic energy dissipated by the brace:

$$E_h = \int P_r d\Delta \tag{2.4}$$

Cumulative Inelastic Axial Deformation Capacity, η

Consider the i^{th} cycle at a deformation level greater than the yield deformation. The total inelastic axial deformation, when normalized by the axial deformation at yield, Δ_{by}, for that cycle is given by:

$$\mu_i = \frac{2(\Delta_i^+ + \Delta_i^-)}{\Delta_{by}} - 4 \tag{2.5}$$

where Δ_i^+ is the maximum tensile Δ and Δ_i^- is the absolute value of the maximum compressive Δ for the i^{th} cycle. The cumulative inelastic axial deformation capacity, η, normalized by Δ_{by}, is determined by the summation of the inelastic axial deformation for each of the i^{th} cycles:

$$\eta = \sum \mu_i \tag{2.5}$$

For uniaxial testing of BRBs, the AISC *Seismic Provisions* requires that the value of η be at least $200\Delta_{by}$. For comparison purposes the η values will be presented in this report.

Table 2.1 Specimen Dimensions

(a) General

Specimen	W1 (in.)	W2 (in.)	W3 (in.)	W4 (in.)	tcp (in.)	Core Plate	HSS Size (in.)
1G, 2G	10	11-3/16	8	--	1-1/2	Flat	14×14×5/16
3G, 4G	16	14	9-3/4	4-1/8	1-1/2	Cruciform	16×16×5/16

(b) Bolting

Specimen	Core PL Hole Dia. (in.)	Gusset PL Hole Dia. (in.)	Rows of Bolts	s (in.)	g1 (in.)	g2 (in.)
1G, 2G	1-9/16	1-11/16	4	6	3-1/8	--
3G, 4G	1-9/16	1-11/16	7	3	3-1/8	6-1/8

(c) Lengths

Specimen	L (in.)	Lb, L1[a] (in.)	Lc (in.)	Ly (in.)	e (in.)	x (in.)	Lt (in.)
1G, 2G	260-1/8	208-3/8	184-3/8	132-1/2	25-7/8	5-1/2	32-7/16
3G, 4G	250-3/16	198-7/16	164-7/16	144-7/16	25-7/8	14	13

[a]See Figure 2.15(a)

Table 2.2 Mechanical Properties of Core Plates

Specimen	Steel Mill	Heat No.	Coupon No.	F_{ya} (ksi)	F_{ua} (ksi)	F_{ua}/F_{ya}	Elong.[a] (%)
1G, 2G, 3G, 4G	Jindal United Steel Corporation	S00442	1	37.0	70.5	1.91	33
			2	37.9	70.0	1.85	31
			Avg.	37.5	70.3	1.88	32

[a]Elongation is based on 2 in. gage length

Table 2.3 Specimen Properties

Specimen	A_{sc} (in^2)	F_{ya} (ksi)	R_y	P_{yn} (kips)	P_{ya} (kips)	Δ_{by} (in.)
1G, 2G	12.0	37.5	1.042	432.0	450.0	0.21
3G, 4G	27.0	37.5	1.042	972.0	1012.5	0.24

Table 2.4 Grout Fill Compressive Strength

Date	Age (day)	Compressive Strength (psi)
10/10/2005	4	5750
10/13/2005	7	6650
11/03/2005	28	8825

Table 2.5 Loading Protocol Peak Displacements

(a) Standard Loading Protocol

Specimen	Longitudinal Deformation (in.)					Transverse Deformation (in.)				
	Number of Cycles					Number of Cycles				
	6	4	4	2	2	6	4	4	2	2
1G, 2G	0.21	0.53	1.06	1.59	2.12	0.43	1.08	2.14	3.20	4.24
3G, 4G	0.24	0.60	1.19	1.78	2.38	0.41	1.03	2.04	3.05	4.05

(b) High-Amplitude Loading Protocol

Specimen	Longitudinal Deformation (in.)				Transverse Deformation (in.)			
	Number of Cycles				Number of Cycles			
	2	2	2	2	2	2	2	2
1G, 2G	2.65	3.17	4.02	4.66	4.87	5.82	6.35	6.27
3G, 4G	2.97	3.57	4.40	5.12	4.67	5.59	6.01	6.02

(c) Low-Cycle Fatigue Loading Protocol

Specimen	Longitudinal Deformation (in.)	Transverse Deformation (in.)
1G, 2G	1.59	3.20
3G, 4G	Not Applicable	Not Applicable

Table 2.6 Shake Table Peak Input Displacements

(a) Standard Loading Protocol

Specimen	Longitudinal Deformation (in.)					Transverse Deformation (in.)				
	Number of Cycles					Number of Cycles				
	6	4	4	2	2	6	4	4	2	2
1G, 2G	0.32	0.65	1.21	1.93[a]	2.48[a]	0.43	1.08	2.14	3.20	4.24
3G	0.74	1.13	1.79	2.42	3.04	0.41	1.03	2.04	3.05	4.05
4G	0.64	1.03	1.69	2.32	2.94	0.41	1.03	2.04	3.05	4.05

[a]Input displacement accidentally accounted for system flexibility twice.

(b) High-Amplitude Loading Protocol

Specimen	Longitudinal Deformation (in.)				Transverse Deformation (in.)			
	Number of Cycles				Number of Cycles			
	2	2	2	2	2	2	2	2
1G, 2G	2.83	3.37	4.23	4.87	4.87	5.82	6.35	6.27
3G	3.65	4.27	5.12	5.84	4.67	5.59	6.01	6.02
4G	3.55	4.17	5.02	5.74	4.67	5.59	6.01	6.02

(c) Low-Cycle Fatigue Cycles

Specimen	Longitudinal Deformation (in.)	Transverse Deformation (in.)
	Number of Cycles	Number of Cycles
	15	15
1G, 2G	1.76	3.20
3G, 4G	Not Applicable	Not Applicable

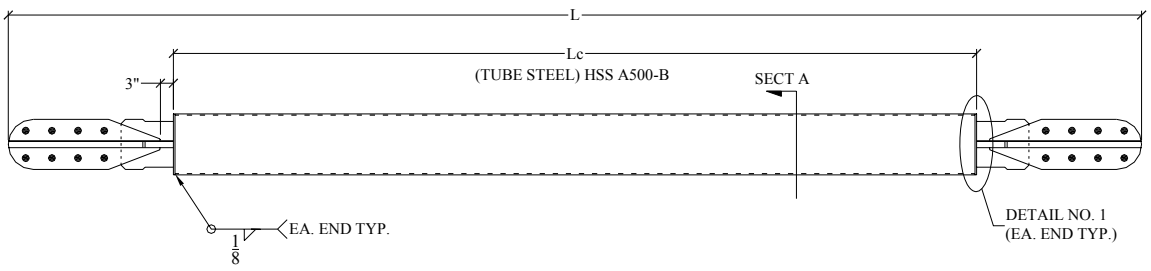

(a) Overall Geometry

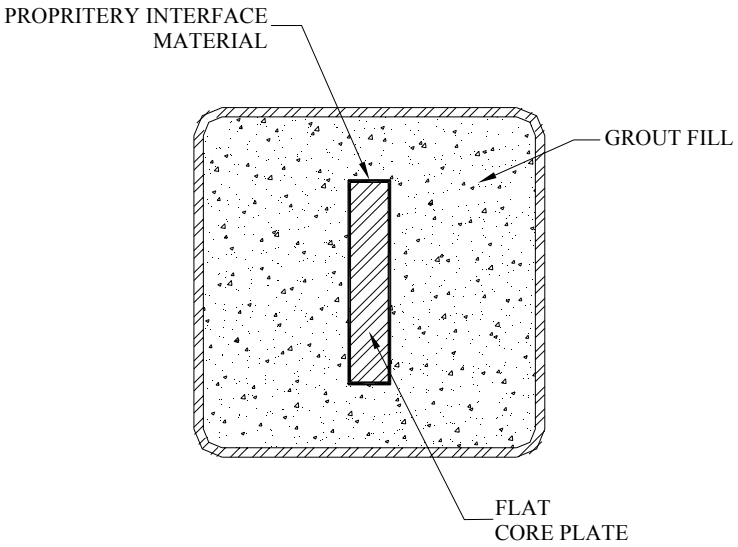

(b) Section A

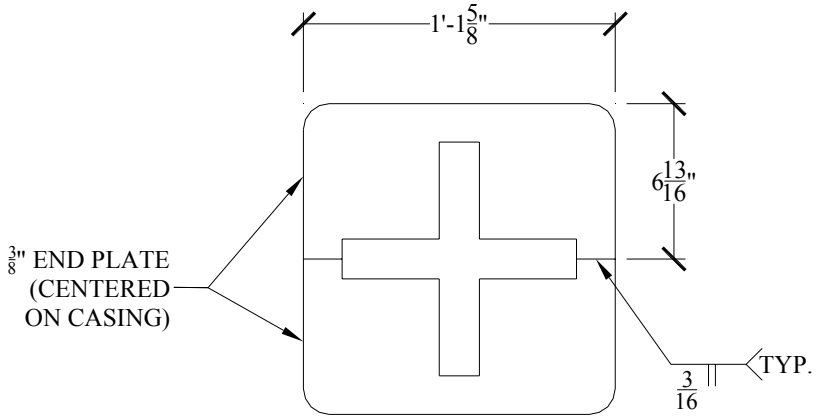

(c) Detail No. 1 (End Plate)

Figure 2.1 Specimens 1G and 2G: Brace Geometry

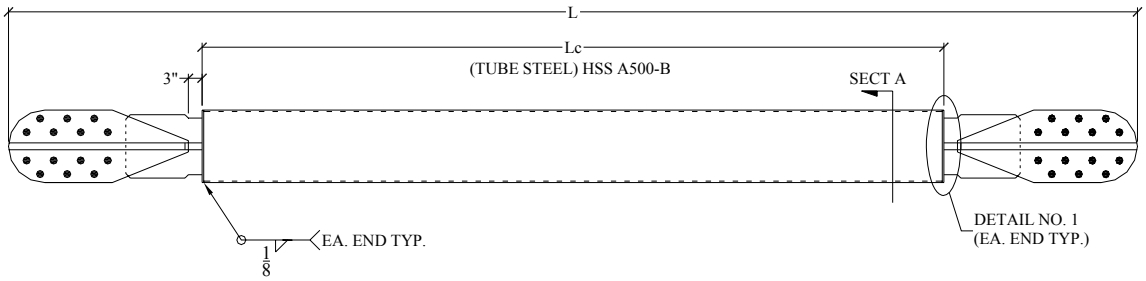

(a) Overall Geometry

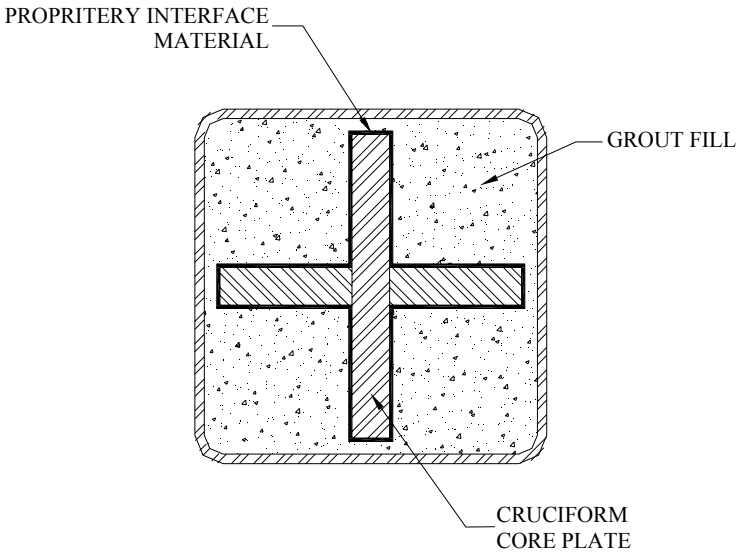

(b) Section A

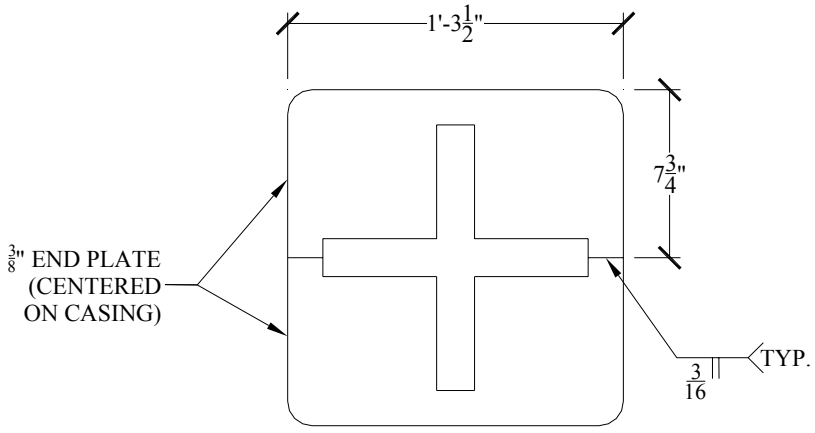

(c) Detail No. 1 (End Plate)

Figure 2.2 Specimens 3G and 4G: Brace Geometry

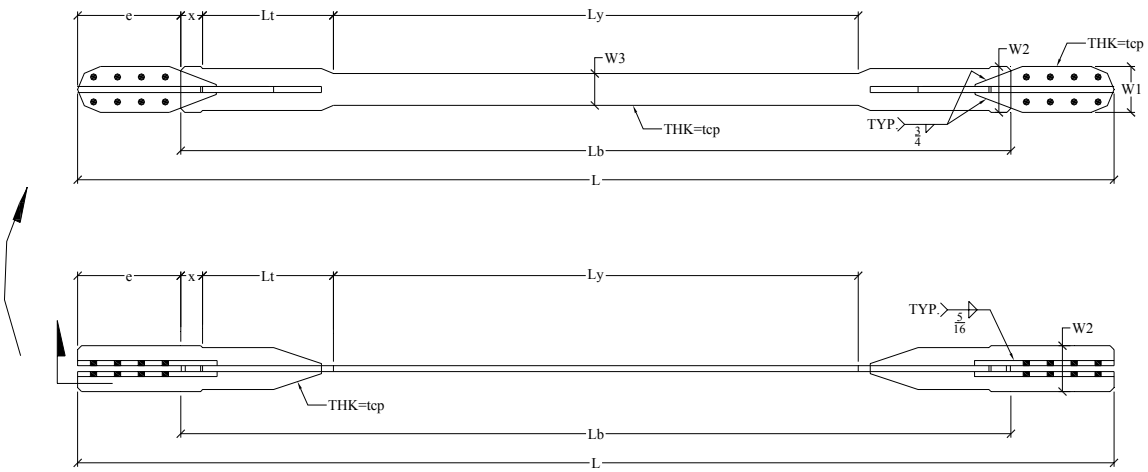

(a) Flat Core Plate

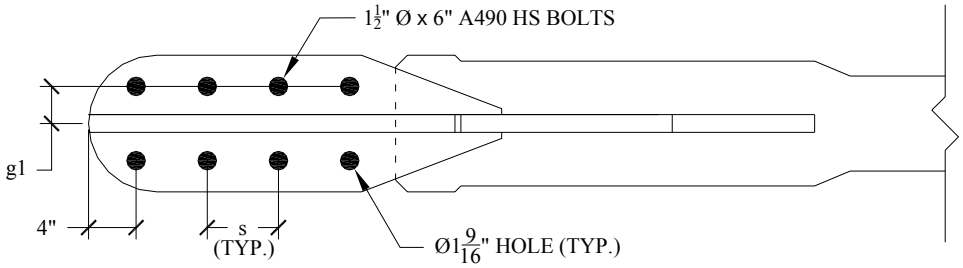

(b) Core Plate End Detail

Figure 2.3 Specimens 1G and 2G: Core Plate Dimensions

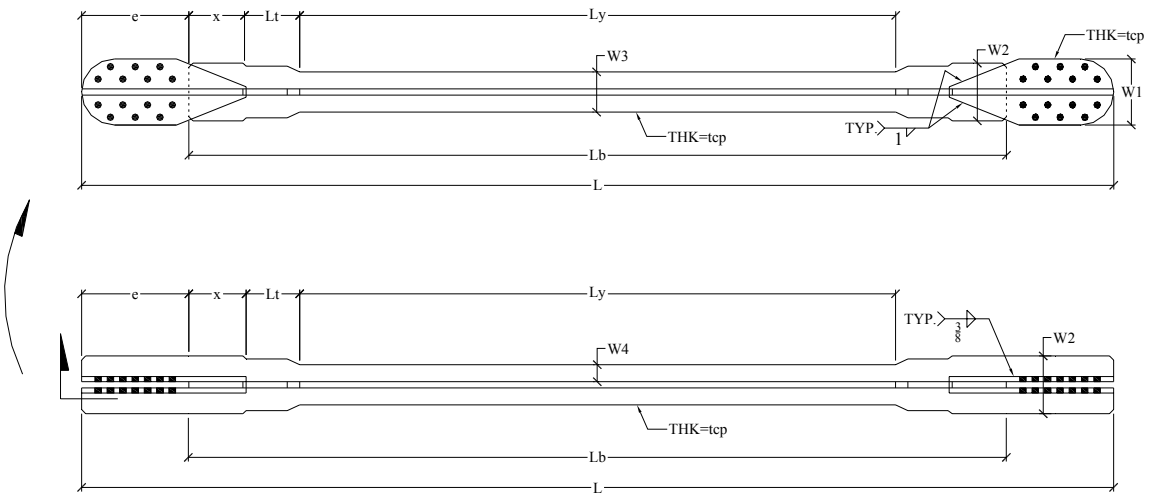

(a) Cruciform Core Plate

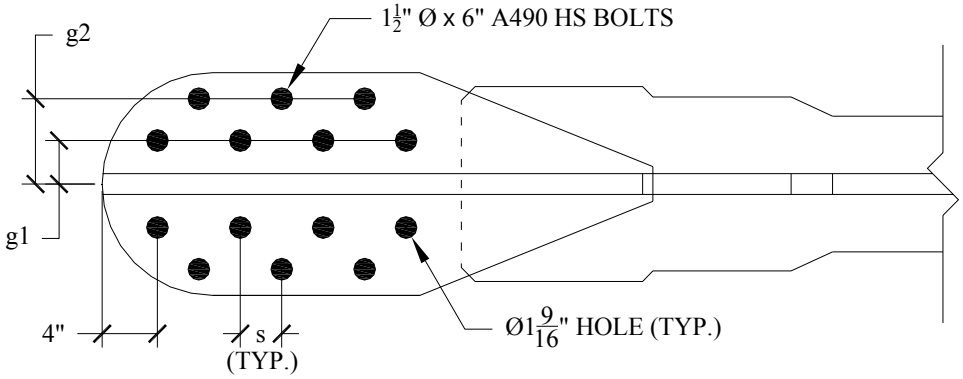

(b) Core Plate End Detail

Figure 2.4 Specimens 3G and 4G: Core Plate Dimensions

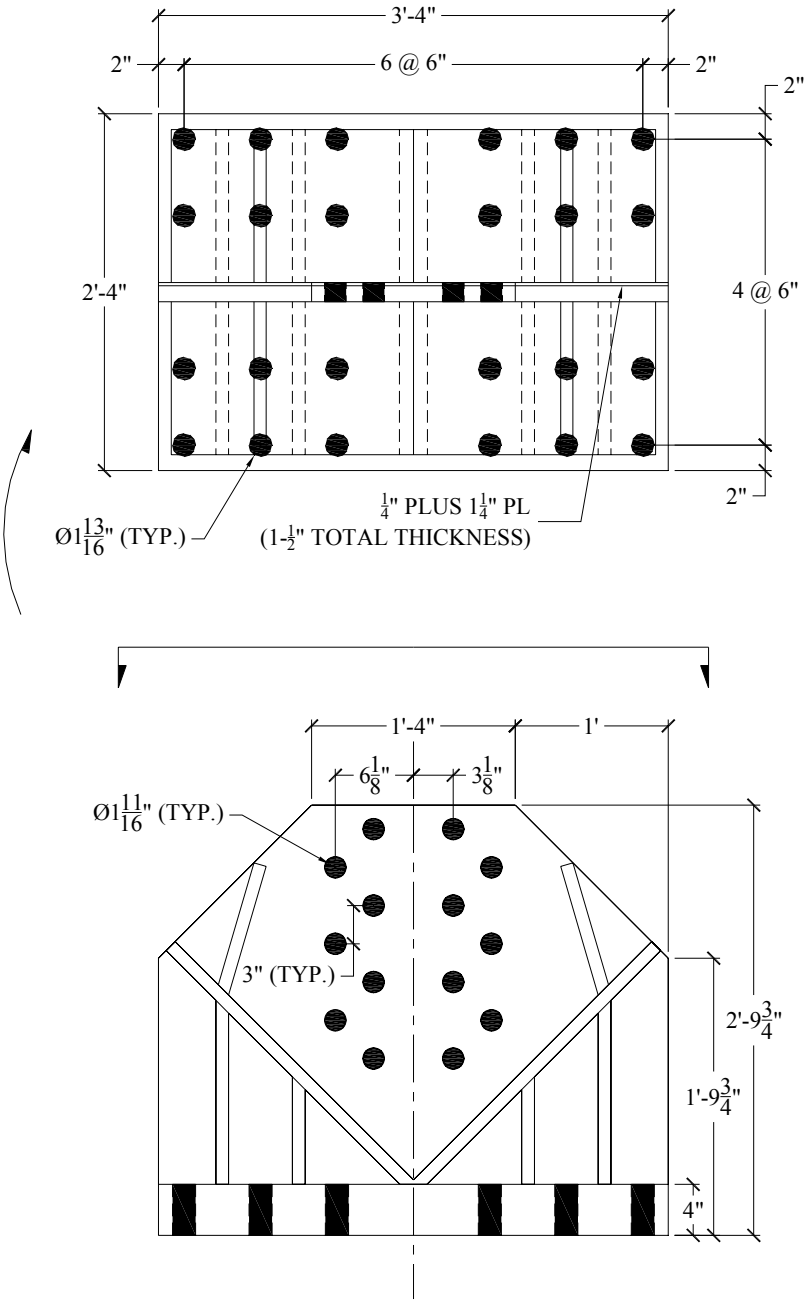

Figure 2.5 End Connection Gusset Bracket

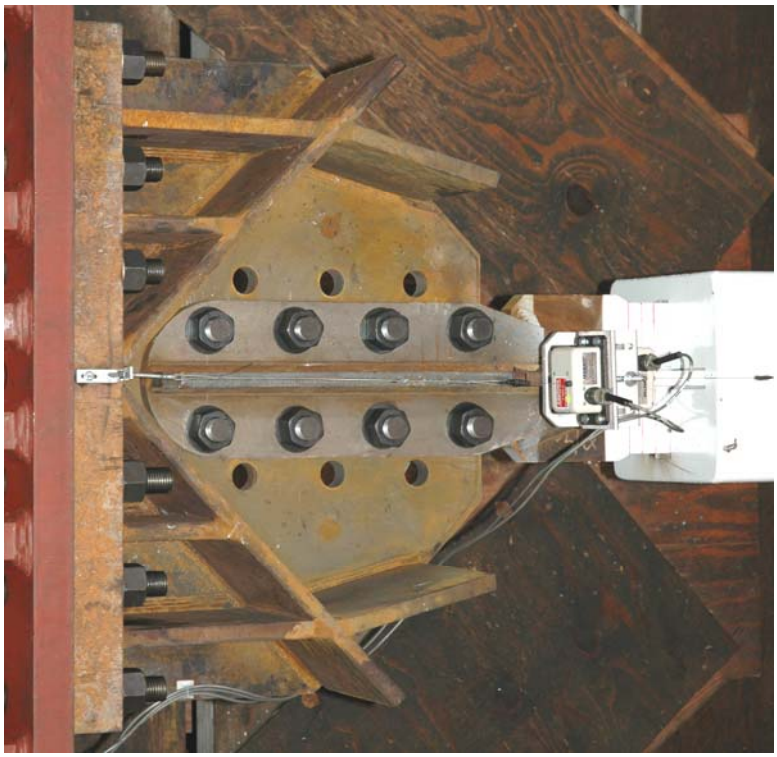

(a) Specimens 1G and 2G

(b) Specimens 3G and 4G

Figure 2.6 End Connections

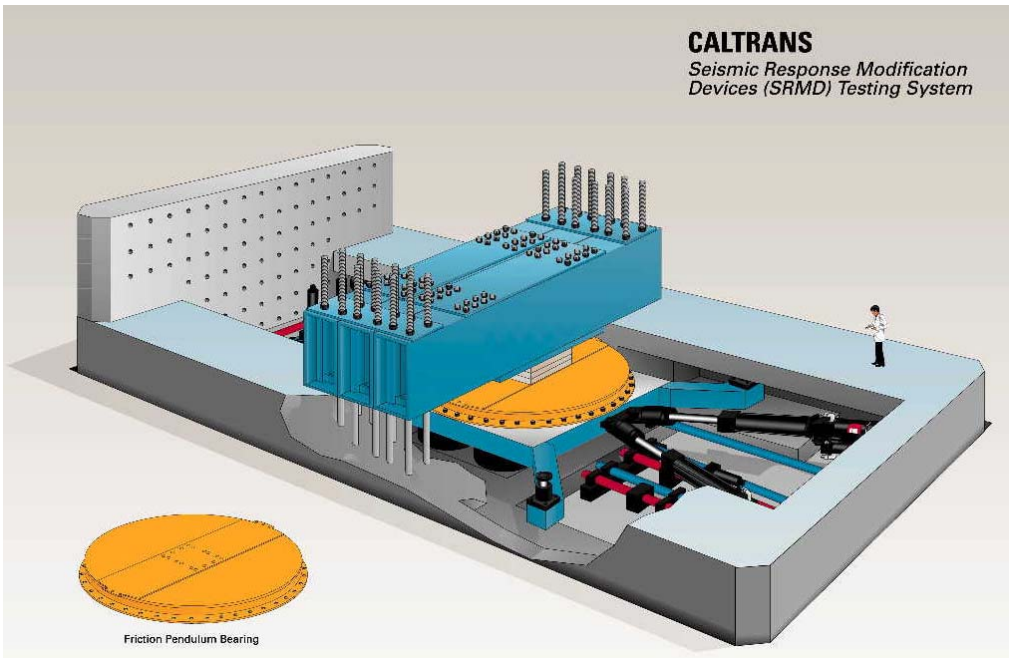

(a) Three-Dimensional Rendering

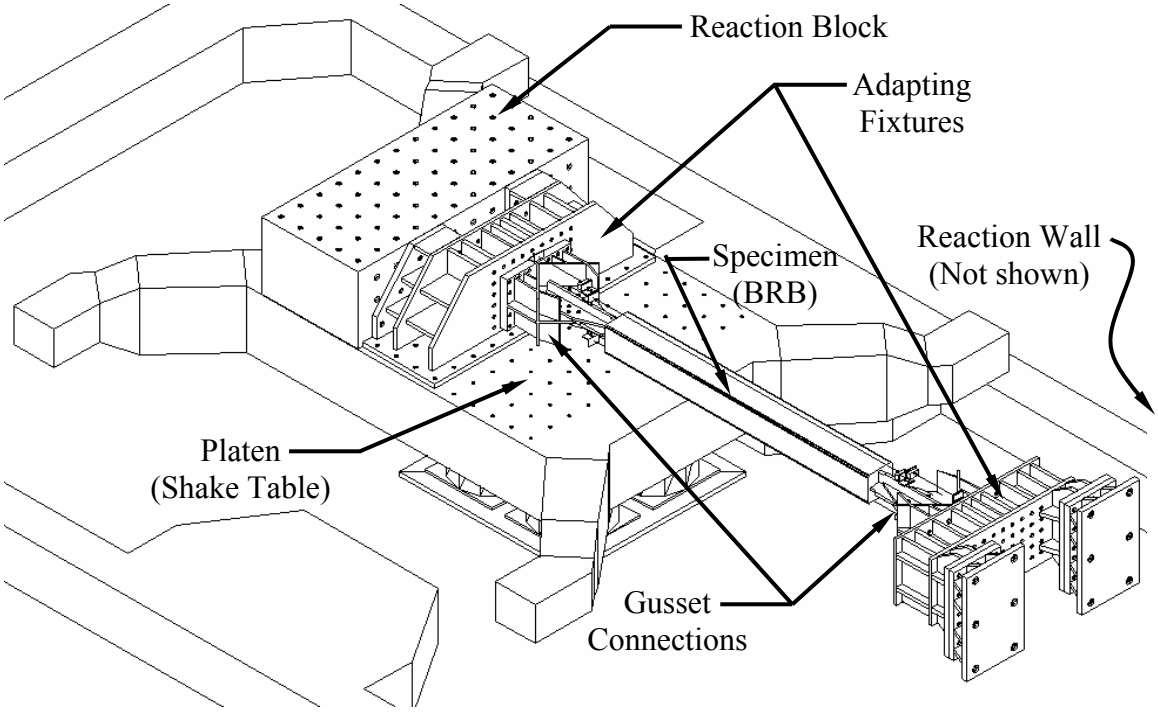

(b) Setup Overview

Figure 2.7 SRMD Test Facility

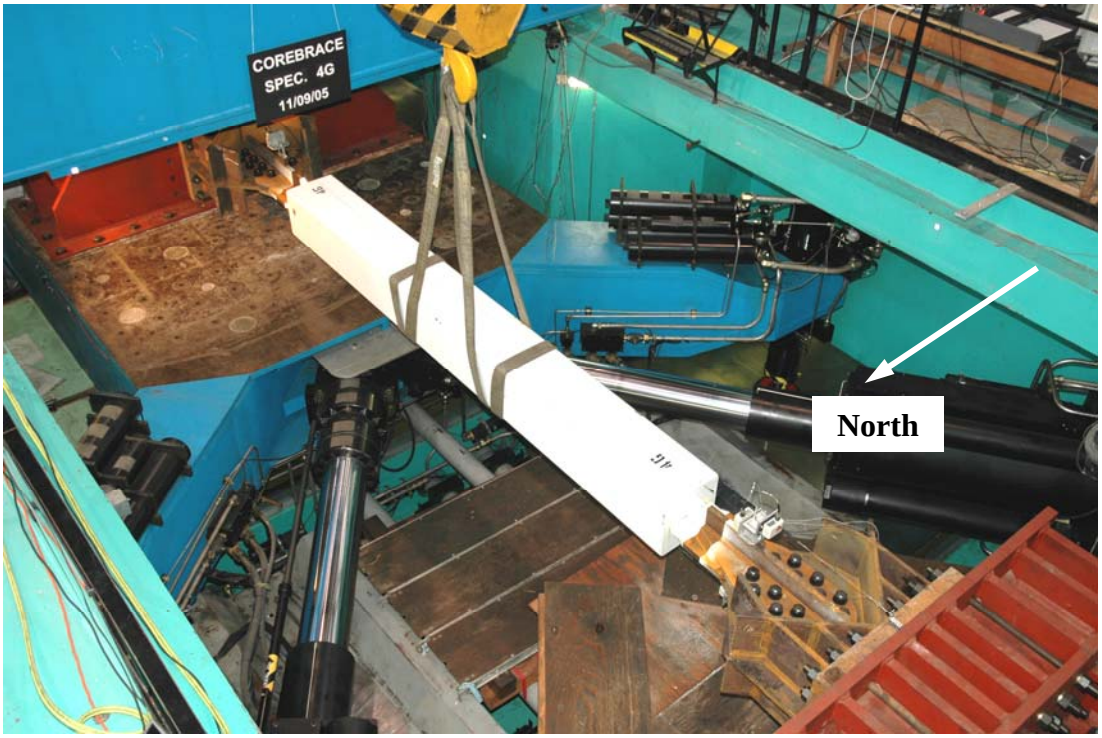

Figure 2.8 Overall View of Specimen and SRMD

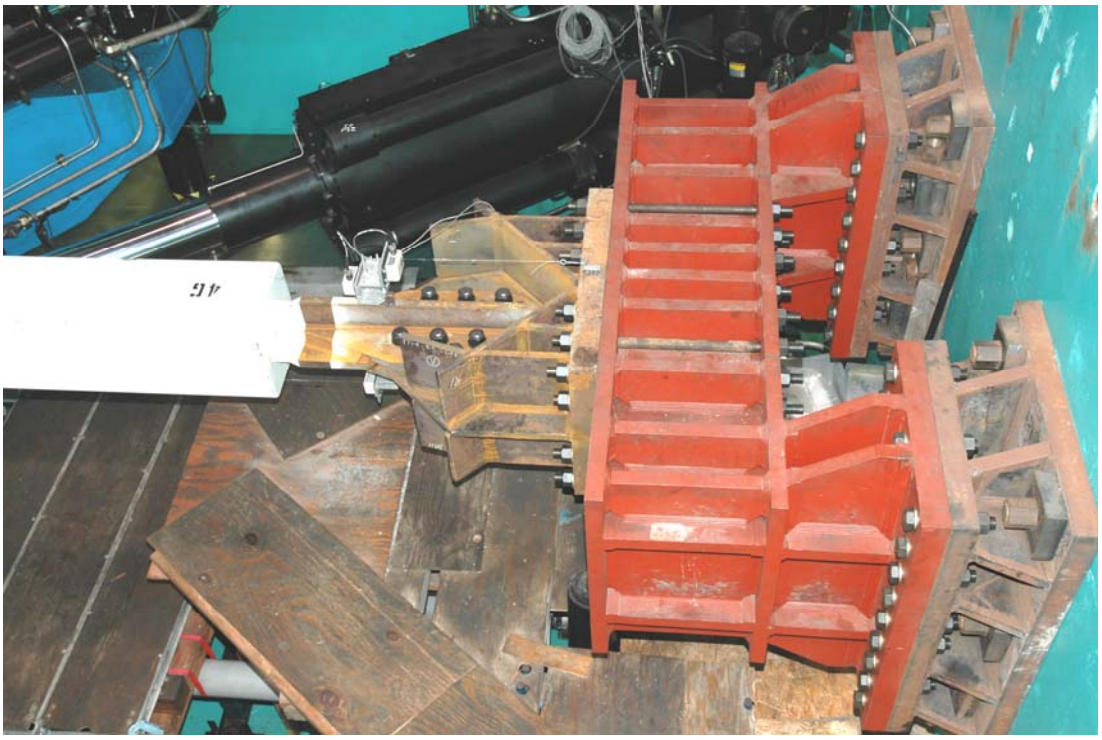

Figure 2.9 Wall End Support (West End)

Figure 2.10 Platen End Support (East End)

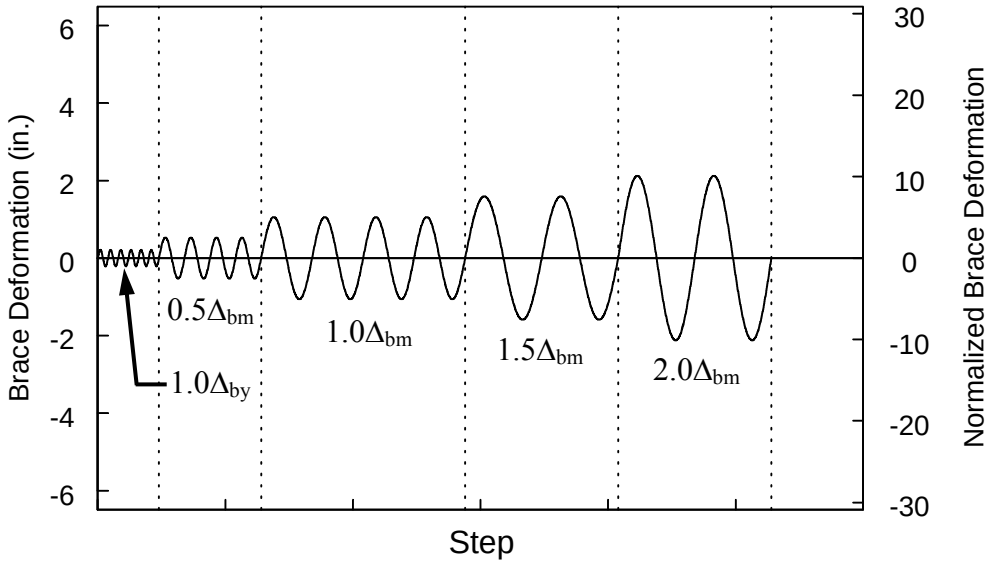

(a) Longitudinal Direction

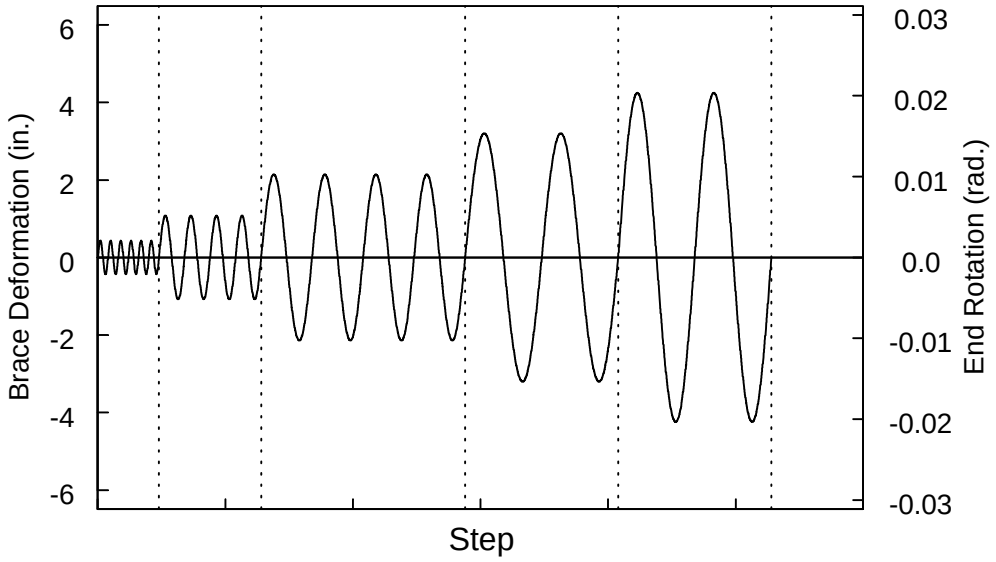

(b) Transverse Direction

Figure 2.11 Specimens 1G and 2G: Standard Loading Protocol

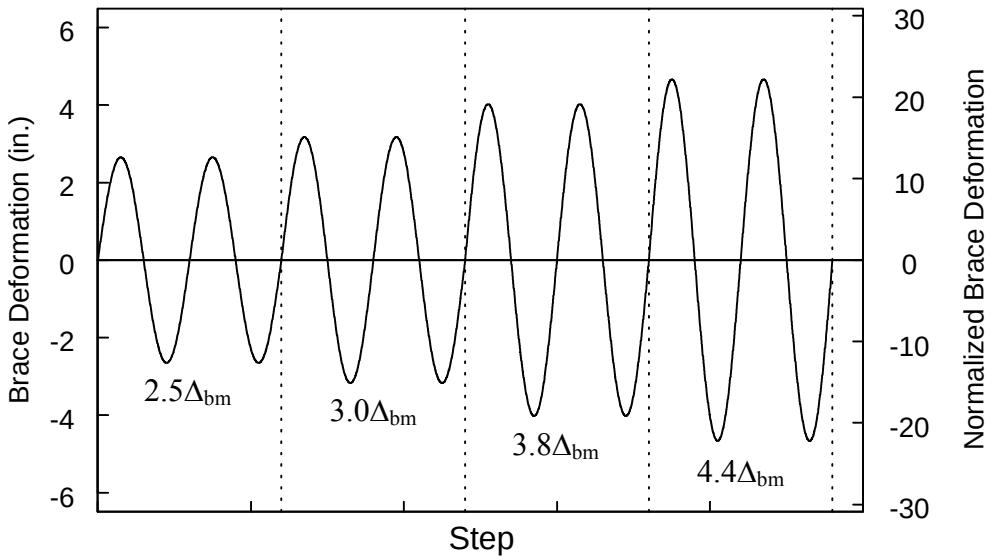

(a) Longitudinal Direction

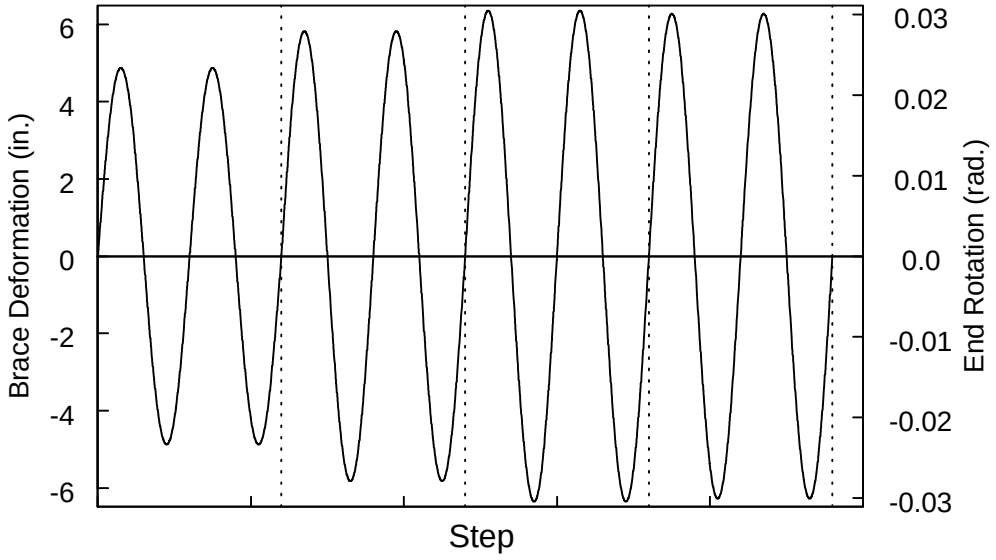

(b) Transverse Direction

Figure 2.12 Specimens 1G and 2G: High-Amplitude Loading Protocol

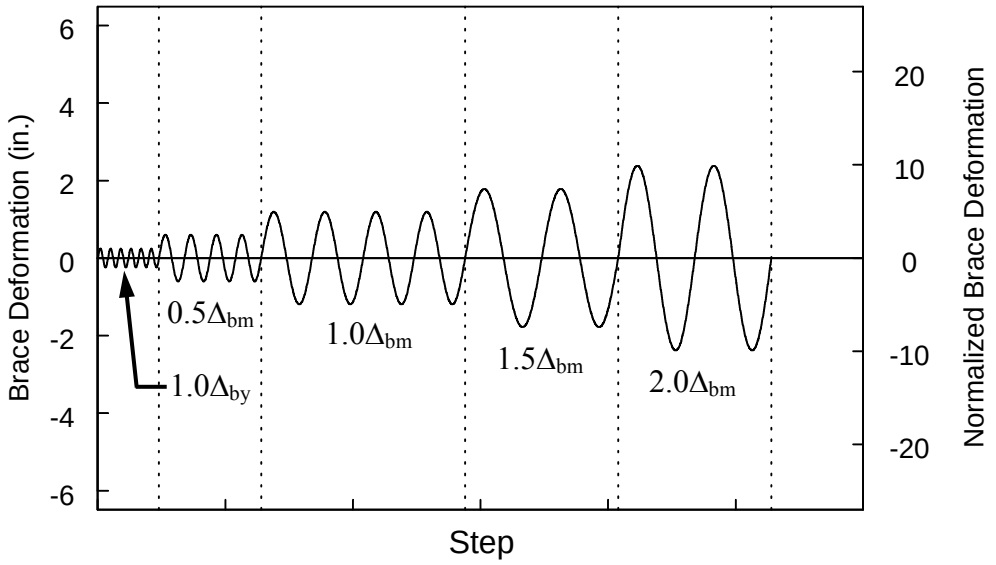

(a) Longitudinal Direction

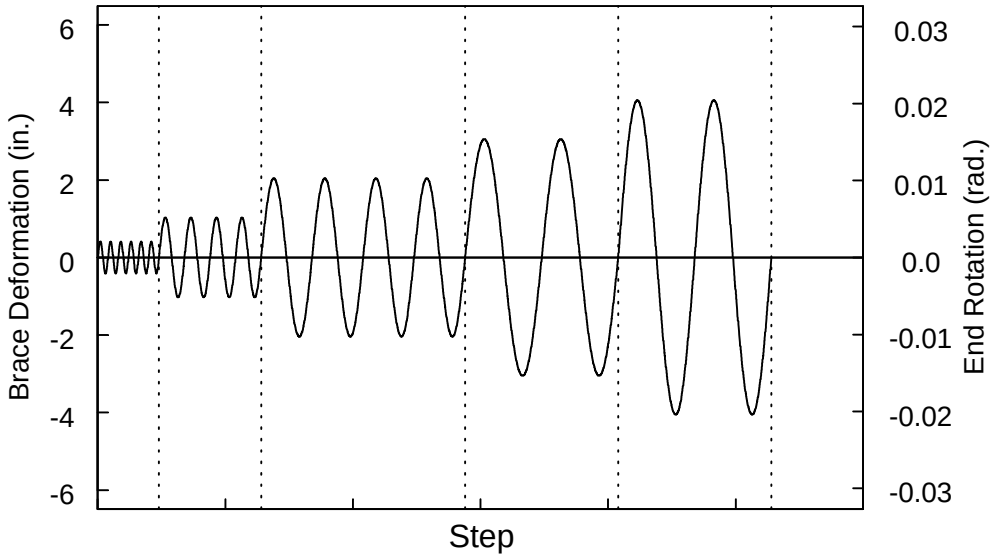

(b) Transverse Direction

Figure 2.13 Specimens 3G and 4G: Standard Loading Protocol

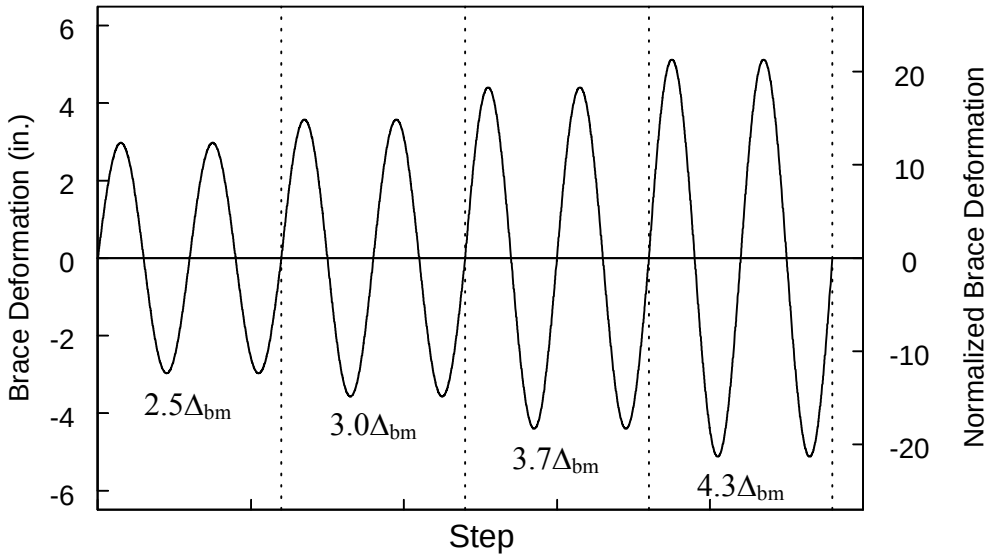

(a) Longitudinal Direction

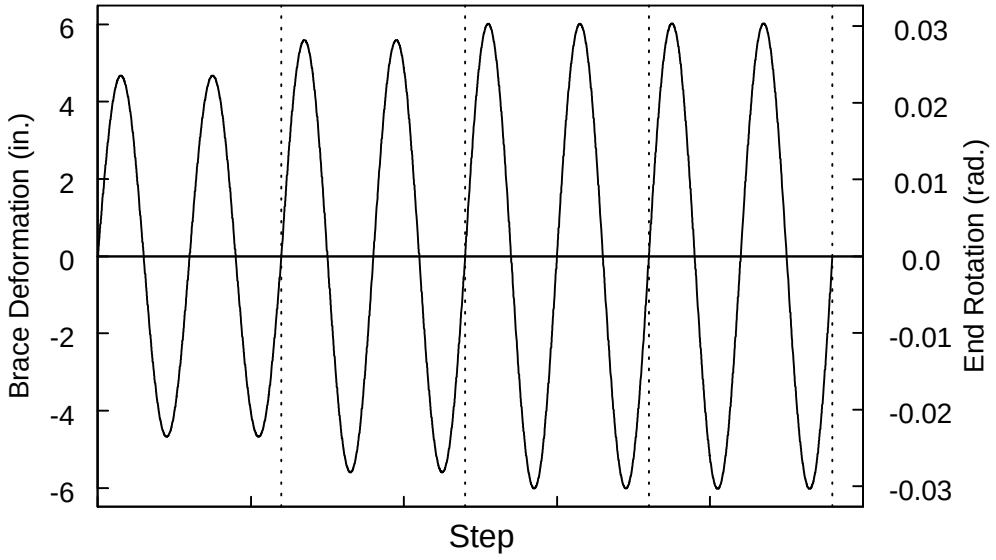

(b) Transverse Direction

Figure 2.14 Specimens 3G and 4G: High-Amplitude Loading Protocol

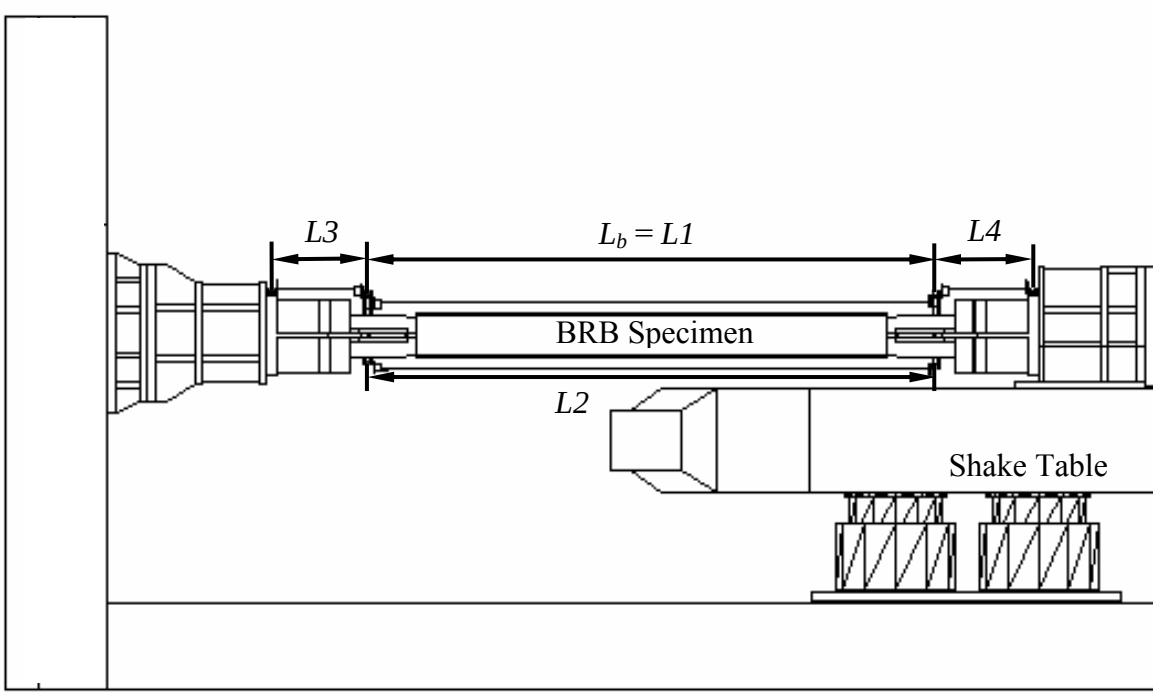

(a) Displacement Transducer Locations

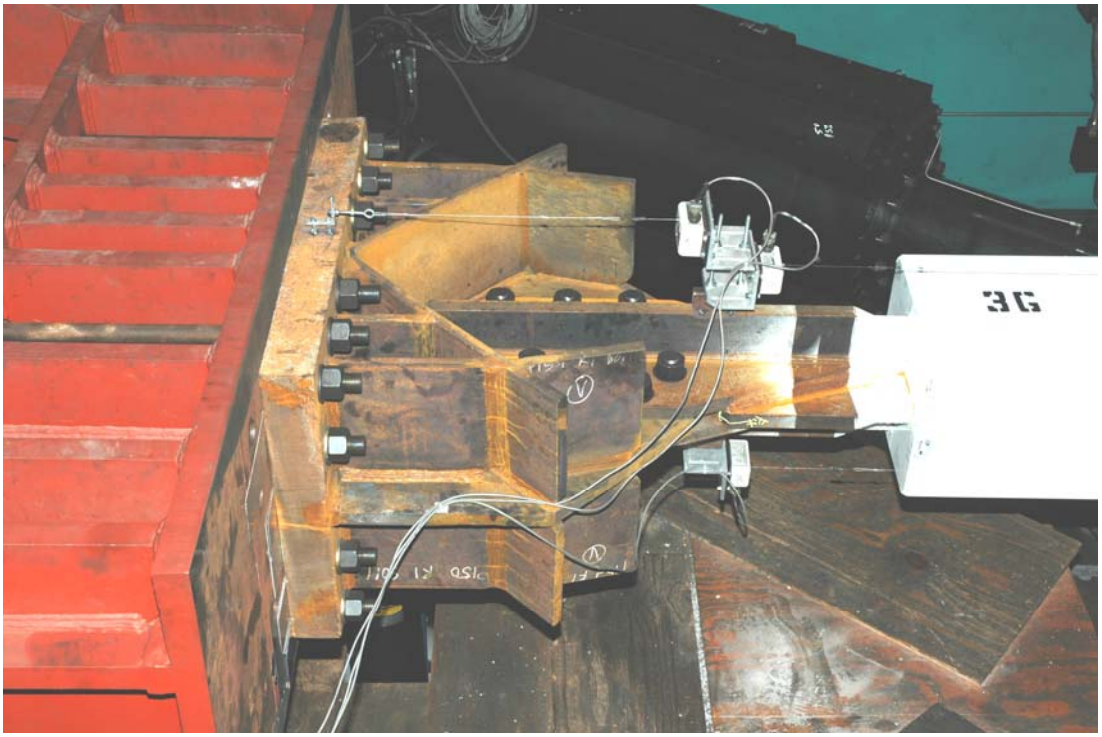

(b) Displacement Transducers

Figure 2.15 Displacement Transducer Instrumentation

3. TEST RESULTS

3.1 Introduction

For each of the test specimens, the following results are presented for the Standard Loading Protocol, High-Amplitude Loading Protocol, and Low-Cycle Fatigue Protocol (Specimens 1G and 2G) tests. In addition to showing results for each loading sequence for each specimen, these results are also combined in another set of plots to demonstrate the accumulative effects.

(1) A table summarizing the peak brace forces and peak brace deformations: The brace axial deformation refers to the average deformation measured by displacement transducers *L1* and *L2* shown in Figure 2.15(a).

(2) Measured shake table displacement time histories in both the longitudinal and transverse directions: These displacements represent the axial deformation and end rotation demand imposed on the specimen-supporting frame assembly.

(3) Measured brace displacement time histories in the longitudinal and transverse directions: These displacements represent the actual axial deformation and end rotation demand experienced by the brace specimen.

(4) Brace resultant force (P_r) versus brace axial deformation (Δ) plot: The calculation of the brace resultant force was presented in Section 2.7.

(5) Gusset bracket displacement time histories measured by displacement transducers *L3* and *L4* shown in Figure 2.15(a).

(6) Hysteretic energy (E_h) time history: The hysteretic energy was computed in accordance with Eq. 2.4.

(7) Tension strength adjustment factor (ω) versus brace axial deformation plot: The calculation of ω is based on Eq. 2.2.

(8) Compression strength adjustment factor (β) versus brace axial deformation plot: See Eq. 2.3 for the calculation of β. The variation of β with respect to the brace axial deformation (Δ) for the Standard Protocol, High-Amplitude Protocol, and Low-Cycle Fatigue Protocol is presented.

3.2 Specimen 1G

Specimen 1G was tested on November 4, 2005. The specimen performed well during the Standard, High-Amplitude, and Low-Cycle Fatigue Loading Protocol tests. Bolt slip was observed during the first cycle of deformation at $4.4\Delta_{bm}$ and occurred on all subsequent cycles at approximately the same axial load. This slip resulted in "polishing" of the gusset brackets (see Figure 3.1) but no deformation of the gusset plate bolt holes was observed. Specimen 1G was subjected to 15 cycles of the Low-Cycle Fatigue Loading Protocol without the steel core plate rupturing. The following results are presented for Specimen 1G:

(1) Standard Loading Protocol test: Figures 3.2 to 3.6,
(2) High-Amplitude Loading Protocol test: Figures 3.7 to 3.11,
(3) Low-Cycle Fatigue test: Figures 3.12 to 3.16,
(4) Combined tests: Figures 3.17 and 3.18,
(5) Peak response values and response envelope: Table 3.1 and Figure 3.19, and
(6) β, ω, and $\beta\omega$ values: Table 3.1 and Figures 3.20 and 3.21.

3.3 Specimen 2G

Specimen 2G was tested on November 7, 2005. The specimen performed well during the Standard Loading Protocol test. Bolt slip was observed during the first cycle of deformation at $3.0\Delta_{bm}$ and occurred on all subsequent cycles at approximately the same axial load. This slip resulted in additional "polishing" of the gusset brackets but no deformation of the bolt holes was visible. Figure 3.22 shows the gusset brackets after testing of Specimen 2G. During the High-Amplitude Protocol the confining HSS shifted towards the platen end of the BRB (problem with centering mechanism) and the majority of core plate deformation relative to the confining HSS occurred on the strong-wall end of the specimen. Previously, balanced deformation (core plate relative to HSS) was observed on both ends of the specimen. Also, the core plate went into bearing against the end of the confining HSS and resulted in increased compressive strength at high deformation levels (see Figure 3.31). Also, during the 15 cycles of the Low-Cycle Fatigue Loading Protocol the majority of deformation (core plate relative to HSS)

occurred on the strong-wall end of the specimen. The Specimen 2G steel core plate did not rupture. The following results are presented for Specimen 2G:

(1) Standard Loading Protocol test: Figures 3.23 to 3.27,
(2) High-Amplitude Loading Protocol test: Figures 3.28 to 3.32,
(3) Low-Cycle Fatigue test: Figures 3.33 to 3.37,
(4) Combined tests: Figures 3.38 and 3.39,
(5) Peak response values and response envelope: Table 3.2 and Figure 3.40, and
(6) β, ω, and βω values: Table 3.2 and Figures 3.41 and 3.42.

3.4 Specimen 3G

Specimen 3G was tested on November 8, 2005. The specimen performed well during the Standard and High-Amplitude Loading Protocol tests. Bolt slip was observed during the fourth cycle of deformation at $0.5\Delta_{bm}$ and occurred on all subsequent cycles at approximately the same axial load. The "polishing" from this slip is shown in Figure 3.43. No deformation of the gusset plate bolt holes was observed. The core plate ruptured on the first $4.3\Delta_{bm}$ tension excursion during the High-Amplitude Loading Protocol. The following results are presented for Specimen 3G:

(1) Standard Loading Protocol test: Figures 3.44 to 3.48,
(2) High-Amplitude Loading Protocol test: Figures 3.49 to 3.53,
(3) Combined tests: Figures 3.54 and 3.55,
(4) Peak response values and response envelope: Table 3.3 and Figure 3.56, and
(5) β, ω, and βω values: Table 3.3 and Figures 3.57 and 3.58.

3.5 Specimen 4G

Specimen 4G was tested on November 9, 2005. Before specimen installation in the test setup the previously "polished" gusset plate faying surfaces were roughened with a file. Figure 3.59 shows the gusset brackets before testing of Specimen 4G. The specimen performed well during the Standard and High-Amplitude Loading Protocol tests. Bolt slip was observed during the second cycle of deformation at $1.0\Delta_{bm}$ and occurred on all subsequent cycles at approximately the same axial load. No deformation of the gusset plate bolt holes was observed. The Specimen 4G steel core plate did not

rupture during the High-Amplitude Loading Protocol but was not subjected to a Low-Cycle Fatigue Loading Protocol. The following results are presented for Specimen 4G:

(1) Standard Loading Protocol test: Figures 3.60 to 3.64,

(2) High-Amplitude Loading Protocol test: Figures 3.65 to 3.69,

(3) Combined tests: Figures 3.70 and 3.71,

(4) Peak response values and response envelope: Table 3.4 and Figure 3.72, and

(5) β, ω, and $\beta\omega$ values: Table 3.4 and Figures 3.73 and 3.74.

Table 3.1 Specimen 1G Peak Response Quantities

Test	Cycle No.	T_{max}	P_{max}	β	ω	βω	Brace Deformations						η
							Longitudinal				Transverse		
							Tension		Compresion				
		(kips)	(kips)				(in.)	ε (%)	(in.)	ε (%)	(in.)	(rad.)	(Δ_{by})
Standard Loading Protocol	1	436	-471	1.08	0.97	1.05	0.22	0.17	-0.24	-0.18	0.43	0.002	0
	2	426	-437	1.03	0.95	0.97	0.21	0.16	-0.24	-0.18	0.42	0.002	1
	3	411	-433	1.05	0.91	0.96	0.21	0.16	-0.23	-0.17	0.42	0.002	1
	4	415	-426	1.03	0.92	0.95	0.21	0.16	-0.23	-0.17	0.42	0.002	1
	5	414	-423	1.02	0.92	0.94	0.22	0.17	-0.23	-0.17	0.41	0.002	1
	6	421	-418	0.99	0.94	0.93	0.22	0.17	-0.23	-0.17	0.42	0.002	2
	7	515	-486	0.94	1.14	1.08	0.54	0.41	-0.56	-0.42	1.10	0.005	8
	8	507	-498	0.98	1.13	1.11	0.54	0.41	-0.56	-0.42	1.09	0.005	15
	9	511	-507	0.99	1.14	1.13	0.54	0.41	-0.56	-0.42	1.09	0.005	21
	10	520	-515	0.99	1.16	1.14	0.53	0.40	-0.55	-0.42	1.09	0.005	27
	11	595	-631	1.06	1.32	1.40	1.24	0.94	-1.24	-0.94	2.42	0.012	47
	12	630	-646	1.03	1.40	1.44	1.23	0.93	-1.23	-0.93	2.42	0.012	66
	13	643	-650	1.01	1.43	1.44	1.23	0.93	-1.23	-0.93	2.42	0.012	86
	14	646	-654	1.01	1.44	1.45	1.22	0.92	-1.23	-0.93	2.43	0.012	105
	15	678	-714	1.05	1.51	1.59	1.80	1.36	-1.78	-1.34	3.22	0.015	135
	16	692	-717	1.04	1.54	1.59	1.79	1.35	-1.77	-1.34	3.23	0.016	165
	17	720	-770	1.07	1.60	1.71	2.36	1.78	-2.30	-1.74	4.27	0.020	206
	18	733	-774	1.06	1.63	1.72	2.35	1.77	-2.30	-1.74	4.28	0.021	246
High-Amplitude Protocol	19	756	-818	1.08	1.68	1.82	2.76	2.08	-2.61	-1.97	4.89	0.023	293
	20	762	-822	1.08	1.69	1.83	2.72	2.05	-2.63	-1.98	4.90	0.023	340
	21	778	-863	1.11	1.73	1.92	3.28	2.48	-3.15	-2.38	5.86	0.028	397
	22	786	-862	1.10	1.75	1.92	3.29	2.48	-3.15	-2.38	5.86	0.028	454
	23	801	-919	1.15	1.78	2.04	4.15	3.13	-3.98	-3.00	6.40	0.031	528
	24	812	-921	1.13	1.80	2.05	4.15	3.13	-3.96	-2.99	6.40	0.031	601
	25	816	-958	1.17	1.81	2.13	4.65	3.51	-4.59	-3.46	6.32	0.030	685
	26	822	-956	1.16	1.83	2.12	4.65	3.51	-4.58	-3.46	6.30	0.030	769
Low-Cycle Fatigue Protocol	29	869	-783	0.90	1.93	1.74	1.45	1.09	-1.53	-1.15	3.22	0.015	793
	30	779	-763	0.98	1.73	1.70	1.45	1.09	-1.54	-1.16	3.22	0.015	818
	31	752	-747	0.99	1.67	1.66	1.44	1.09	-1.55	-1.17	3.22	0.015	842
	32	735	-738	1.00	1.63	1.64	1.45	1.09	-1.55	-1.17	3.22	0.015	867
	33	725	-730	1.01	1.61	1.62	1.45	1.09	-1.57	-1.18	3.23	0.015	892
	34	717	-726	1.01	1.59	1.61	1.46	1.10	-1.56	-1.18	3.22	0.015	916
	35	711	-721	1.01	1.58	1.60	1.46	1.10	-1.58	-1.19	3.22	0.015	941
	36	706	-717	1.02	1.57	1.59	1.46	1.10	-1.58	-1.19	3.22	0.015	966
	37	702	-715	1.02	1.56	1.59	1.47	1.11	-1.58	-1.19	3.22	0.015	991
	38	699	-714	1.02	1.55	1.59	1.48	1.12	-1.59	-1.20	3.22	0.015	1017
	39	697	-712	1.02	1.55	1.58	1.47	1.11	-1.59	-1.20	3.22	0.015	1042
	40	694	-709	1.02	1.54	1.58	1.48	1.12	-1.60	-1.21	3.23	0.016	1067
	41	693	-708	1.02	1.54	1.57	1.48	1.12	-1.59	-1.20	3.22	0.015	1092
	42	691	-708	1.02	1.54	1.57	1.48	1.12	-1.59	-1.20	3.22	0.015	1118
	43	691	-709	1.03	1.54	1.58	1.49	1.12	-1.59	-1.20	3.23	0.015	1143

Table 3.2 Specimen 2G Peak Response Quantities

Test	Cycle No.	T_{max}	P_{max}	β	ω	βω	Brace Deformations						η
							Longitudinal				Transverse		
							Tension		Compresion				
		(kips)	(kips)				(in.)	ε (%)	(in.)	ε (%)	(in.)	(rad.)	(Δ_{by})
Standard Loading Protocol	1	416	-469	1.13	0.92	1.04	0.21	0.16	-0.24	-0.18	0.43	0.002	0
	2	395	-435	1.10	0.88	0.97	0.21	0.16	-0.23	-0.17	0.42	0.002	0
	3	405	-417	1.03	0.90	0.93	0.21	0.16	-0.23	-0.17	0.42	0.002	1
	4	390	-417	1.07	0.87	0.93	0.21	0.16	-0.23	-0.17	0.42	0.002	1
	5	400	-423	1.06	0.89	0.94	0.21	0.16	-0.23	-0.17	0.42	0.002	1
	6	394	-417	1.06	0.88	0.93	0.22	0.17	-0.23	-0.17	0.42	0.002	1
	7	492	-483	0.98	1.09	1.07	0.54	0.41	-0.56	-0.42	1.09	0.005	8
	8	504	-493	0.98	1.12	1.10	0.53	0.40	-0.55	-0.42	1.10	0.005	14
	9	506	-497	0.98	1.12	1.10	0.53	0.40	-0.54	-0.41	1.10	0.005	20
	10	514	-506	0.98	1.14	1.12	0.53	0.40	-0.54	-0.41	1.09	0.005	26
	11	569	-617	1.08	1.26	1.37	1.23	0.93	-1.23	-0.93	2.43	0.012	46
	12	614	-635	1.03	1.36	1.41	1.21	0.91	-1.21	-0.91	2.44	0.012	65
	13	627	-641	1.02	1.39	1.42	1.21	0.91	-1.21	-0.91	2.43	0.012	84
	14	631	-642	1.02	1.40	1.43	1.21	0.91	-1.21	-0.91	2.43	0.012	103
	15	661	-698	1.06	1.47	1.55	1.78	1.34	-1.77	-1.34	3.24	0.016	133
	16	676	-701	1.04	1.50	1.56	1.77	1.34	-1.76	-1.33	3.24	0.016	162
	17	704	-762	1.08	1.56	1.69	2.33	1.76	-2.28	-1.72	4.28	0.021	202
	18	718	-769	1.07	1.60	1.71	2.33	1.76	-2.28	-1.72	4.28	0.021	242
High-Amplitude Protocol	19	742	-808	1.09	1.65	1.80	2.76	2.08	-2.56	-1.93	4.92	0.024	289
	20	749	-819	1.09	1.66	1.82	2.71	2.05	-2.61	-1.97	4.91	0.024	336
	21	753	-856	1.14	1.67	1.90	3.05	2.30	-3.13	-2.36	5.87	0.028	390
	22	765	-855	1.12	1.70	1.90	3.04	2.29	-3.12	-2.35	5.88	0.028	445
	23	778	-941	1.21	1.73	2.09	3.90	2.94	-3.93	-2.97	6.41	0.031	516
	24	793	-945	1.19	1.76	2.10	3.90	2.94	-3.85	-2.91	6.41	0.031	586
	25	797	-1018	1.28	1.77	2.26	4.47	3.37	-4.47	-3.37	6.33	0.030	667
	26	805	-1027	1.28	1.79	2.28	4.47	3.37	-4.47	-3.37	6.31	0.030	748
Low-Cycle Fatigue Protocol	29	852	-762	0.89	1.89	1.69	1.29	0.97	-1.43	-1.08	3.24	0.016	770
	30	770	-743	0.96	1.71	1.65	1.29	0.97	-1.45	-1.09	3.23	0.016	792
	31	744	-733	0.99	1.65	1.63	1.28	0.97	-1.45	-1.09	3.23	0.016	814
	32	727	-726	1.00	1.62	1.61	1.28	0.97	-1.46	-1.10	3.23	0.015	836
	33	715	-723	1.01	1.59	1.61	1.28	0.97	-1.49	-1.12	3.23	0.016	858
	34	706	-715	1.01	1.57	1.59	1.28	0.97	-1.49	-1.12	3.24	0.016	881
	35	699	-712	1.02	1.55	1.58	1.28	0.97	-1.49	-1.12	3.23	0.016	903
	36	694	-709	1.02	1.54	1.58	1.28	0.97	-1.49	-1.12	3.23	0.016	925
	37	689	-708	1.03	1.53	1.57	1.29	0.97	-1.50	-1.13	3.23	0.015	948
	38	685	-707	1.03	1.52	1.57	1.29	0.97	-1.50	-1.13	3.23	0.016	971
	39	682	-705	1.03	1.52	1.57	1.29	0.97	-1.49	-1.12	3.23	0.016	993
	40	680	-703	1.03	1.51	1.56	1.29	0.97	-1.50	-1.13	3.22	0.015	1016
	41	678	-701	1.03	1.51	1.56	1.29	0.97	-1.50	-1.13	3.23	0.015	1038
	42	676	-701	1.04	1.50	1.56	1.29	0.97	-1.50	-1.13	3.22	0.015	1061
	43	676	-702	1.04	1.50	1.56	1.29	0.97	-1.50	-1.13	3.22	0.015	1083

Table 3.3 Specimen 3G Peak Response Quantities

Test	Cycle No.	T_{max}	P_{max}	β	ω	βω	Brace Deformations						η
							Longitudinal				Transverse		
							Tension		Compresion				
		(kips)	(kips)				(in.)	ε (%)	(in.)	ε (%)	(in.)	(rad.)	(Δ_{by})
Standard Loading Protocol	1	1130	-1020	0.90	1.12	1.01	0.51	0.35	-0.52	-0.36	0.43	0.002	5
	2	1049	-1047	1.00	1.04	1.04	0.50	0.35	-0.50	-0.35	0.41	0.002	9
	3	1070	-1061	0.99	1.06	1.05	0.49	0.34	-0.49	-0.34	0.42	0.002	13
	4	1090	-1070	0.98	1.08	1.06	0.48	0.33	-0.48	-0.33	0.41	0.002	17
	5	1099	-1077	0.98	1.09	1.07	0.48	0.33	-0.47	-0.33	0.41	0.002	21
	6	1103	-1079	0.98	1.09	1.07	0.48	0.33	-0.47	-0.33	0.41	0.002	25
	7	1201	-1210	1.01	1.19	1.20	0.85	0.59	-0.84	-0.58	1.03	0.005	35
	8	1235	-1238	1.00	1.22	1.22	0.84	0.58	-0.84	-0.58	1.05	0.005	45
	9	1256	-1253	1.00	1.24	1.24	0.83	0.57	-0.83	-0.57	1.04	0.005	55
	10	1259	-1243	0.99	1.25	1.23	0.76	0.53	-0.78	-0.54	1.04	0.005	64
	11	1336	-1377	1.03	1.32	1.36	1.37	0.95	-1.42	-0.98	2.07	0.010	83
	12	1380	-1401	1.02	1.36	1.39	1.35	0.93	-1.41	-0.98	2.08	0.010	102
	13	1398	-1411	1.01	1.38	1.40	1.35	0.93	-1.41	-0.98	2.08	0.010	121
	14	1402	-1414	1.01	1.39	1.40	1.35	0.93	-1.40	-0.97	2.07	0.010	140
	15	1451	-1511	1.04	1.44	1.49	2.01	1.39	-2.03	-1.41	3.10	0.016	170
	16	1489	-1528	1.03	1.47	1.51	2.01	1.39	-2.02	-1.40	3.10	0.016	199
	17	1530	-1606	1.05	1.51	1.59	2.51	1.74	-2.54	-1.76	4.11	0.021	237
	18	1562	-1620	1.04	1.55	1.60	2.50	1.73	-2.54	-1.76	4.11	0.021	275
High-Amplitude Protocol	19	1614	-1712	1.06	1.60	1.69	3.17	2.19	-3.11	-2.15	4.71	0.024	324
	20	1643	-1720	1.05	1.63	1.70	3.11	2.15	-3.11	-2.15	4.73	0.024	371
	21	1671	-1792	1.07	1.65	1.77	3.74	2.59	-3.69	-2.55	5.66	0.028	429
	22	1690	-1798	1.06	1.67	1.78	3.74	2.59	-3.69	-2.55	5.65	0.028	487
	23	1719	-1883	1.10	1.70	1.86	4.61	3.19	-4.52	-3.13	6.07	0.031	559
	24	1744	-1890	1.08	1.73	1.87	4.60	3.18	-4.52	-3.13	6.07	0.031	631

Table 3.4 Specimen 4G Peak Response Quantities

Test	Cycle No.	T_{max}	P_{max}	β	ω	βω	Brace Deformations						η
							Longitudinal				Transverse		
							Tension		Compresion				
		(kips)	(kips)				(in.)	ε (%)	(in.)	ε (%)	(in.)	(rad.)	(Δ_{by})
Standard Loading Protocol	1	1137	-1006	0.88	1.12	1.00	0.40	0.28	-0.41	-0.28	0.42	0.002	3
	2	1038	-1000	0.96	1.03	0.99	0.41	0.28	-0.40	-0.28	0.42	0.002	6
	3	1043	-999	0.96	1.03	0.99	0.40	0.28	-0.39	-0.27	0.41	0.002	8
	4	1053	-1010	0.96	1.04	1.00	0.39	0.27	-0.39	-0.27	0.42	0.002	11
	5	1042	-1001	0.96	1.03	0.99	0.38	0.26	-0.39	-0.27	0.41	0.002	13
	6	1047	-1015	0.97	1.04	1.00	0.38	0.26	-0.38	-0.26	0.41	0.002	15
	7	1171	-1157	0.99	1.16	1.14	0.76	0.53	-0.75	-0.52	1.04	0.005	24
	8	1215	-1190	0.98	1.20	1.18	0.75	0.52	-0.74	-0.51	1.04	0.005	32
	9	1236	-1207	0.98	1.22	1.19	0.74	0.51	-0.73	-0.51	1.04	0.005	41
	10	1252	-1217	0.97	1.24	1.20	0.74	0.51	-0.73	-0.51	1.05	0.005	49
	11	1348	-1372	1.02	1.33	1.36	1.40	0.97	-1.39	-0.96	2.08	0.010	68
	12	1387	-1382	1.00	1.37	1.37	1.29	0.89	-1.26	-0.87	2.08	0.010	85
	13	1411	-1391	0.99	1.40	1.38	1.29	0.89	-1.25	-0.87	2.09	0.011	103
	14	1417	-1395	0.98	1.40	1.38	1.29	0.89	-1.25	-0.87	2.09	0.011	120
	15	1470	-1496	1.02	1.45	1.48	1.95	1.35	-1.89	-1.31	3.10	0.016	148
	16	1500	-1501	1.00	1.48	1.48	1.85	1.28	-1.79	-1.24	3.11	0.016	174
	17	1546	-1594	1.03	1.53	1.58	2.49	1.72	-2.39	-1.65	4.11	0.021	211
	18	1584	-1611	1.02	1.57	1.59	2.48	1.72	-2.38	-1.65	4.12	0.021	247
High-Amplitude Protocol	19	1638	-1712	1.05	1.62	1.69	3.15	2.18	-2.96	-2.05	4.71	0.024	294
	20	1669	-1725	1.03	1.65	1.71	3.08	2.13	-2.96	-2.05	4.73	0.024	340
	21	1700	-1830	1.08	1.68	1.81	3.73	2.58	-3.53	-2.44	5.65	0.028	397
	22	1725	-1827	1.06	1.71	1.81	3.72	2.58	-3.53	-2.44	5.65	0.028	453
	23	1751	-1929	1.10	1.73	1.91	4.58	3.17	-4.36	-3.02	6.07	0.031	524
	24	1778	-1931	1.09	1.76	1.91	4.58	3.17	-4.34	-3.00	6.07	0.031	594
	25	1794	-2028	1.13	1.77	2.01	5.32	3.68	-5.05	-3.50	6.08	0.031	677
	26	1819	-2033	1.12	1.80	2.01	5.32	3.68	-4.96	-3.43	6.14	0.031	758

(a) Platen Bracket (East End)

(b) Wall Bracket (West End)

Figure 3.1 Specimen 1G: Gusset Bracket after Test

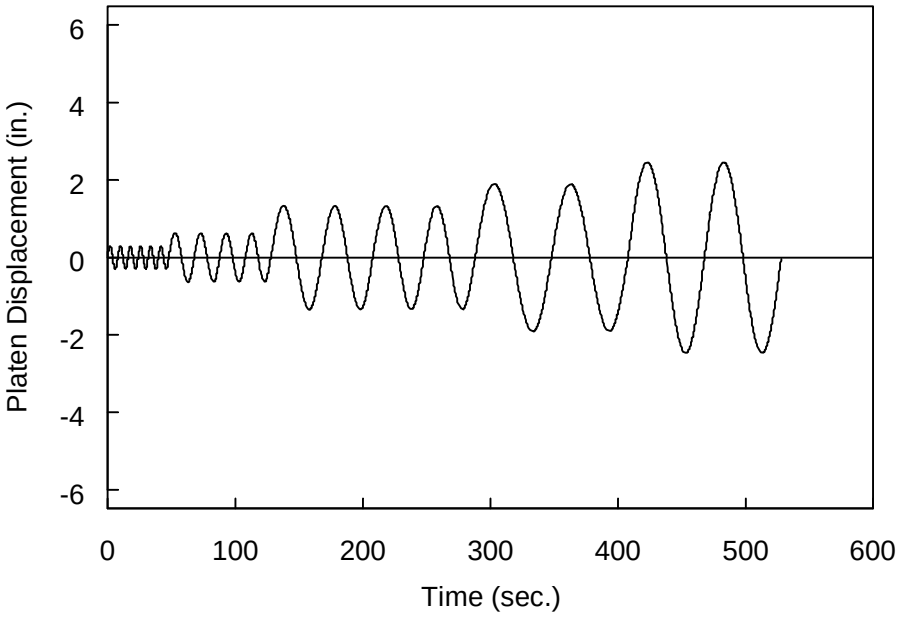

(a) Longitudinal Direction

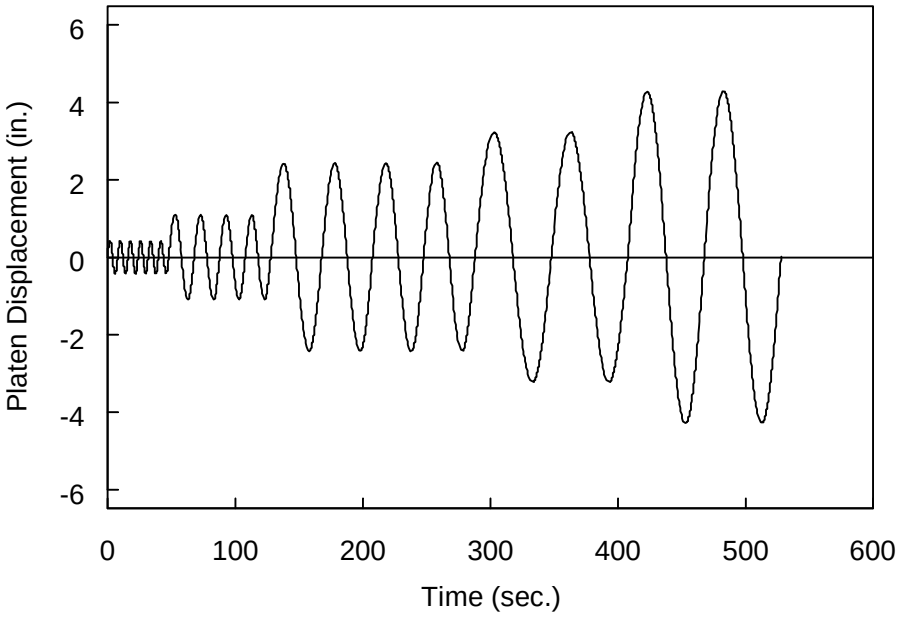

(b) Transverse Direction

Figure 3.2 Specimen 1G: Table Displacement Time Histories (Standard Protocol)

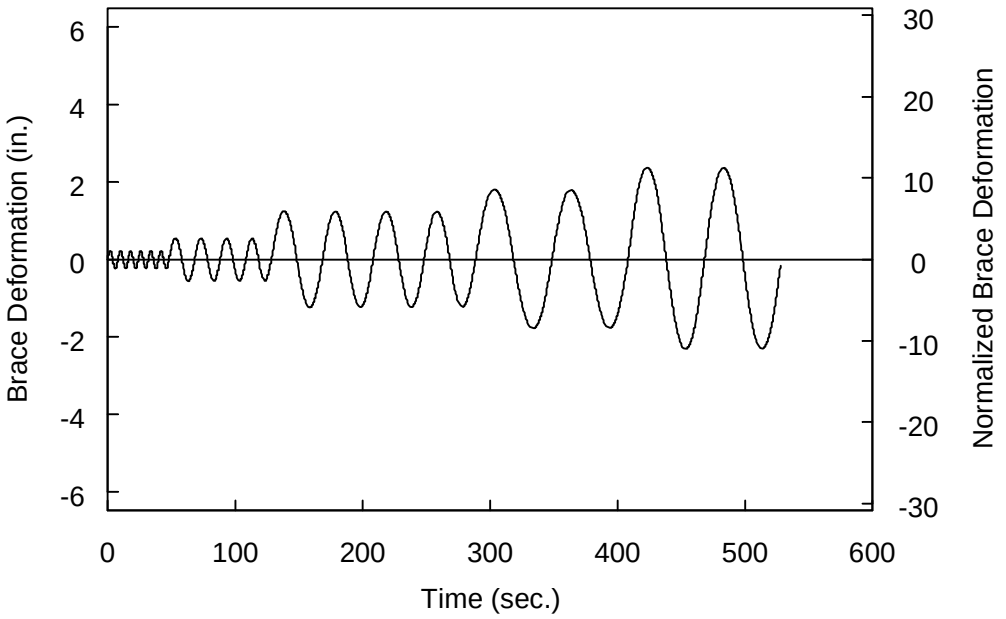

(a) Axial Direction

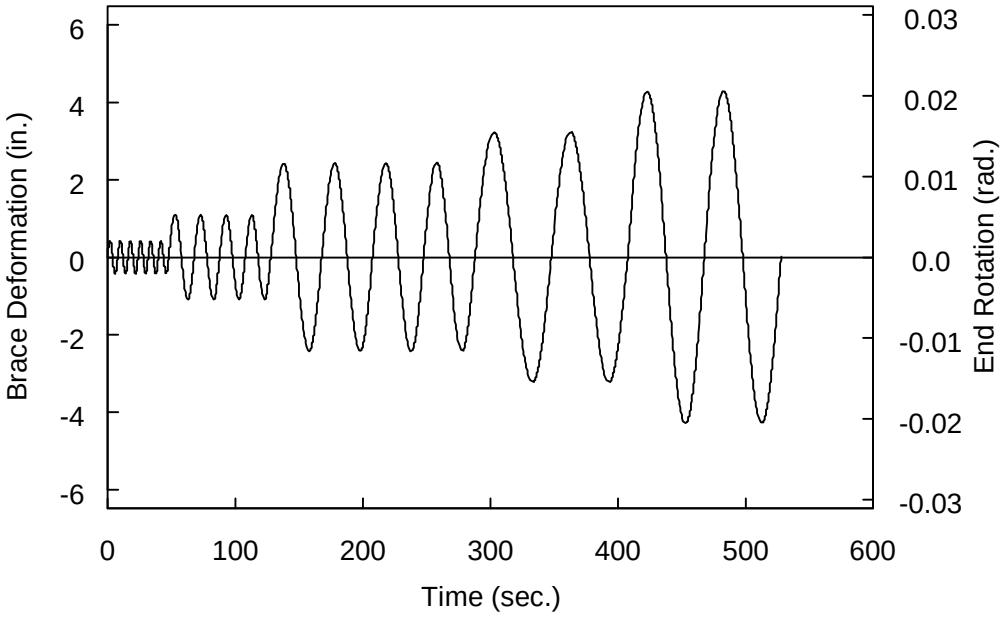

(b) Transverse Direction

Figure 3.3 Specimen 1G: Brace Deformation Time Histories (Standard Protocol)

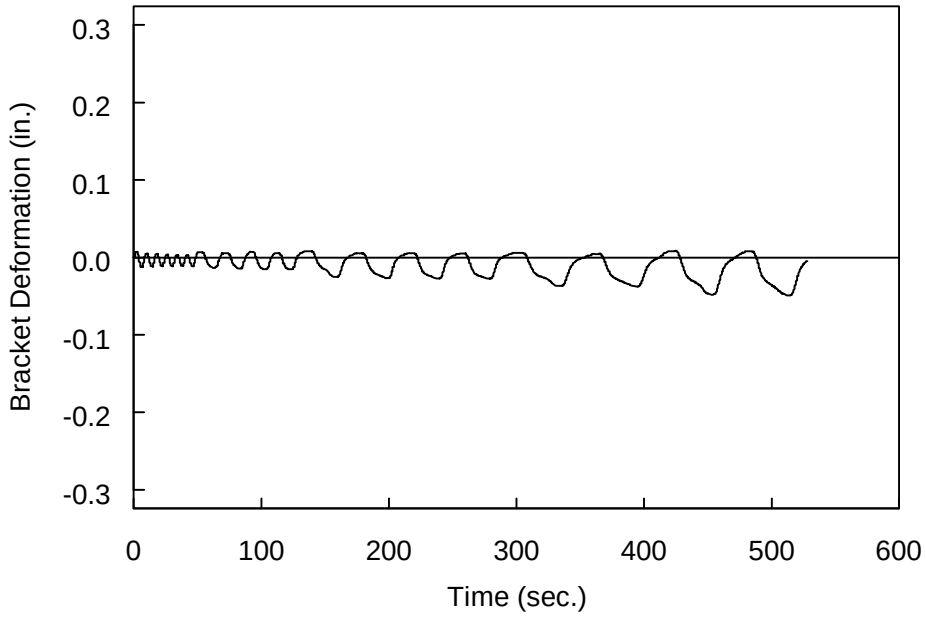

(a) Platen End Bracket

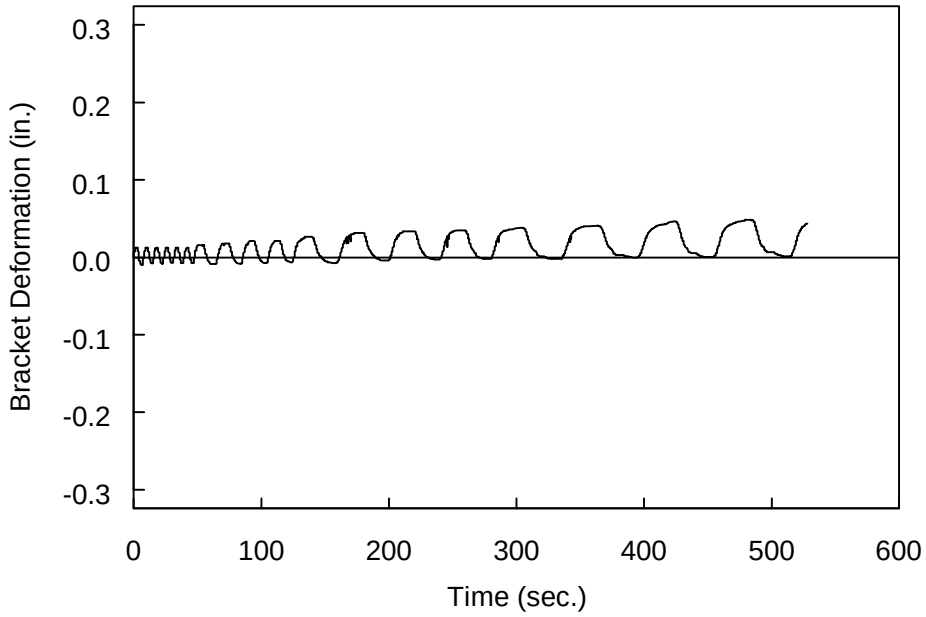

(b) Wall End Bracket

Figure 3.4 Specimen 1G: Bracket Deformation Time Histories (Standard Protocol)

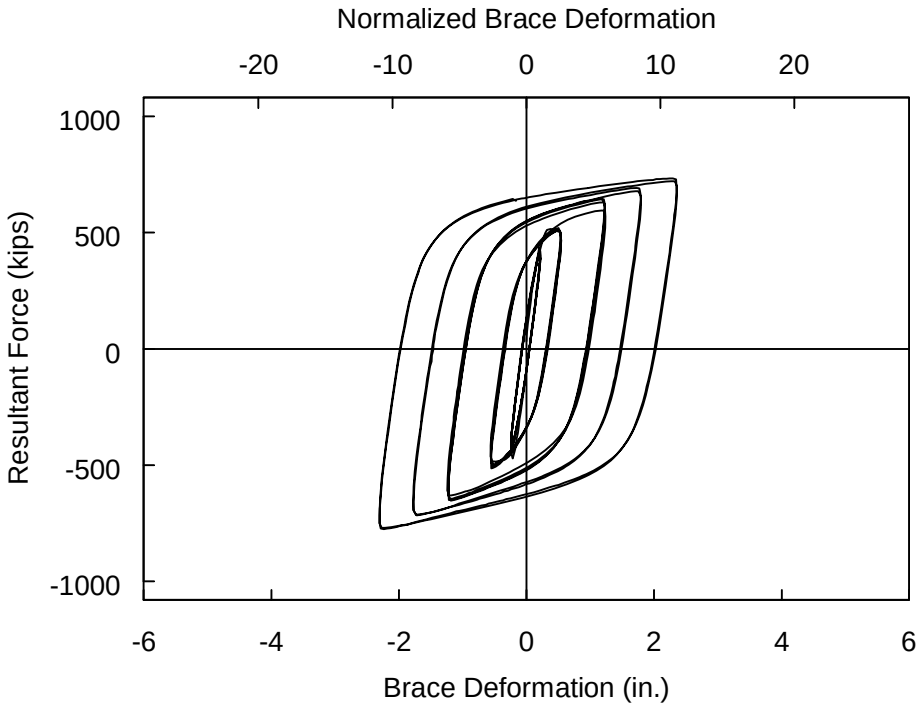

Figure 3.5 Specimen 1G: Brace Force versus Axial Deformation (Standard Protocol)

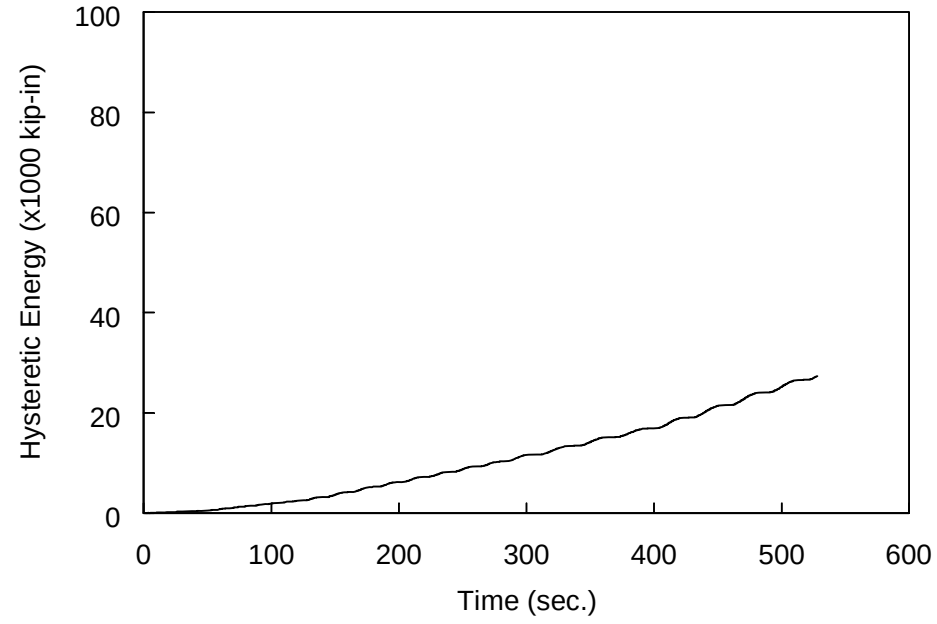

Figure 3.6 Specimen 1G: Hysteretic Energy Time History (Standard Protocol)

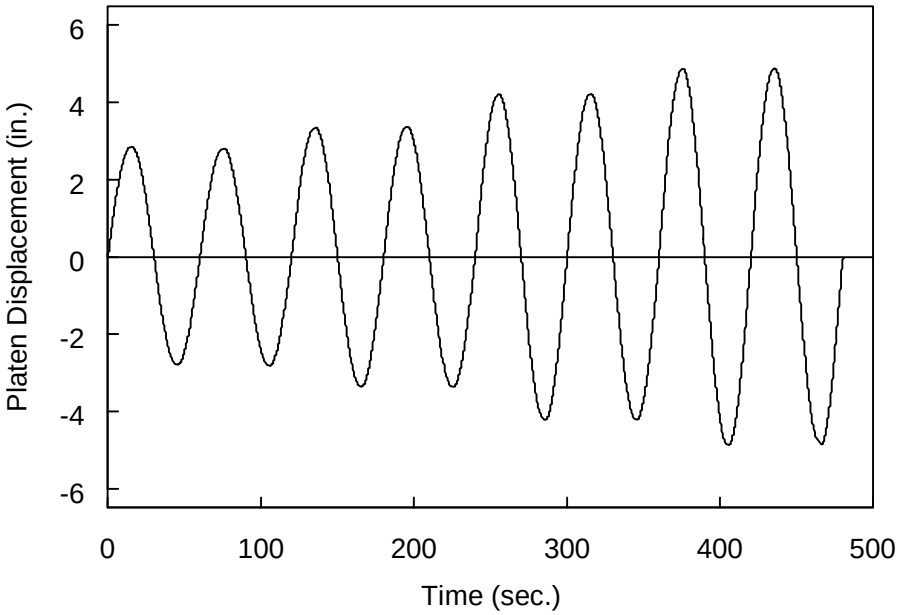

(a) Longitudinal Direction

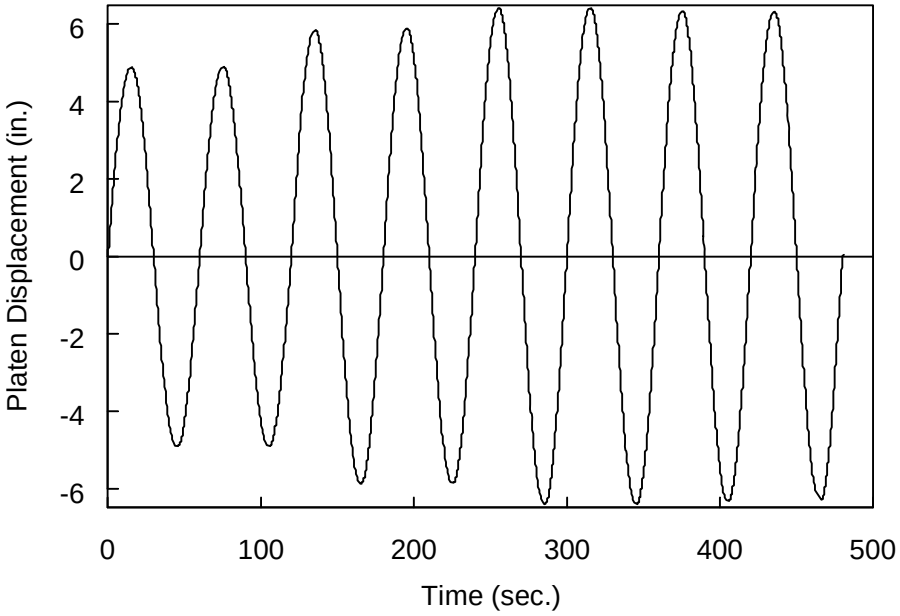

(b) Transverse Direction

Figure 3.7 Specimen 1G: Table Displacement Time Histories (High-Amplitude Protocol)

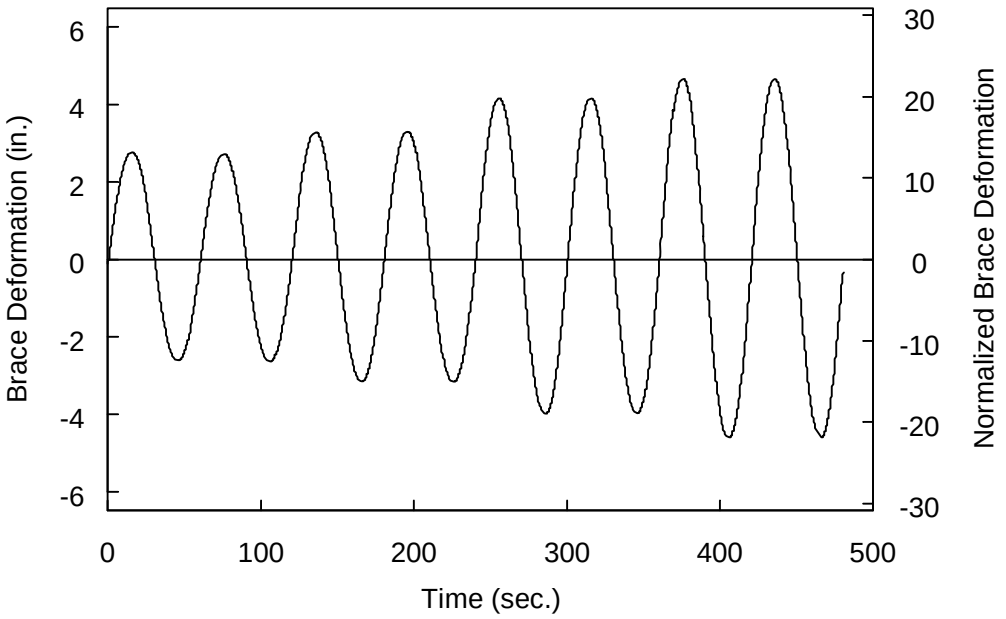

(a) Axial Direction

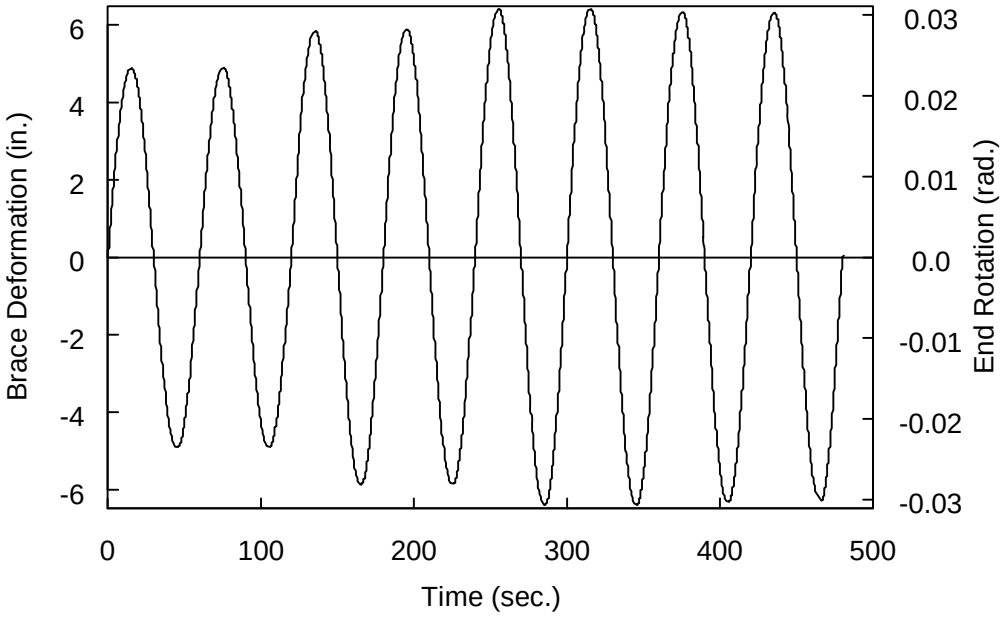

(b) Transverse Direction

Figure 3.8 Specimen 1G: Brace Deformation Time Histories (High-Amplitude Protocol)

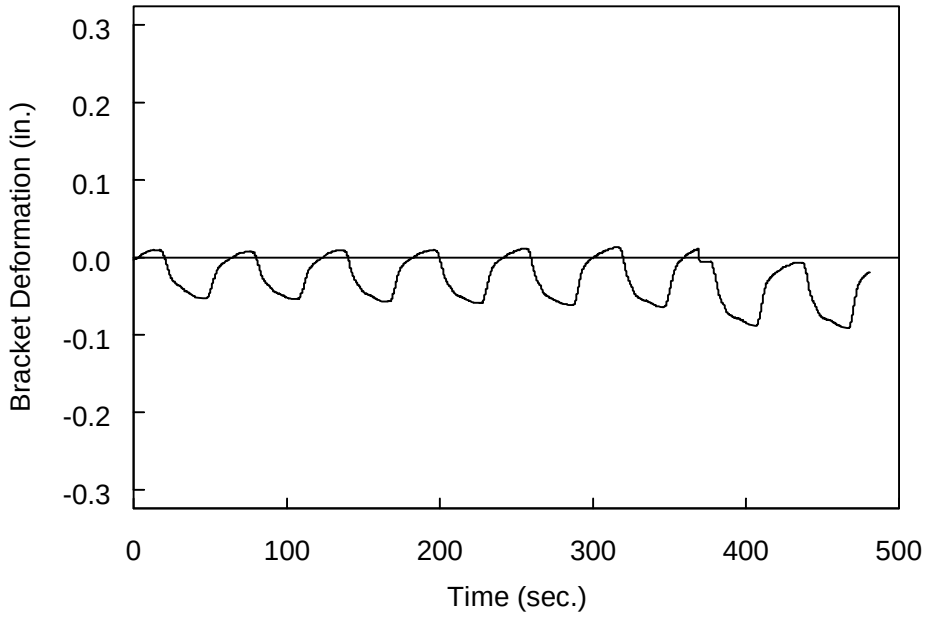

(a) Platen End Bracket

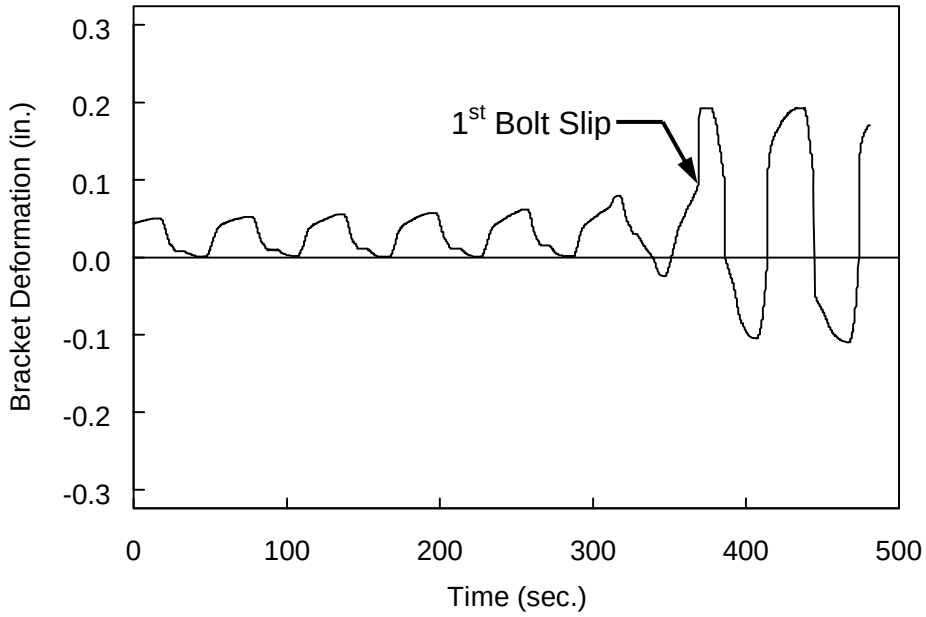

(b) Wall End Bracket

Figure 3.9 Specimen 1G: Bracket Deformation Time Histories (High-Amplitude Protocol)

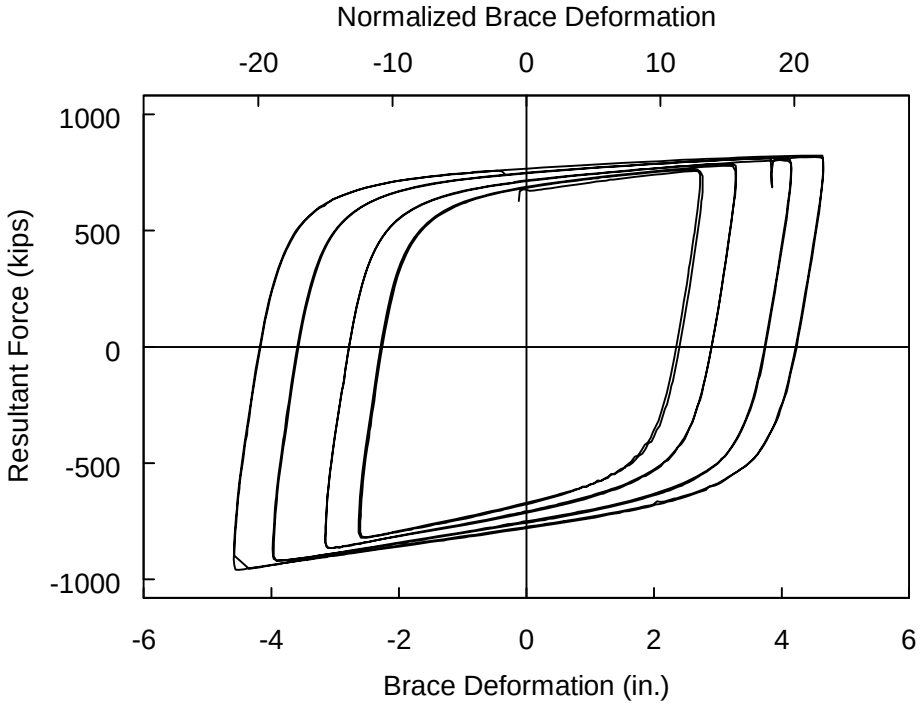

Figure 3.10 Specimen 1G: Brace Force versus Axial Deformation (High-Amplitude Protocol)

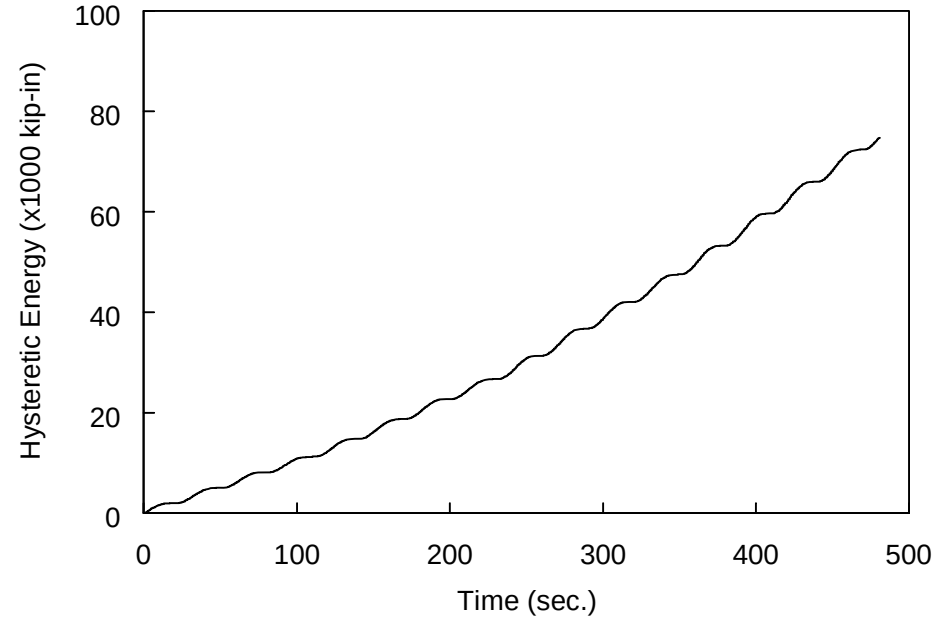

Figure 3.11 Specimen 1G: Hysteretic Energy Time History (High-Amplitude Protocol)

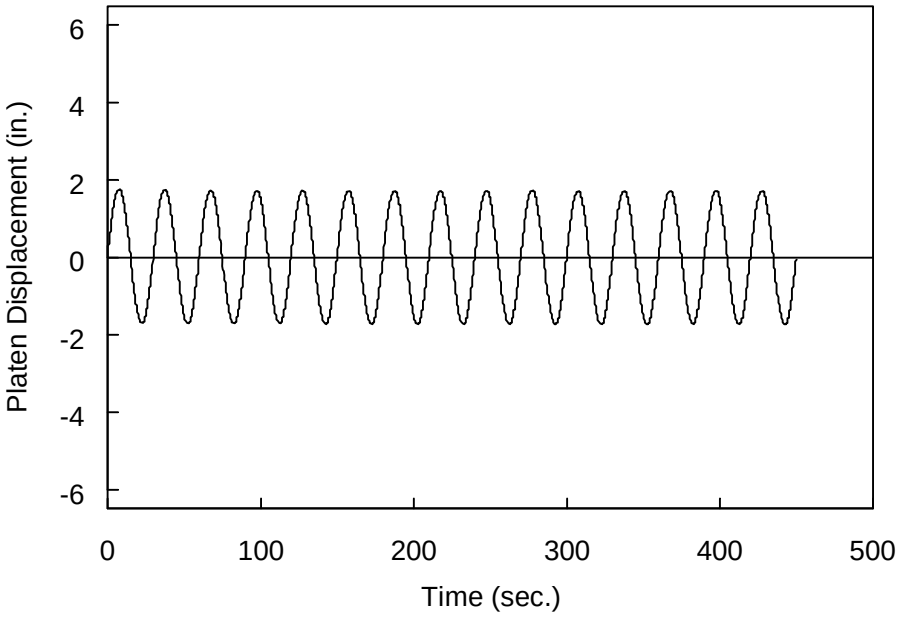

(a) Longitudinal Direction

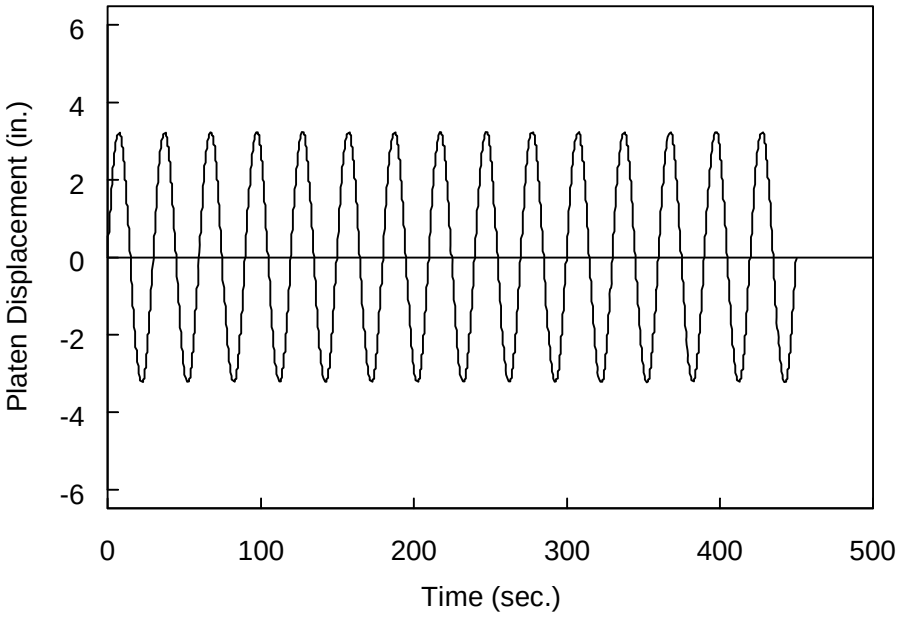

(b) Transverse Direction

Figure 3.12 Specimen 1G: Table Displacement Time Histories (Low-Cycle Fatigue Protocol)

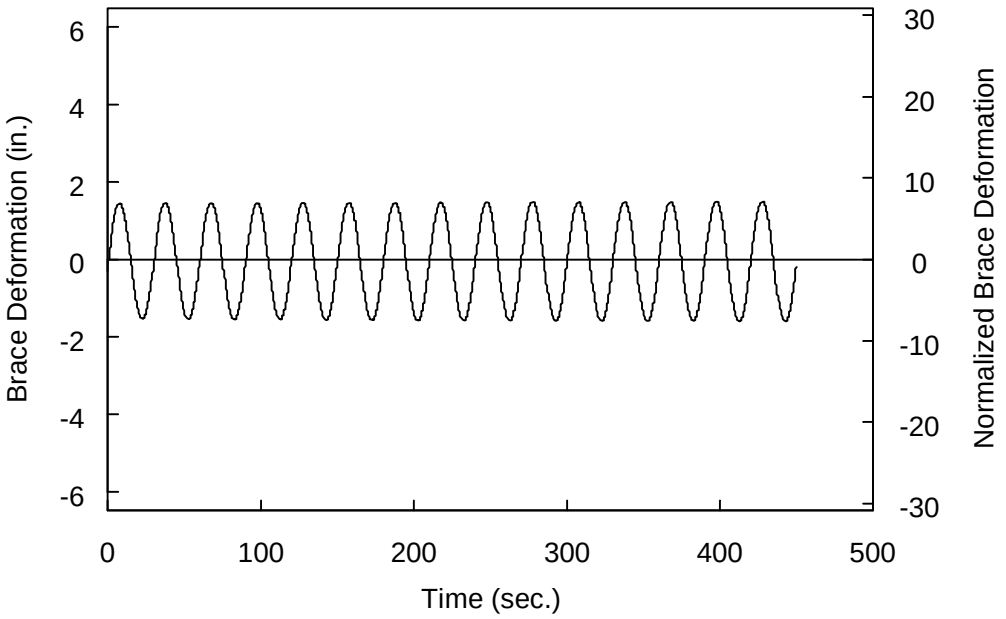

(a) Axial Direction

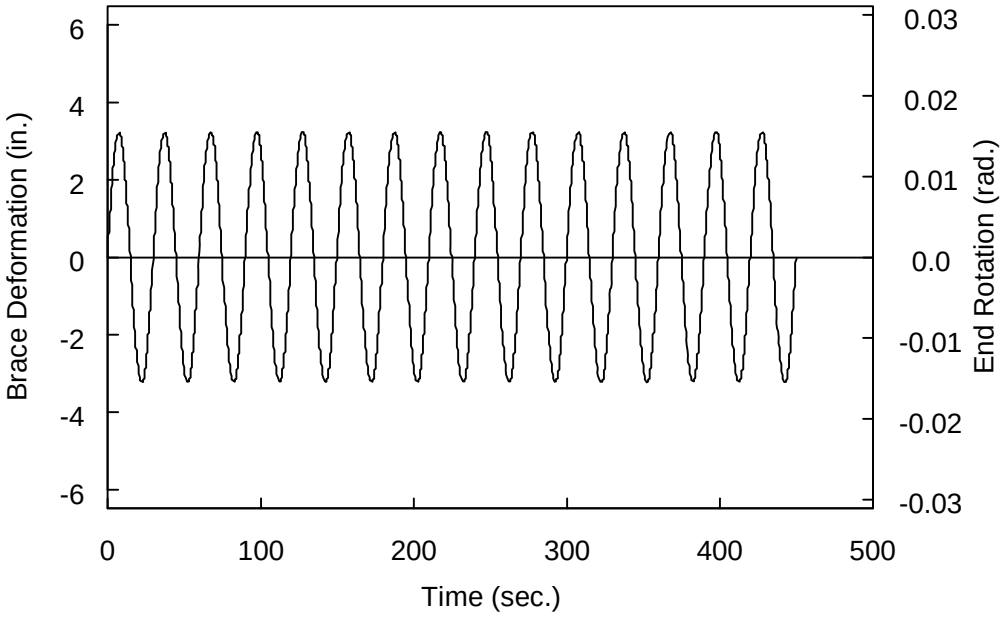

(b) Transverse Direction

Figure 3.13 Specimen 1G: Brace Deformation Time Histories (Low-Cycle Fatigue Protocol)

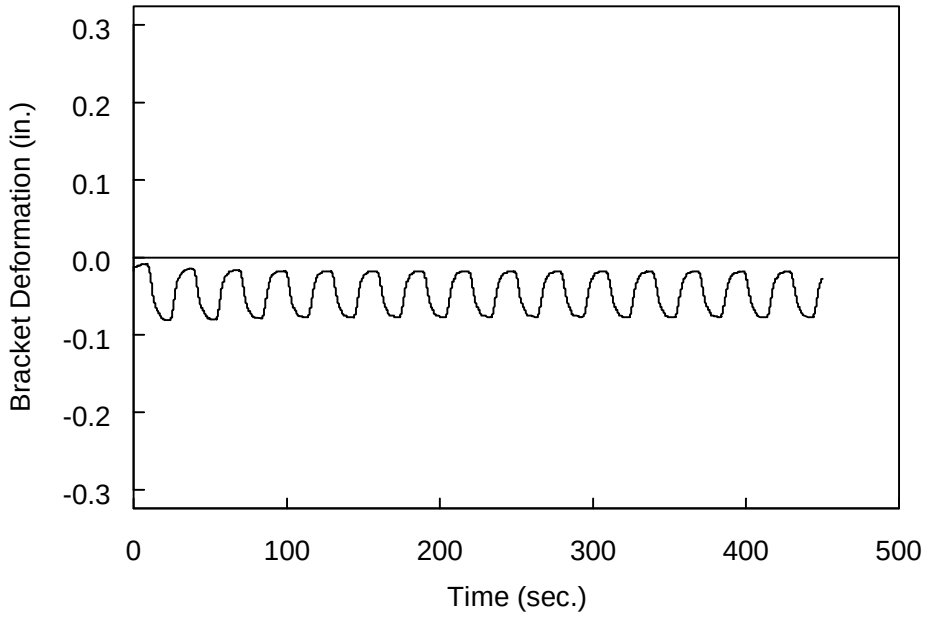

(a) Platen End Bracket

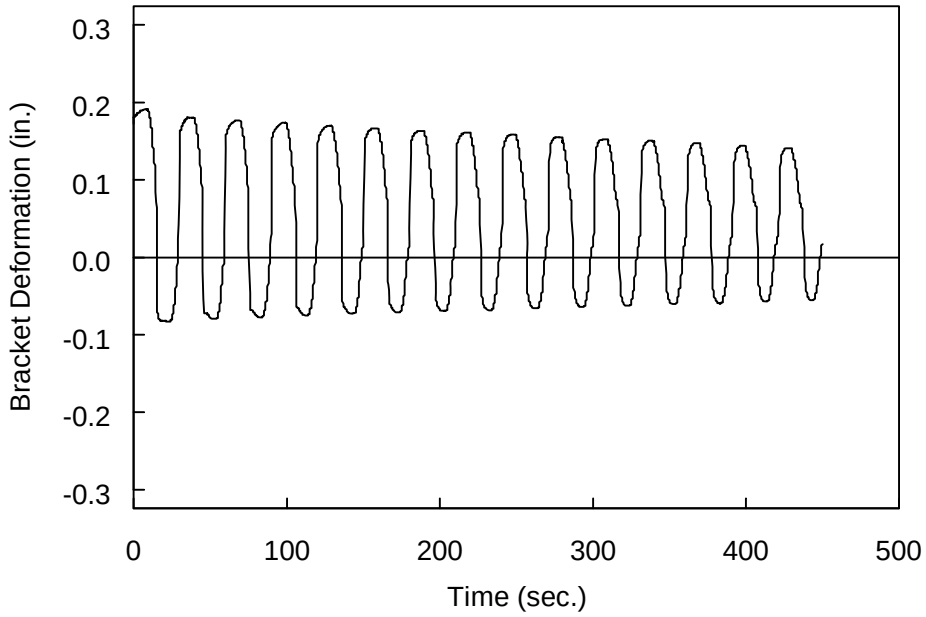

(b) Wall End Bracket

Figure 3.14 Specimen 1G: Bracket Deformation Time Histories (Low-Cycle Fatigue Protocol)

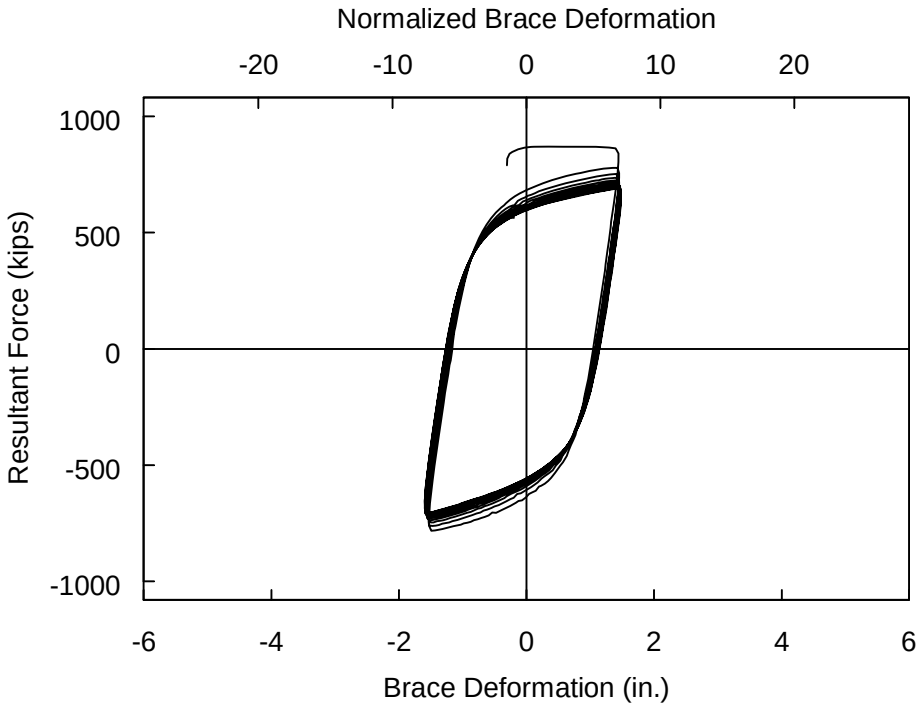

Figure 3.15 Specimen 1G: Brace Force versus Axial Deformation (Low-Cycle Fatigue Protocol)

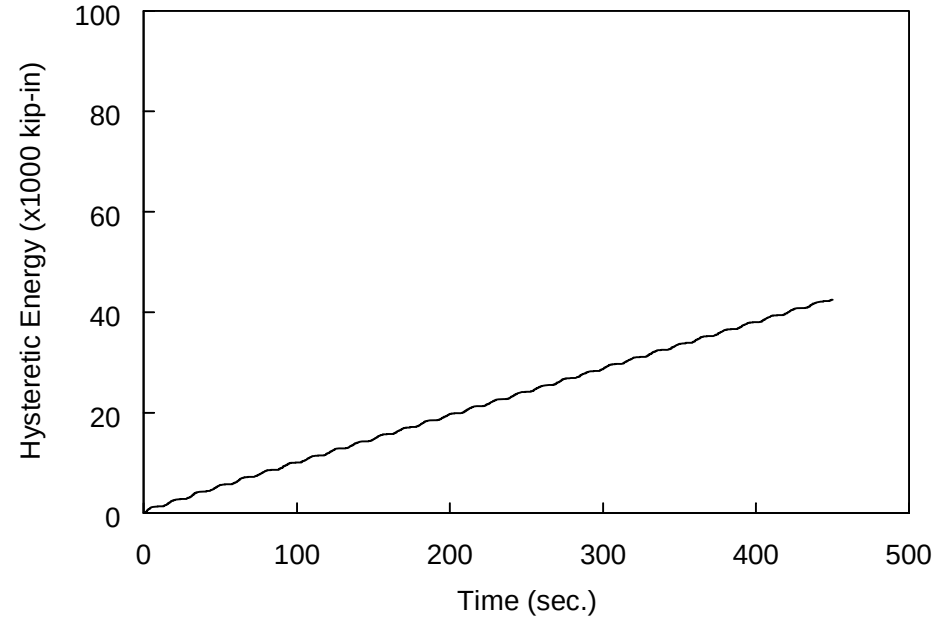

Figure 3.16 Specimen 1G: Hysteretic Energy Time History (Low-Cycle Fatigue Protocol)

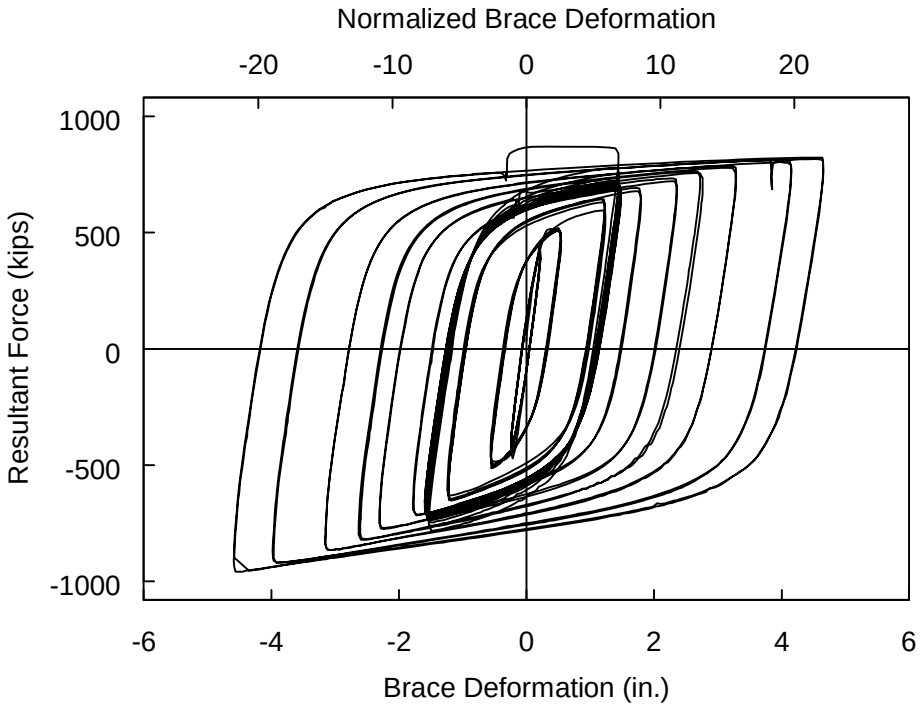

Figure 3.17 Specimen 1G: Brace Force versus Axial Deformation (All Cycles)

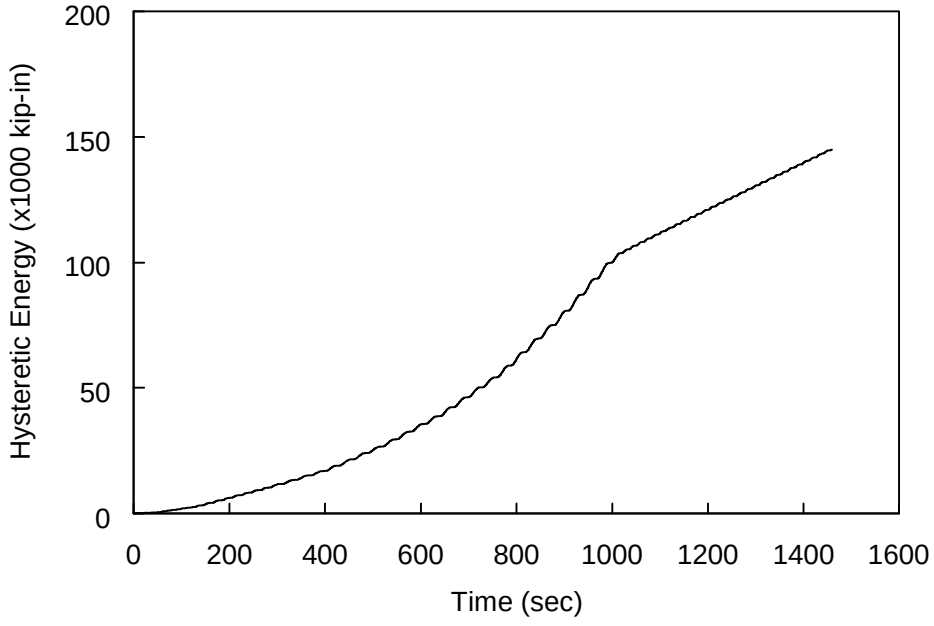

Figure 3.18 Specimen 1G: Hysteretic Energy Time History (All Cycles)

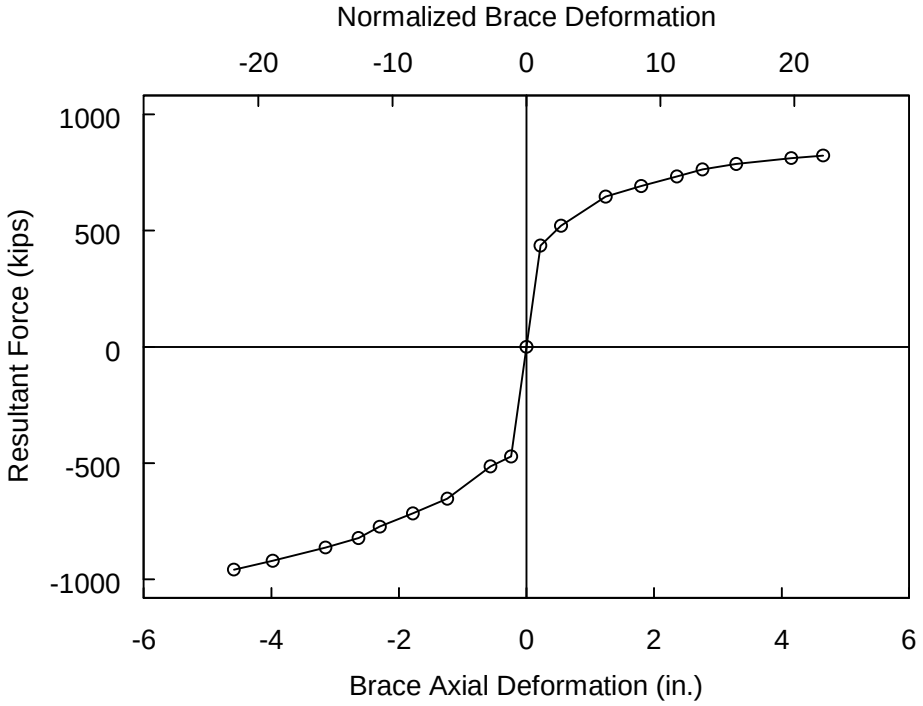

Figure 3.19 Specimen 1G: Brace Response Envelope

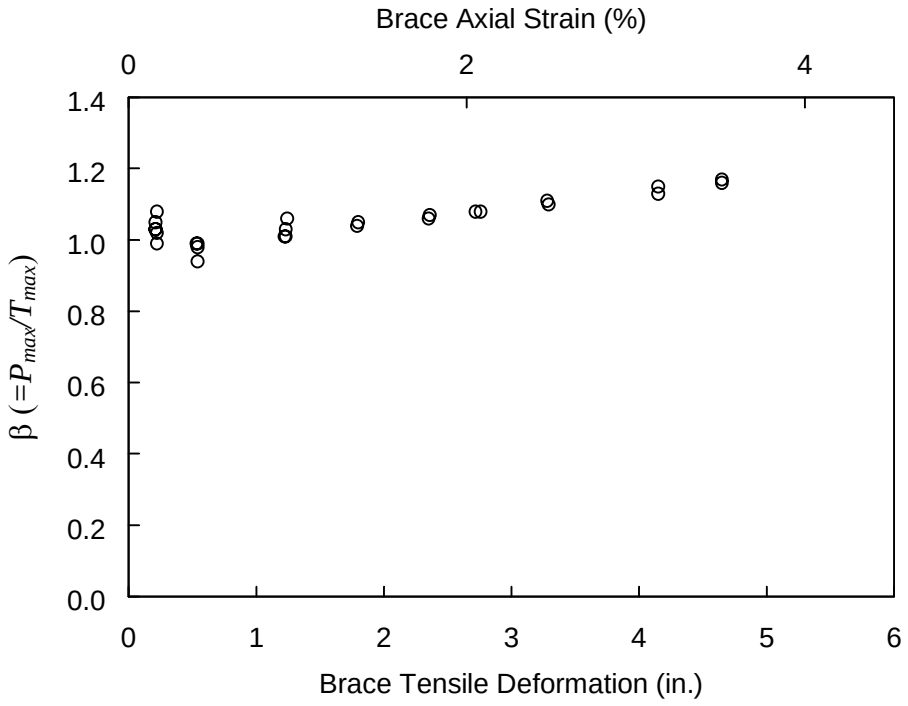

Figure 3.20 Specimen 1G: β versus Axial Deformation Level

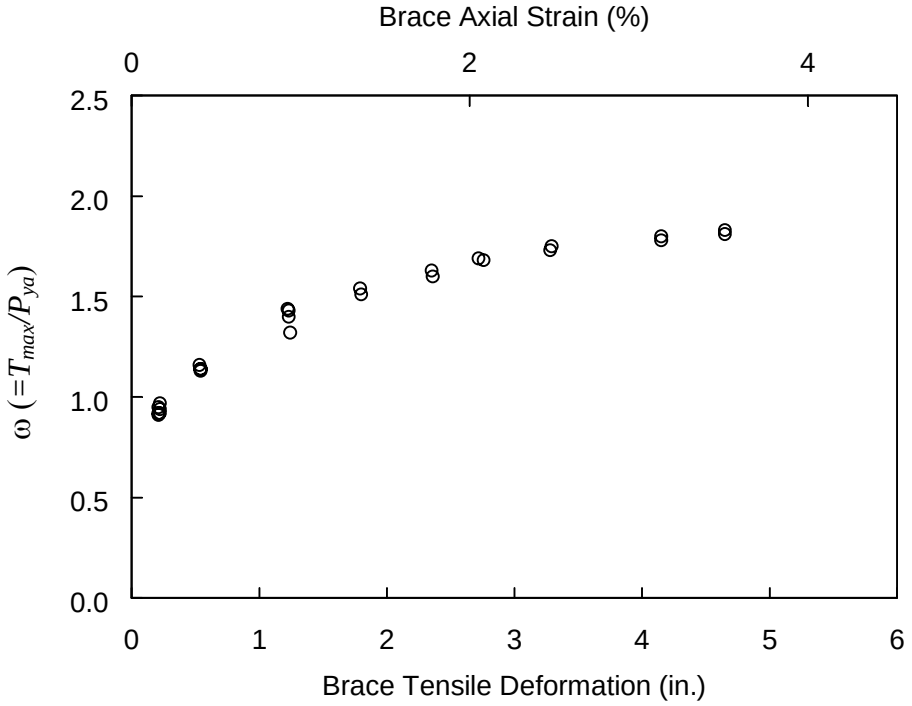

(a) Tension

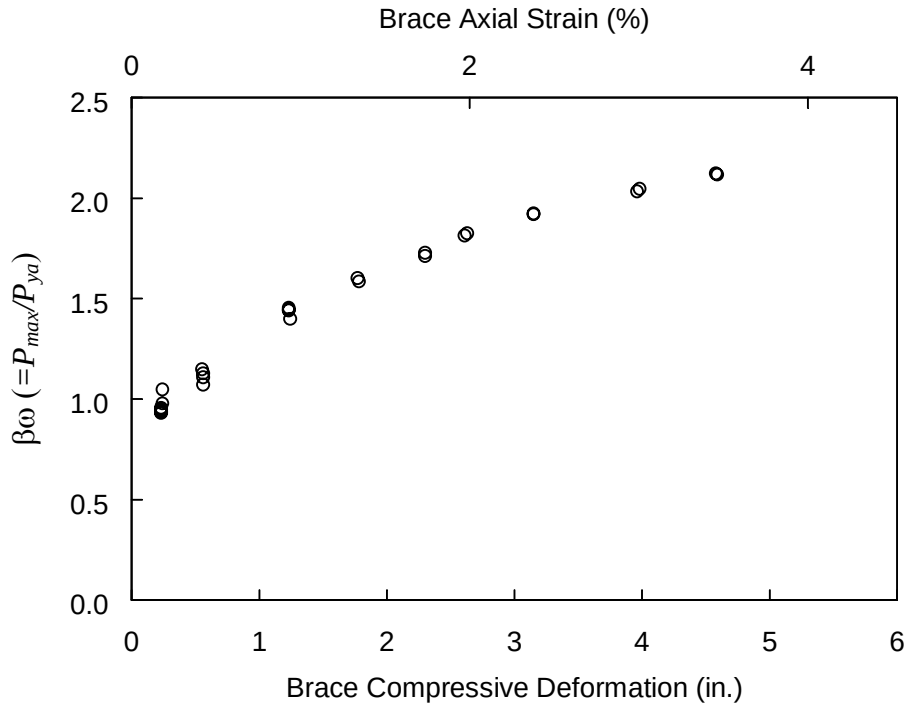

(b) Compression

Figure 3.21 Specimen 1G: ω and βω versus Axial Deformation Level

(a) Platen Bracket (East End)

(b) Wall Bracket (West End)

Figure 3.22 Specimen 2G: Gusset Bracket after Test

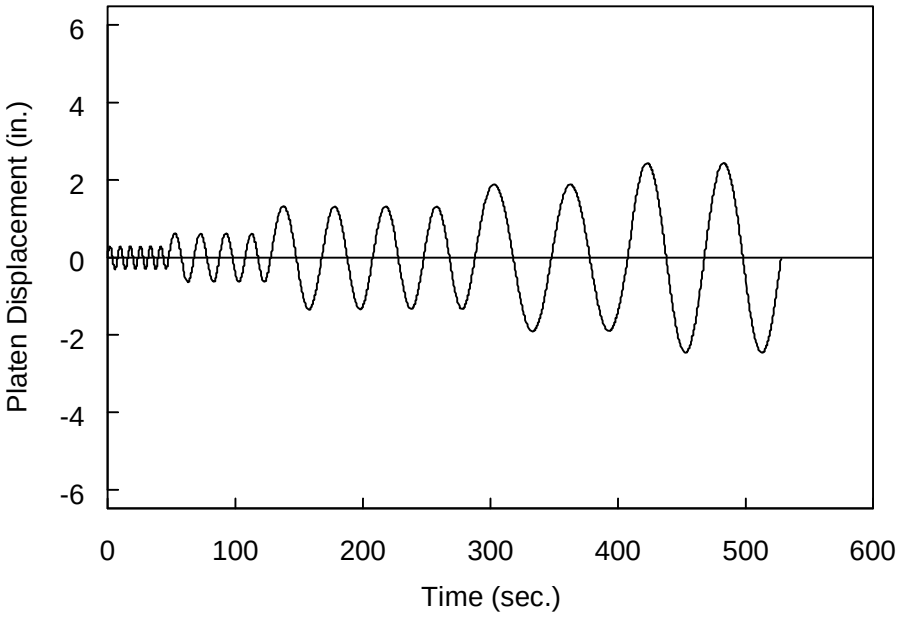

(a) Longitudinal Direction

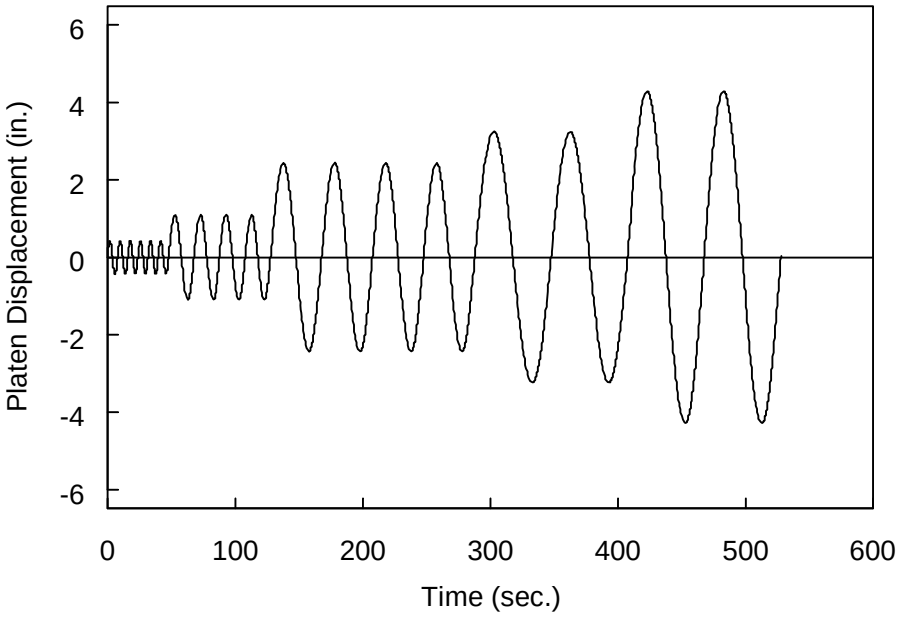

(b) Transverse Direction

Figure 3.23 Specimen 2G: Table Displacement Time Histories (Standard Protocol)

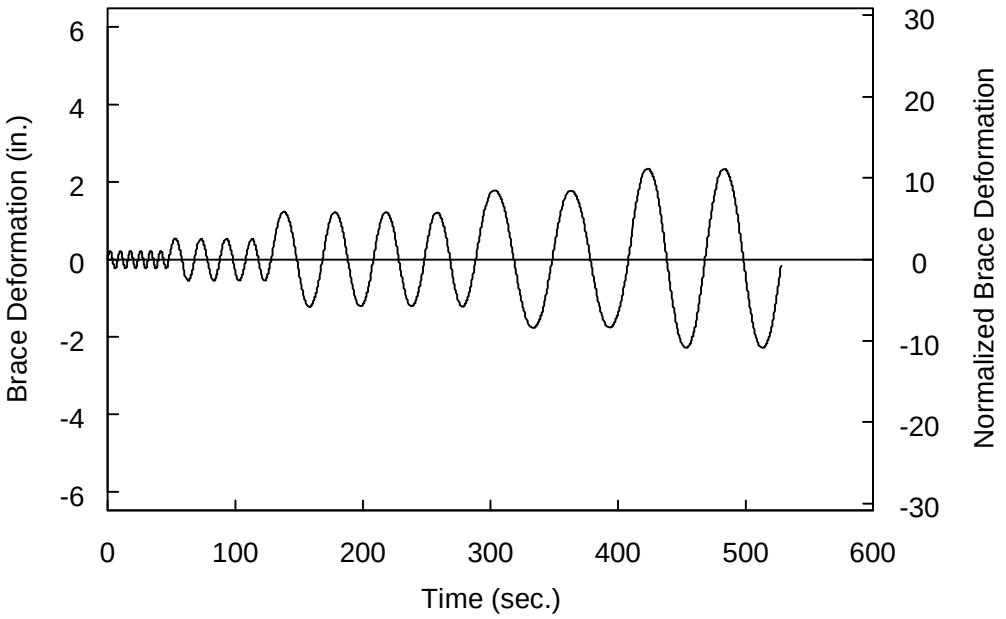

(a) Axial Direction

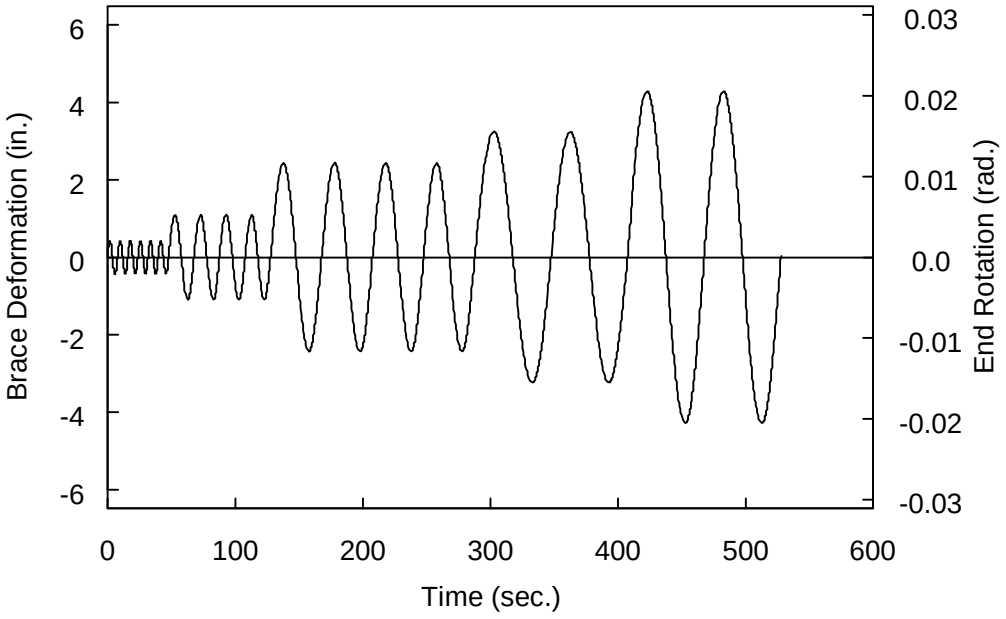

(b) Transverse Direction

Figure 3.24 Specimen 2G: Brace Deformation Time Histories (Standard Protocol)

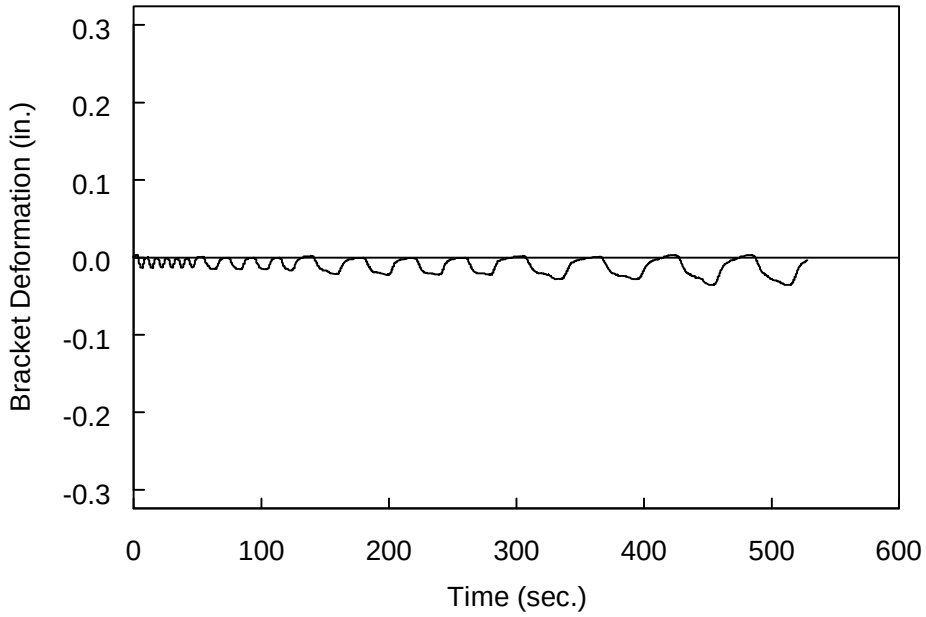

(a) Platen End Bracket

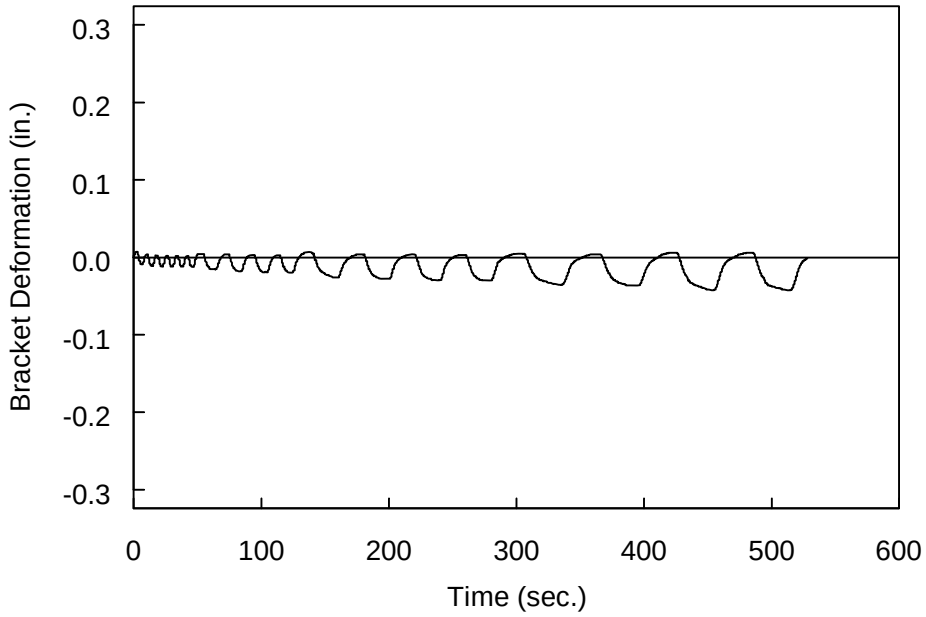

(b) Wall End Bracket

Figure 3.25 Specimen 2G: Bracket Deformation Time Histories (Standard Protocol)

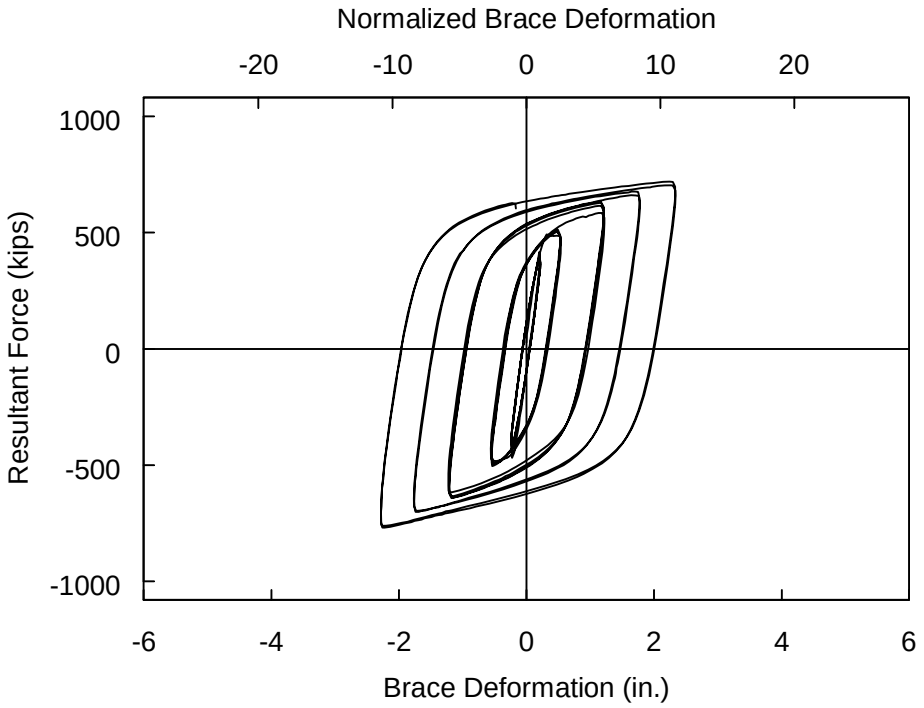

Figure 3.26 Specimen 2G: Brace Force versus Axial Deformation (Standard Protocol)

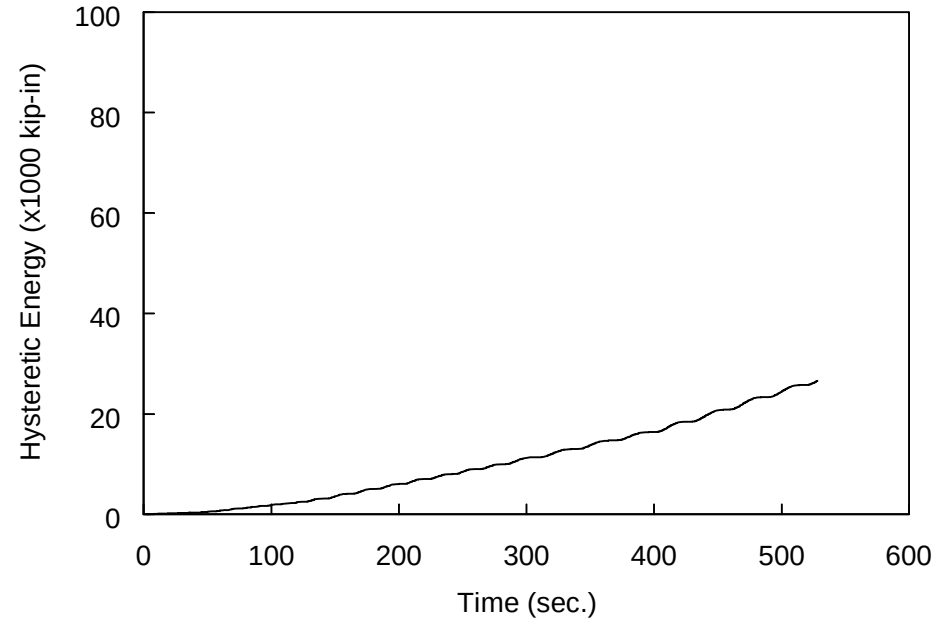

Figure 3.27 Specimen 2G: Hysteretic Energy Time History (Standard Protocol)

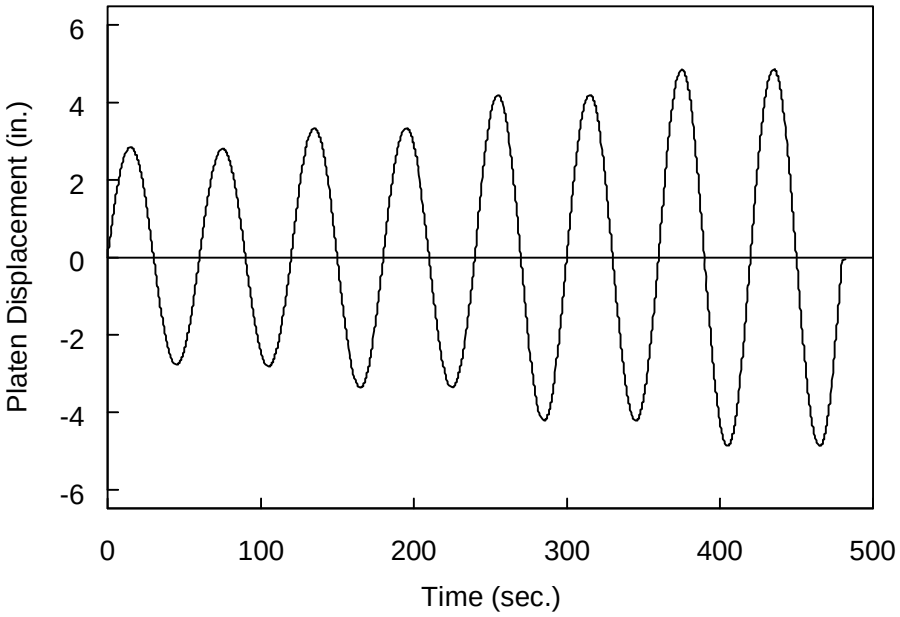

(a) Longitudinal Direction

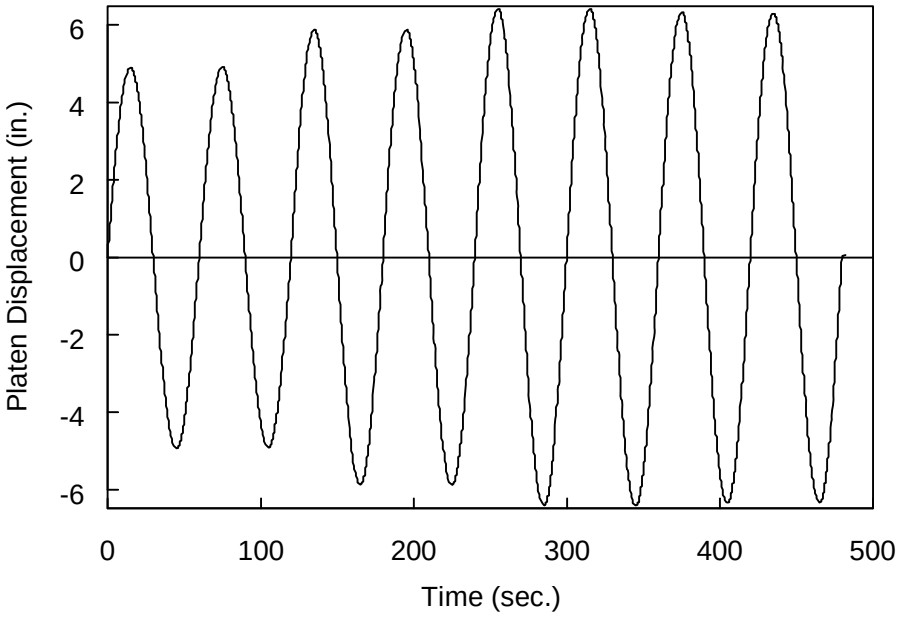

(b) Transverse Direction

Figure 3.28 Specimen 2G: Table Displacement Time Histories (High-Amplitude Protocol)

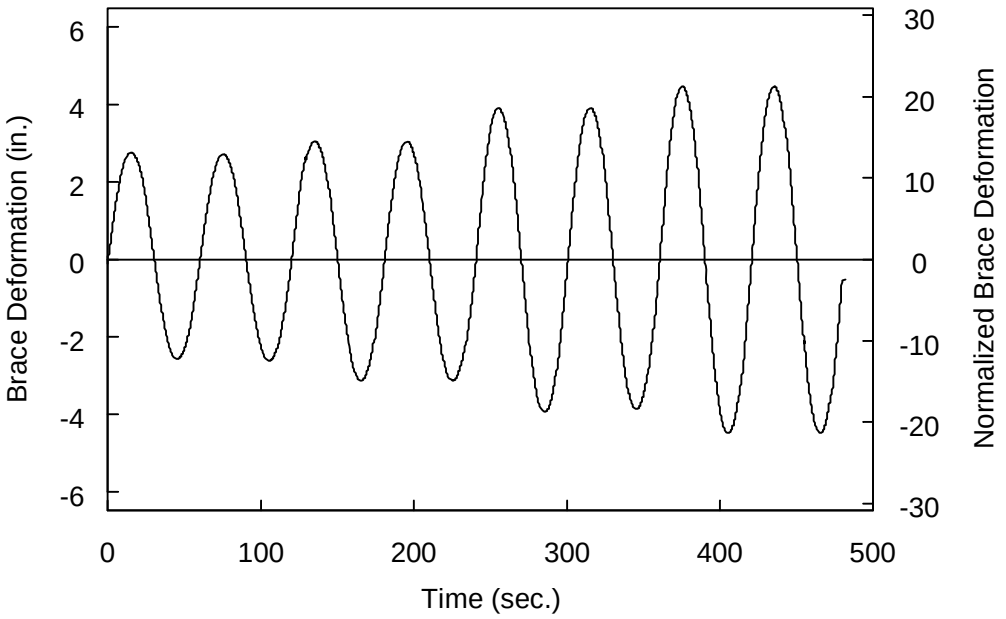

(a) Axial Direction

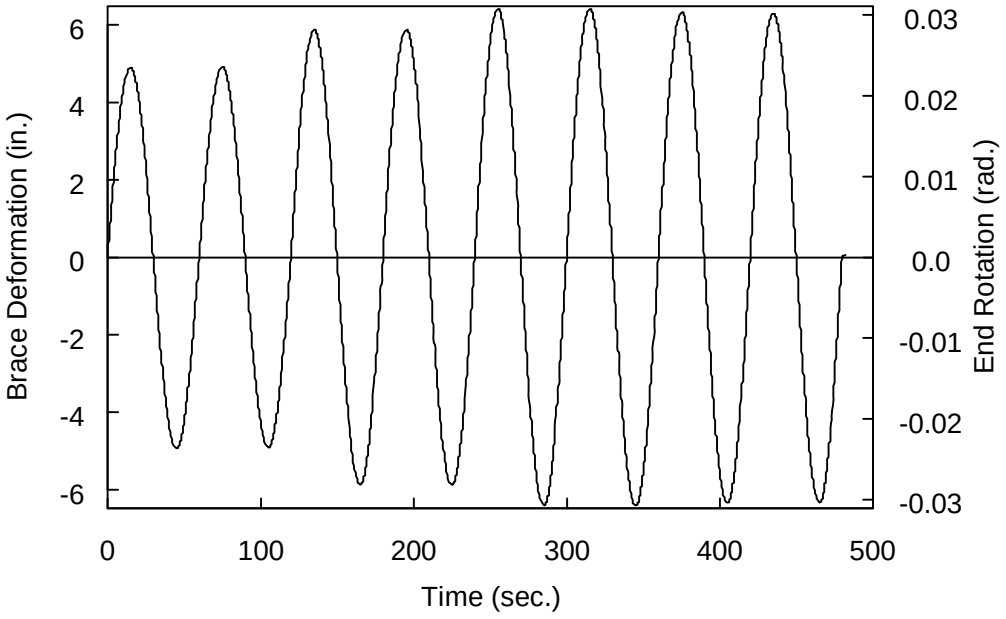

(b) Transverse Direction

Figure 3.29 Specimen 2G: Brace Deformation Time Histories (High-Amplitude Protocol)

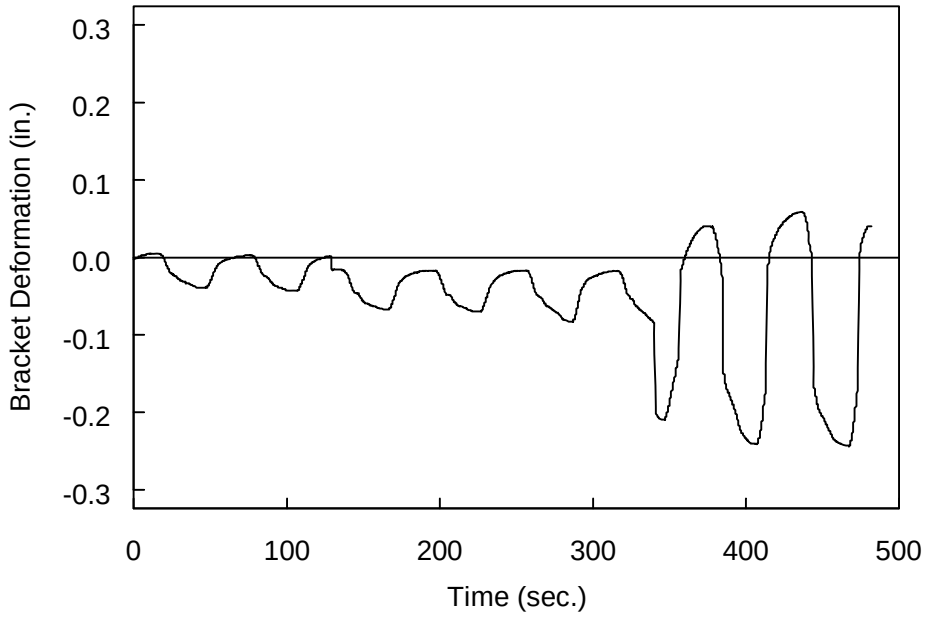

(a) Platen End Bracket

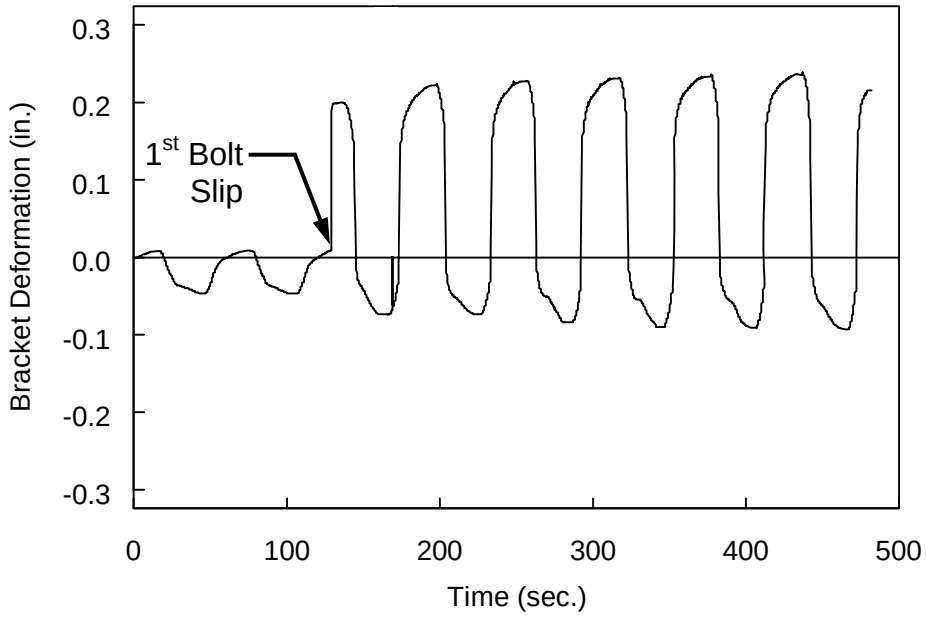

(b) Wall End Bracket

Figure 3.30 Specimen 2G: Bracket Deformation Time Histories (High-Amplitude Protocol)

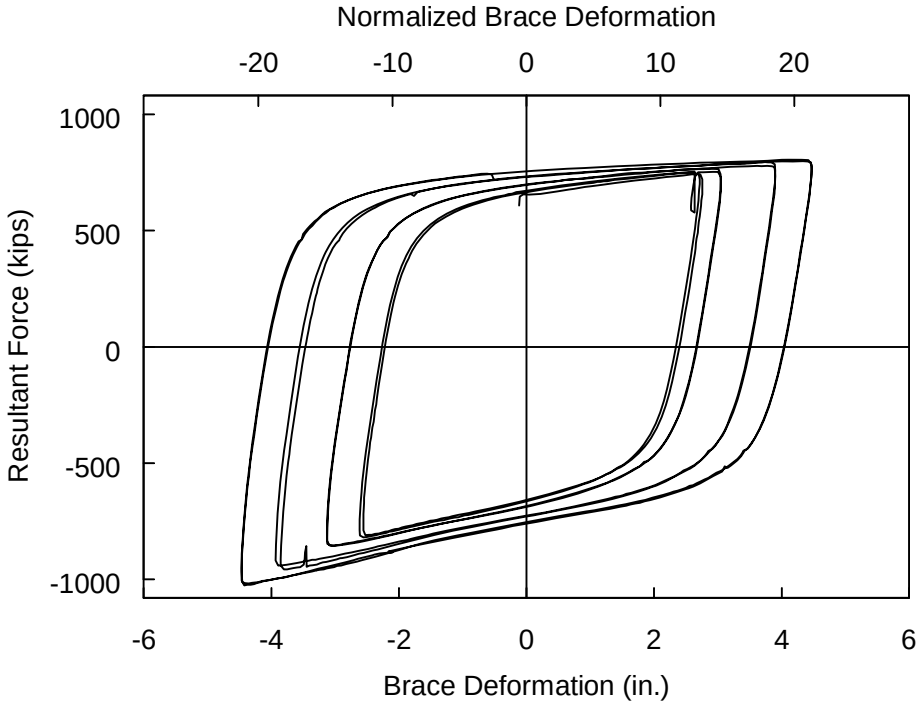

Figure 3.31 Specimen 2G: Brace Force versus Axial Deformation (High-Amplitude Protocol)

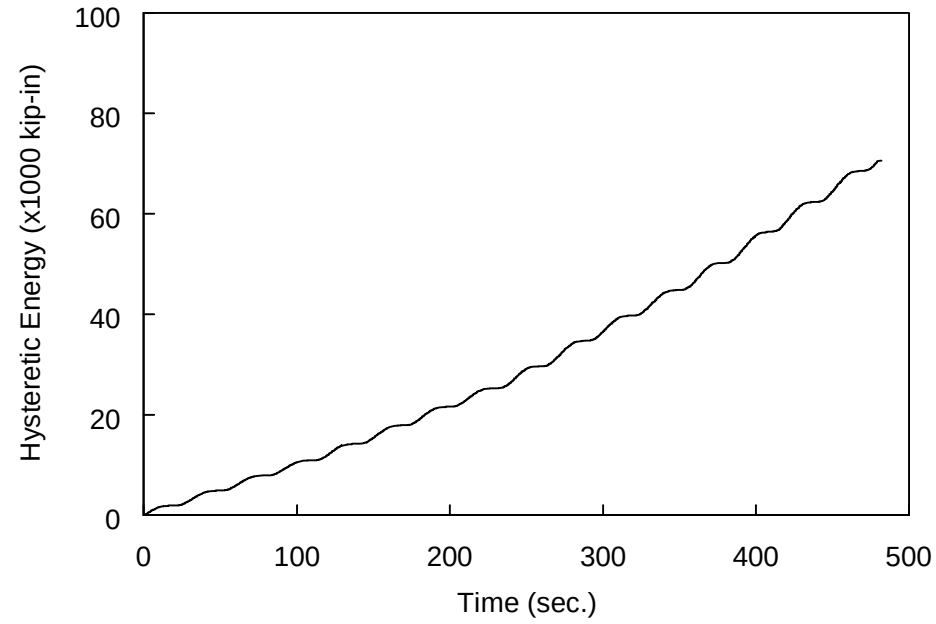

Figure 3.32 Specimen 2G: Hysteretic Energy Time History (High-Amplitude Protocol)

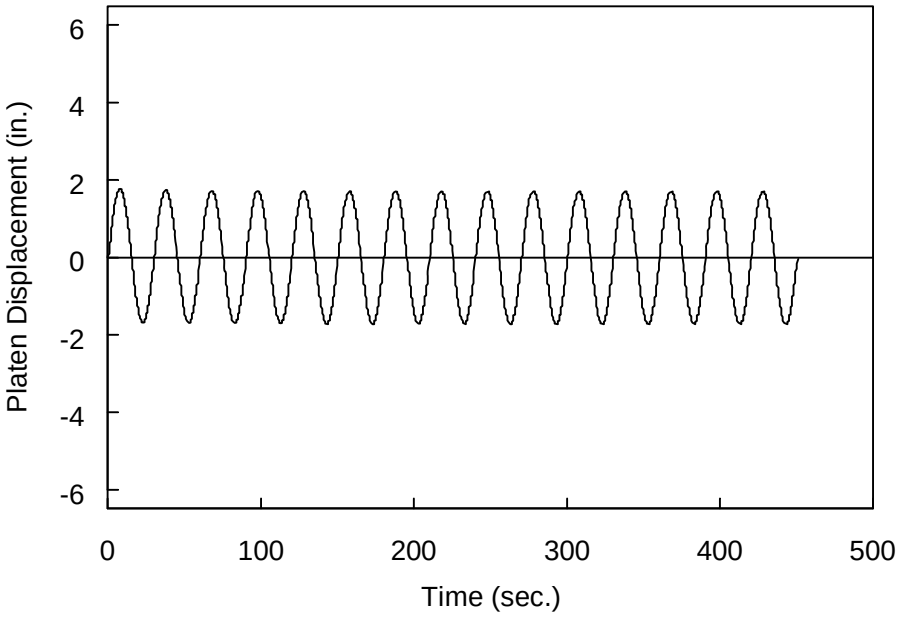

(a) Longitudinal Direction

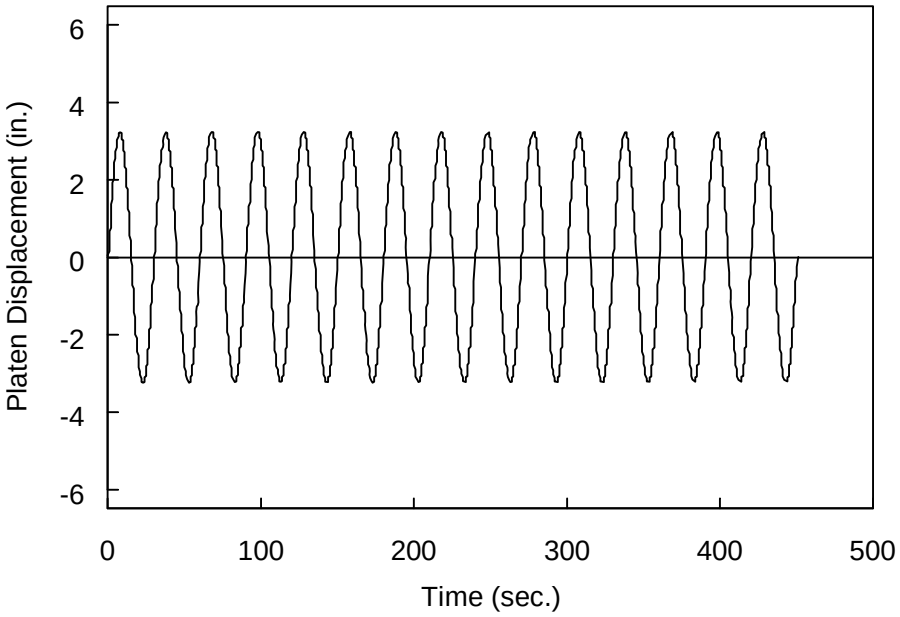

(b) Transverse Direction

Figure 3.33 Specimen 2G: Table Displacement Time Histories (Low-Cycle Fatigue Protocol)

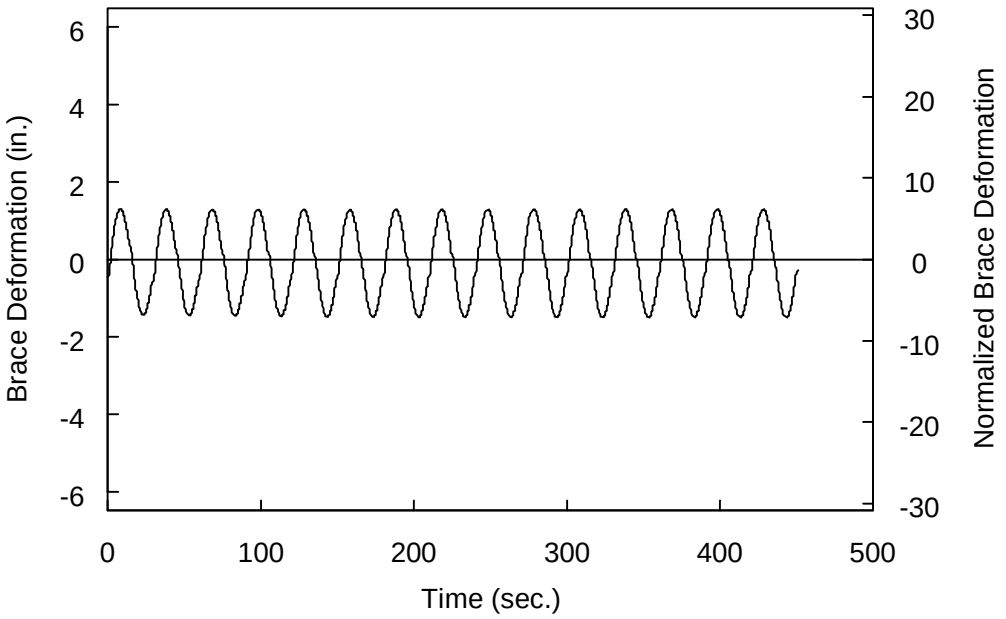

(a) Axial Direction

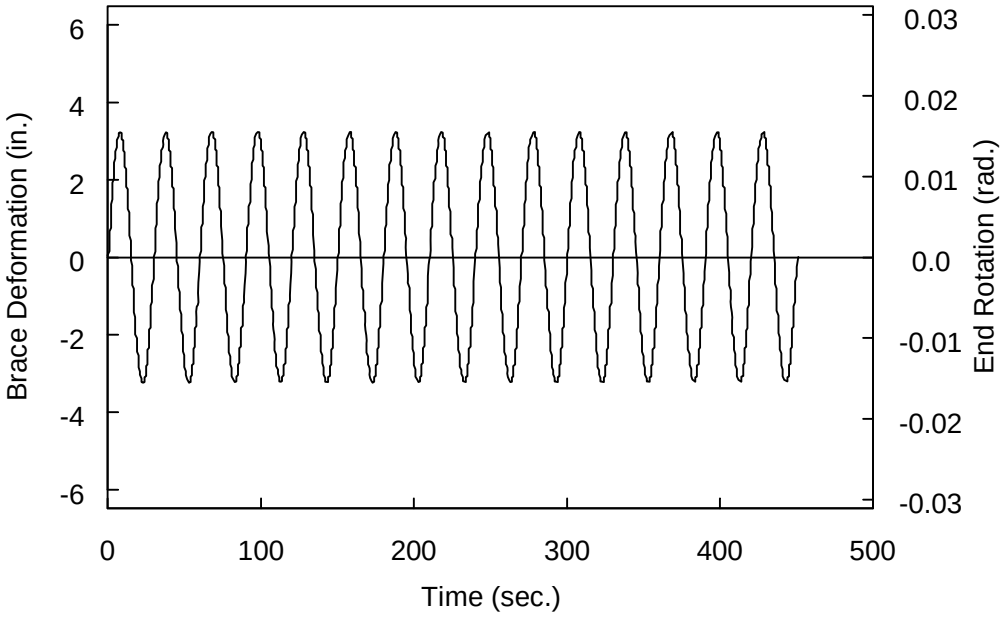

(b) Transverse Direction

Figure 3.34 Specimen 2G: Brace Deformation Time Histories (Low-Cycle Fatigue Protocol)

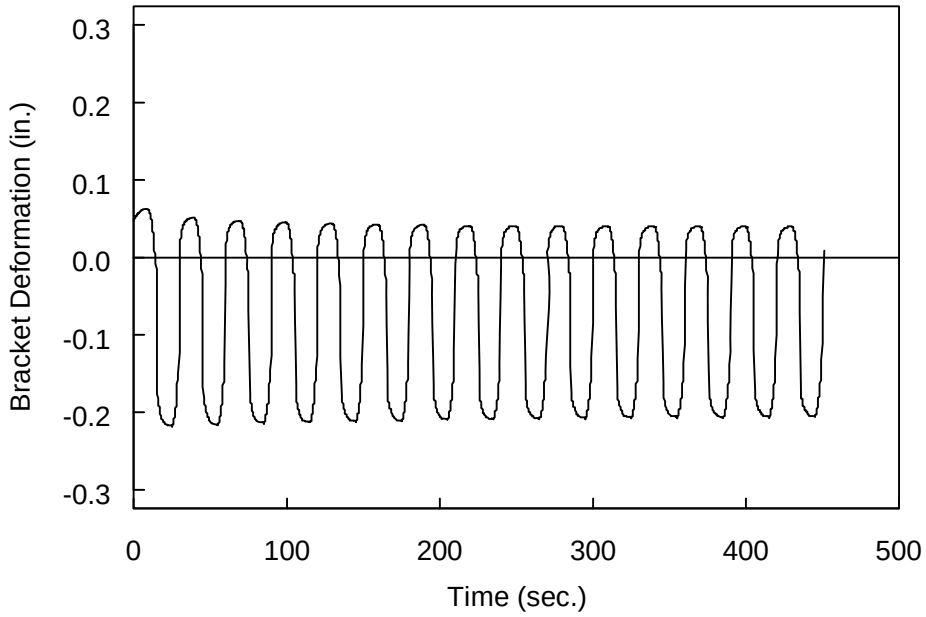

(a) Platen End Bracket

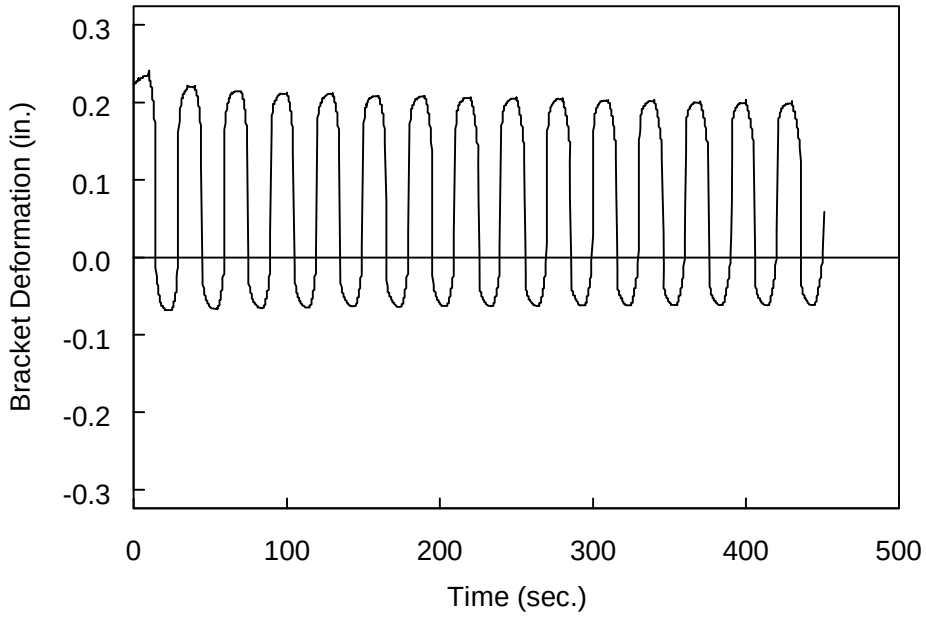

(b) Wall End Bracket

Figure 3.35 Specimen 2G: Bracket Deformation Time Histories (Low-Cycle Fatigue Protocol)

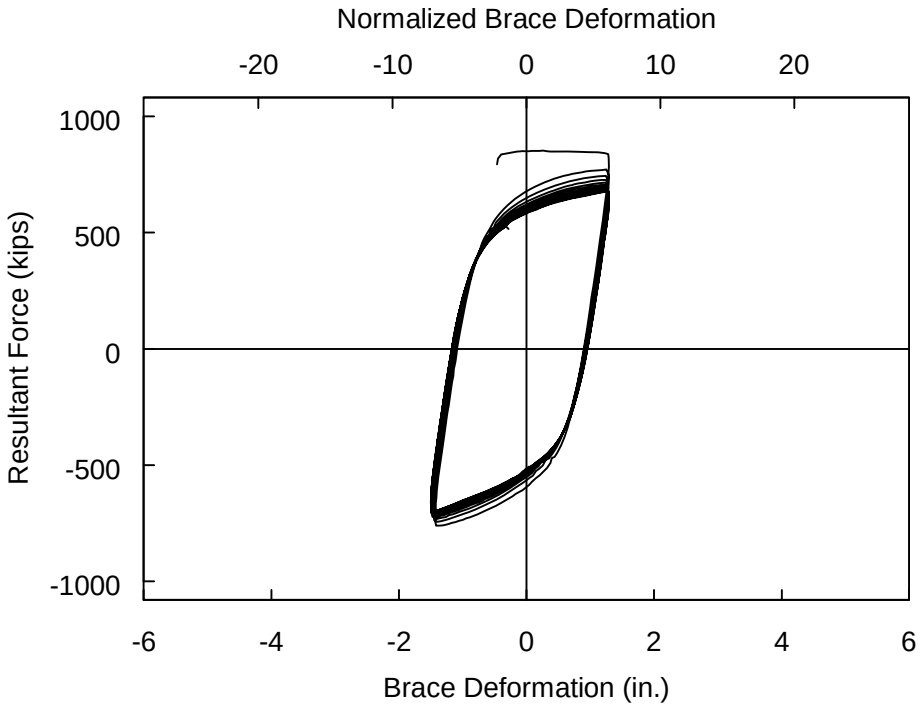

Figure 3.36 Specimen 2G: Brace Force versus Axial Deformation (Low-Cycle Fatigue Protocol)

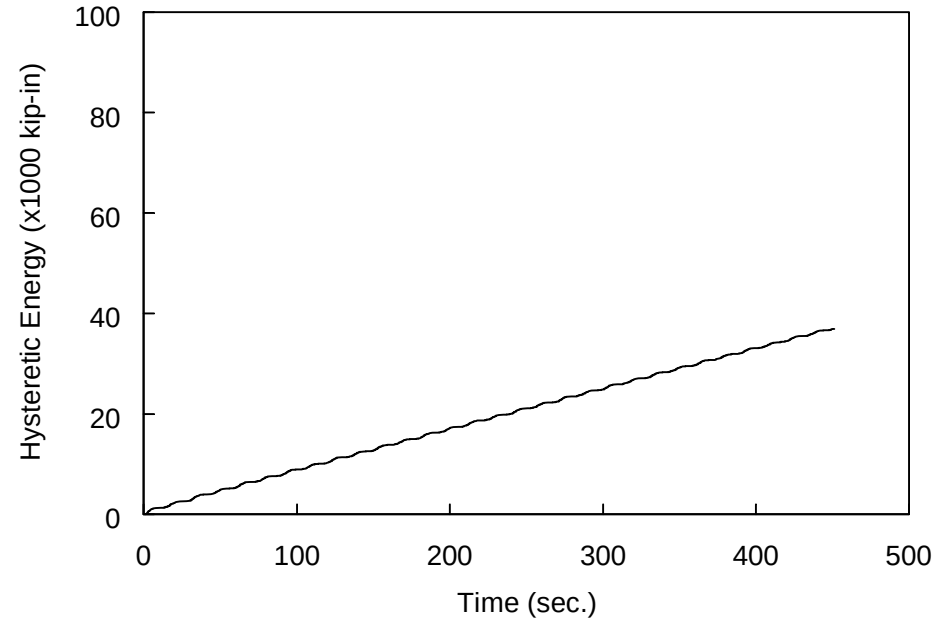

Figure 3.37 Specimen 2G: Hysteretic Energy Time History (Low-Cycle Fatigue Protocol)

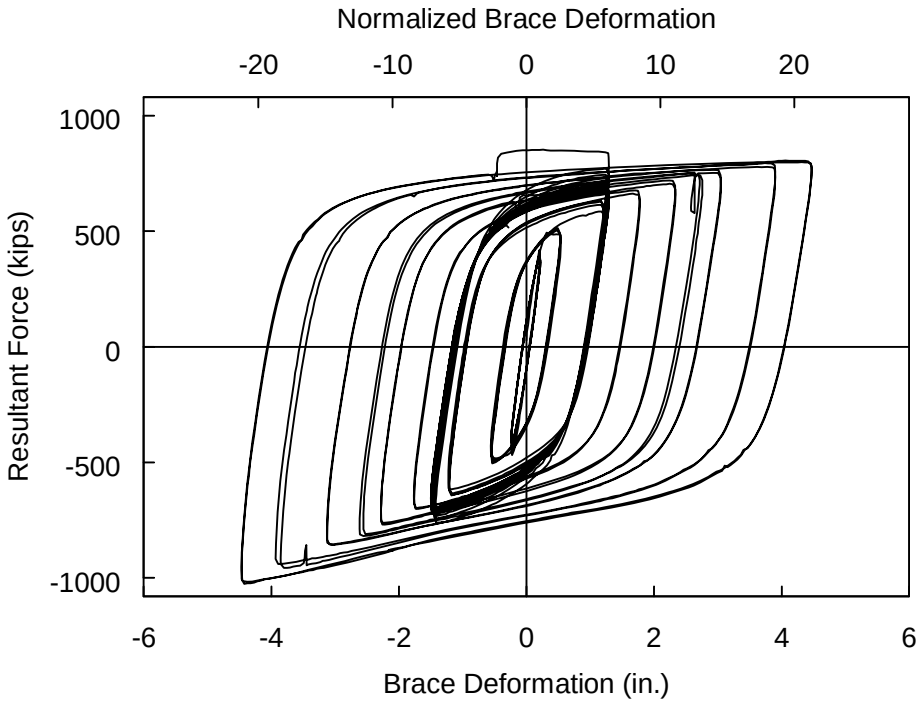

Figure 3.38 Specimen 2G: Brace Force versus Axial Deformation (All Cycles)

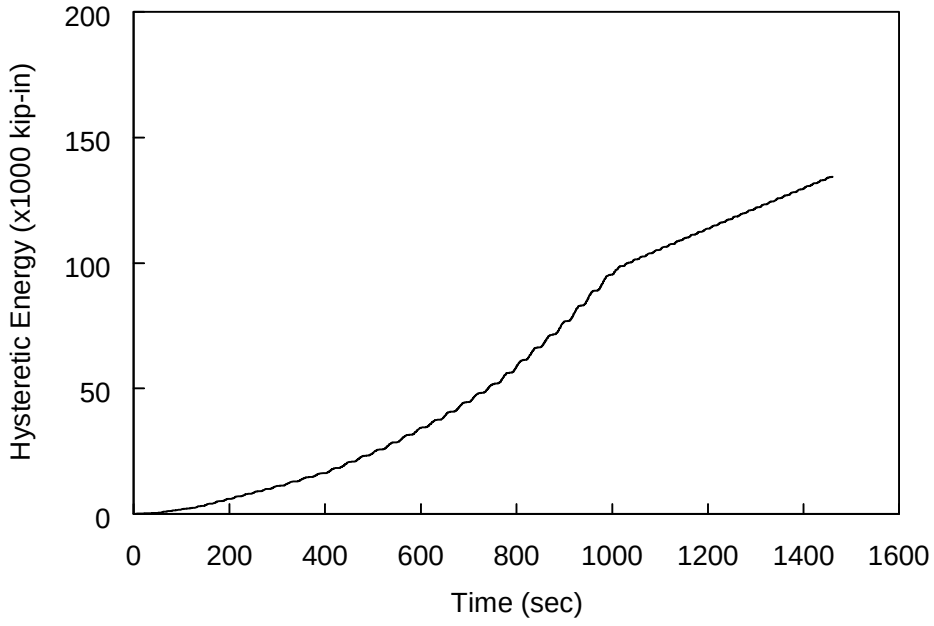

Figure 3.39 Specimen 2G: Hysteretic Energy Time History (All Cycles)

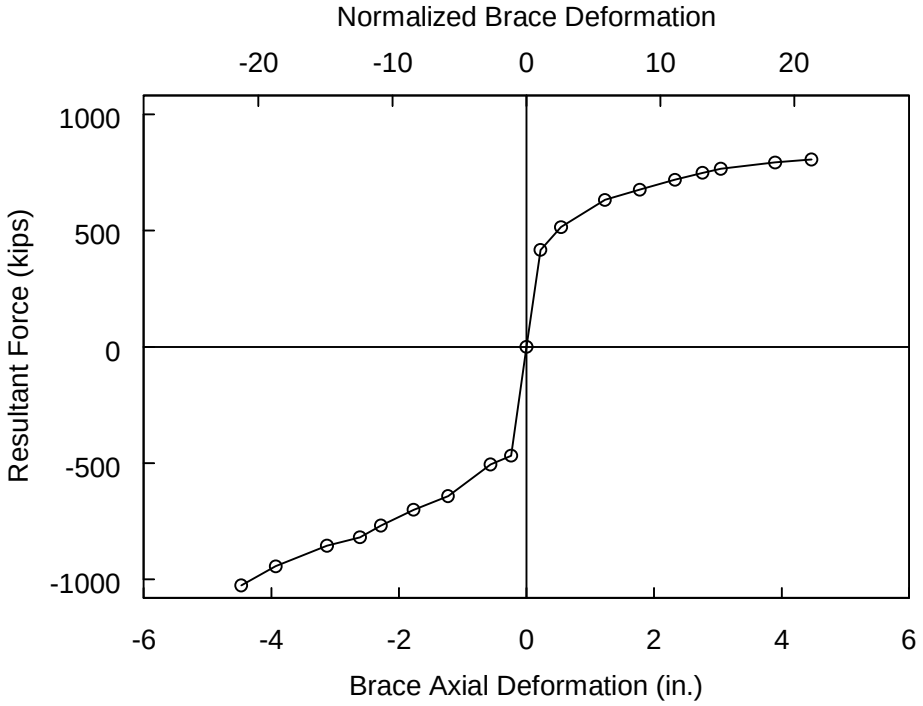

Figure 3.40 Specimen 2G: Brace Response Envelope

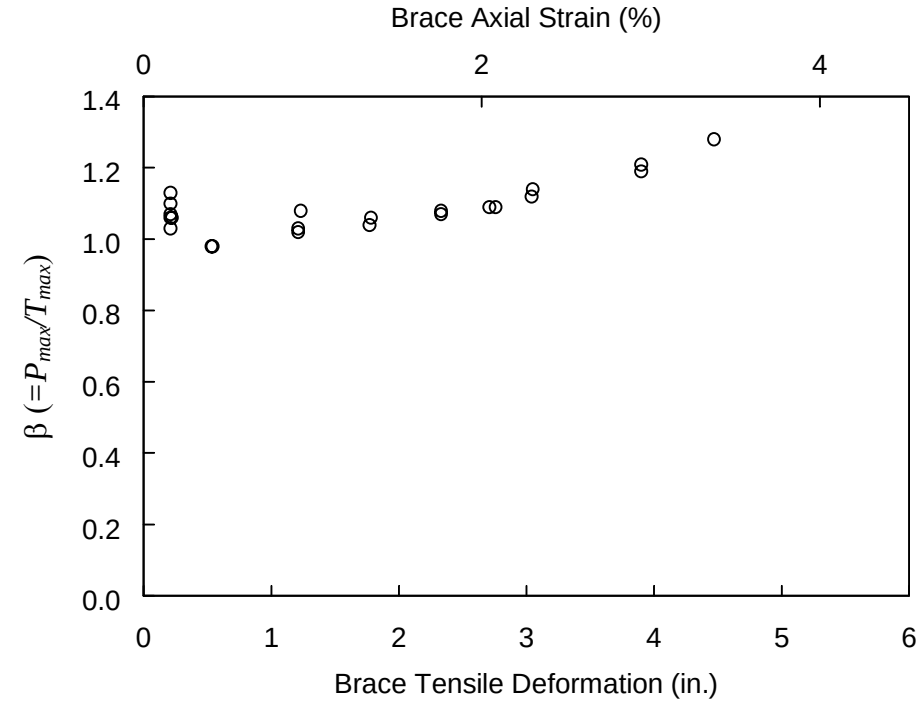

Figure 3.41 Specimen 2G: β versus Axial Deformation Level

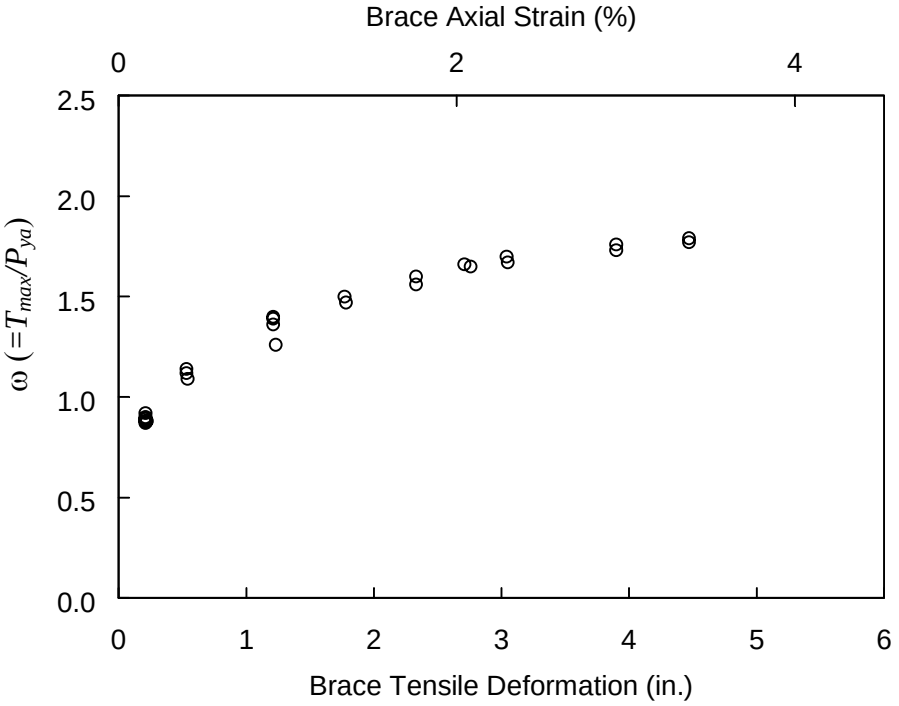

(a) Tension

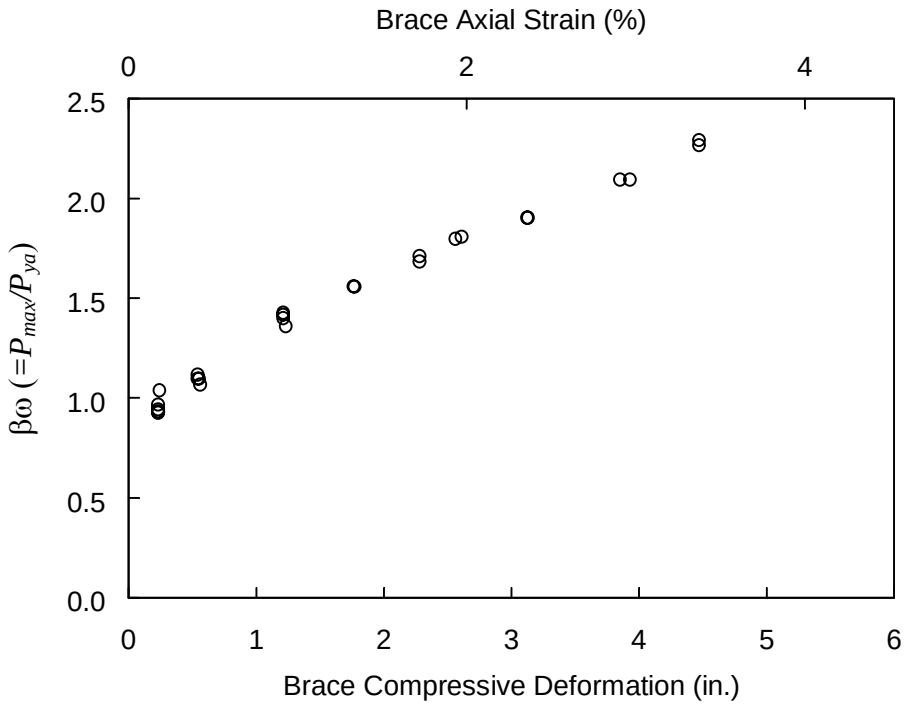

(b) Compression

Figure 3.42 Specimen 2G: ω and βω versus Axial Deformation Level

(a) Platen Bracket (East End)

(b) Wall Bracket (West End)

Figure 3.43 Specimen 3G: Gusset Bracket after Test

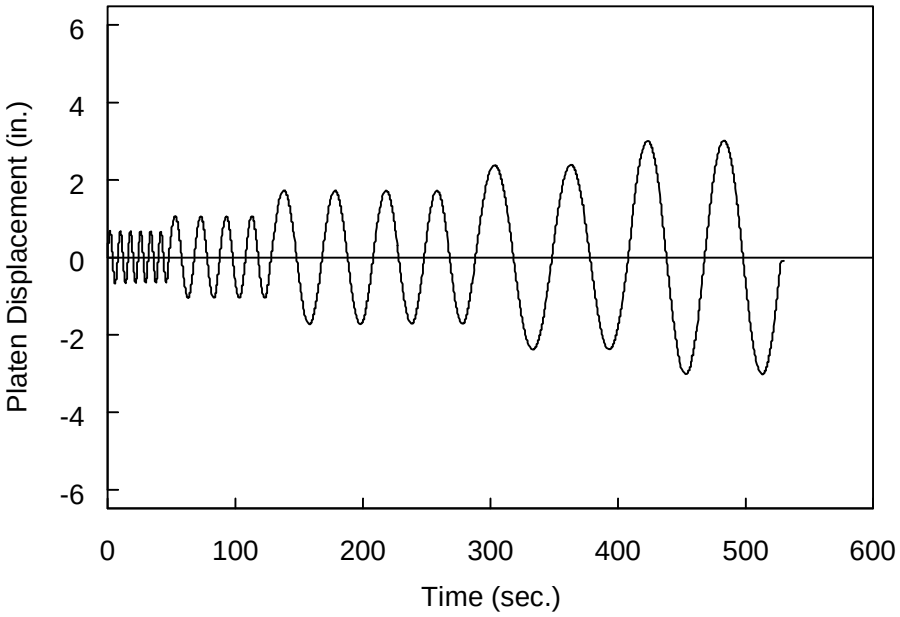

(a) Longitudinal Direction

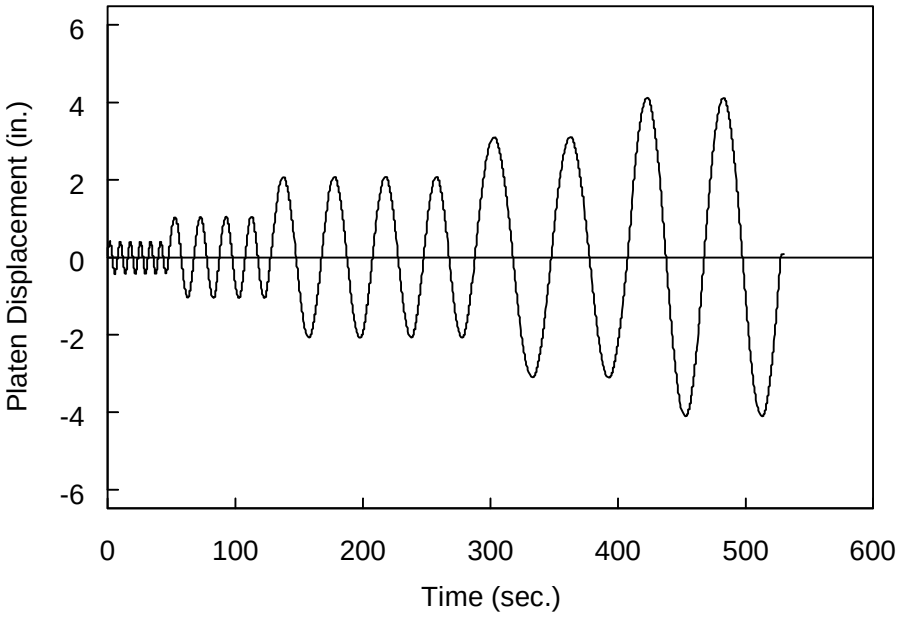

(b) Transverse Direction

Figure 3.44 Specimen 3G: Table Displacement Time Histories (Standard Protocol)

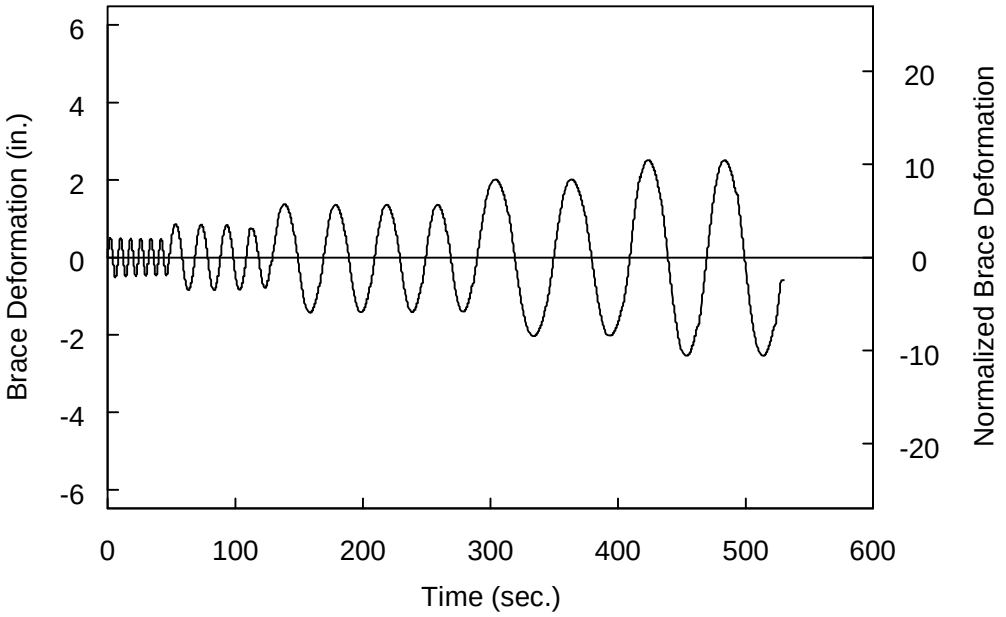

(a) Axial Direction

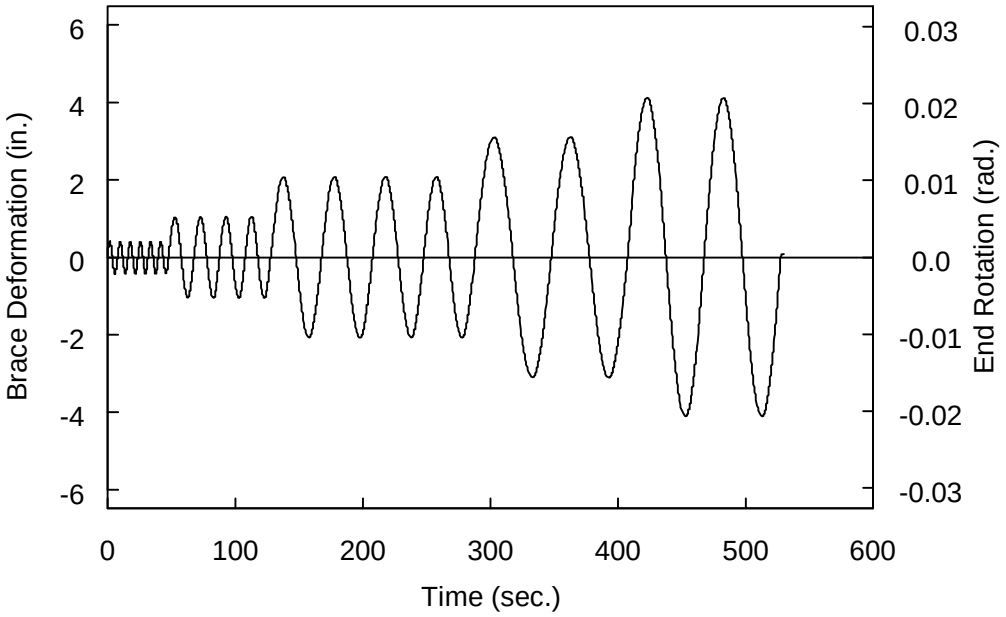

(b) Transverse Direction

Figure 3.45 Specimen 3G: Brace Deformation Time Histories (Standard Protocol)

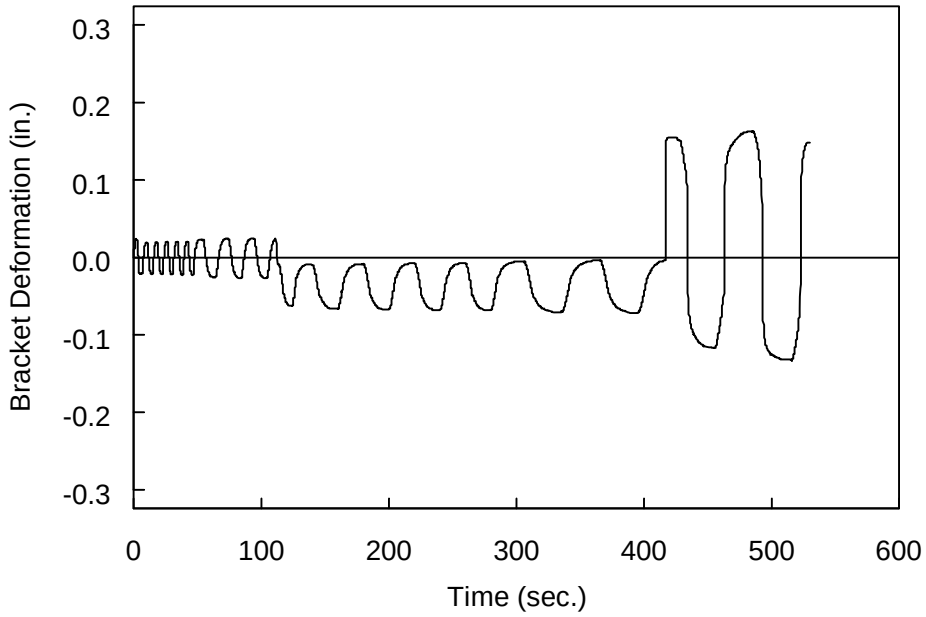

(a) Platen End Bracket

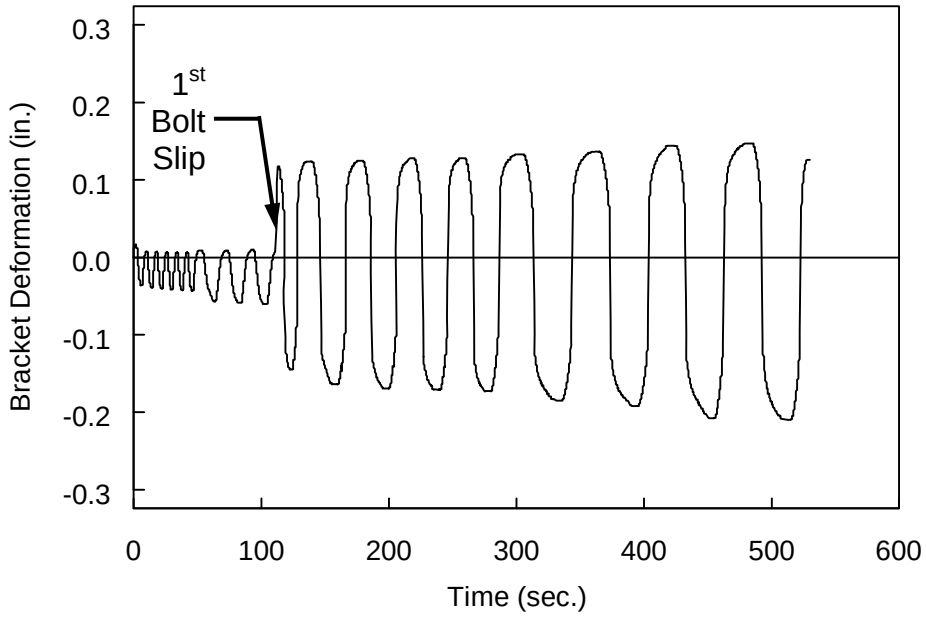

(b) Wall End Bracket

Figure 3.46 Specimen 3G: Bracket Deformation Time Histories (Standard Protocol)

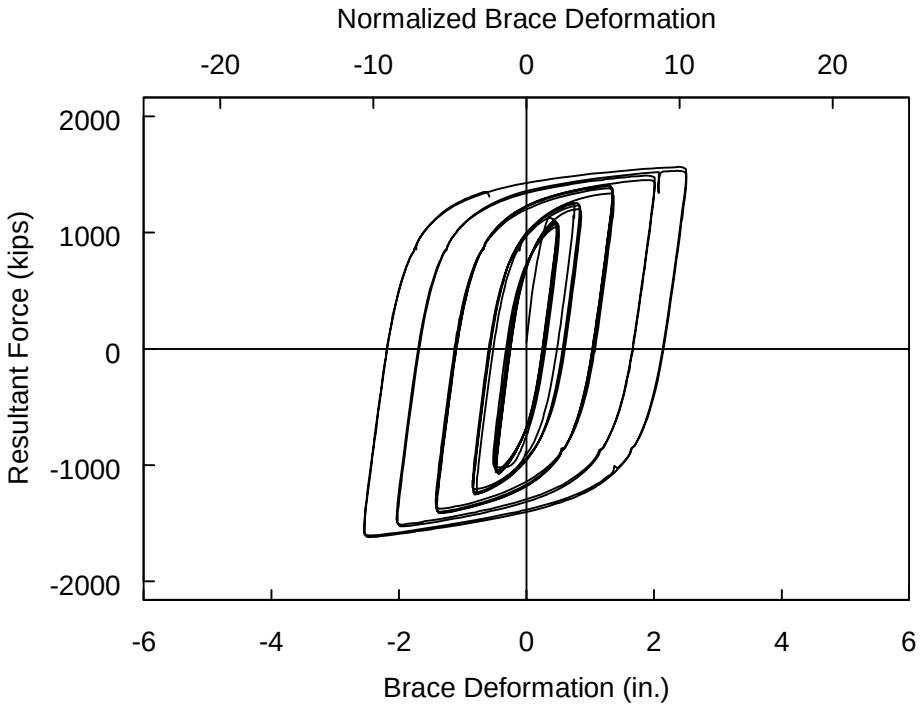

Figure 3.47 Specimen 3G: Brace Force versus Axial Deformation (Standard Protocol)

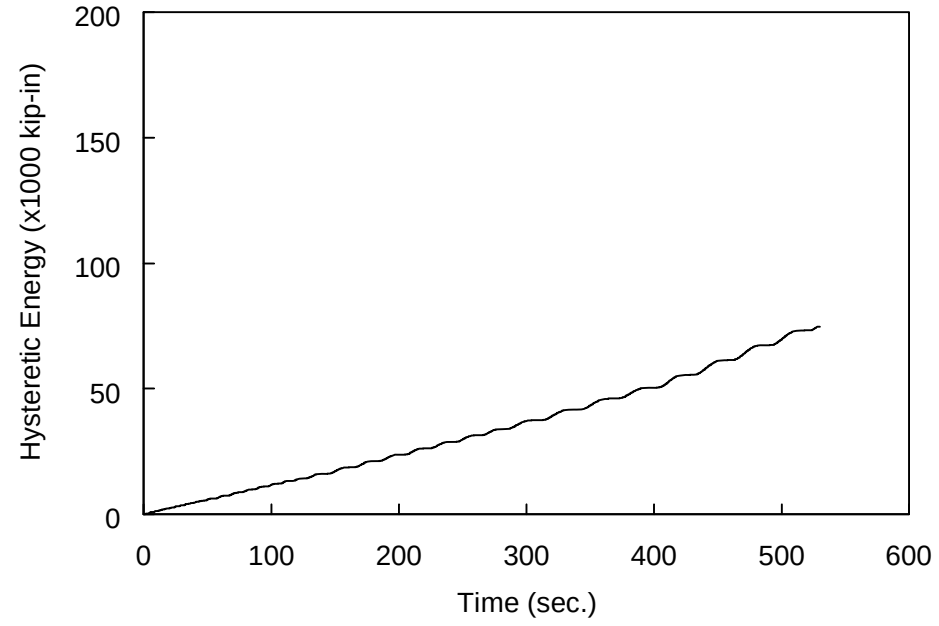

Figure 3.48 Specimen 3G: Hysteretic Energy Time History (Standard Protocol)

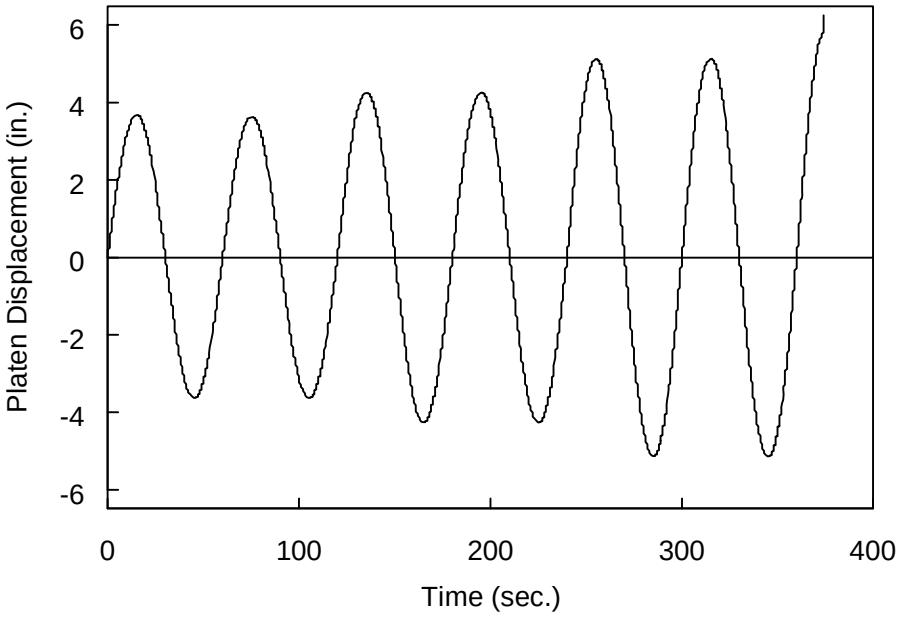

(a) Longitudinal Direction

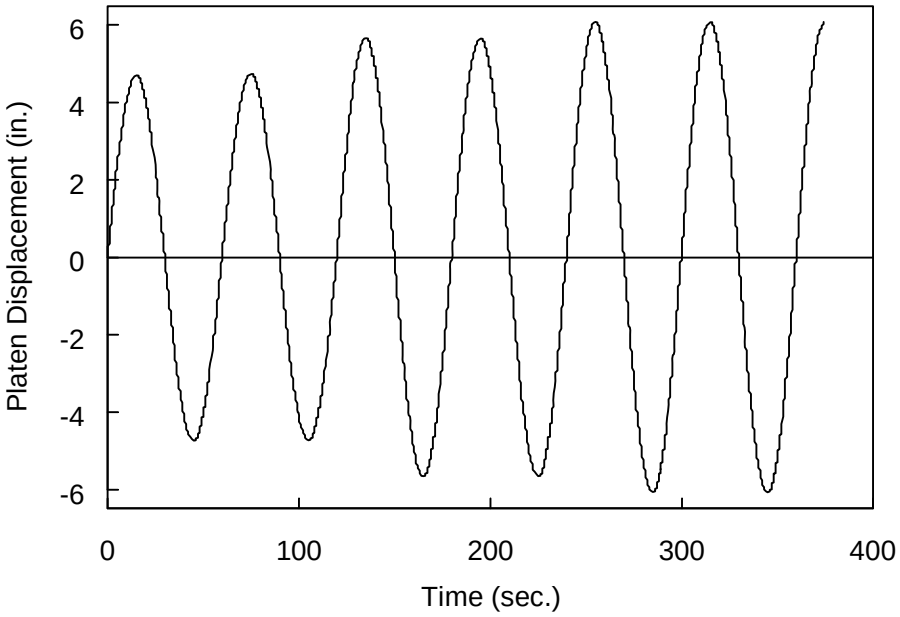

(b) Transverse Direction

Figure 3.49 Specimen 3G: Table Displacement Time Histories (High-Amplitude Protocol)

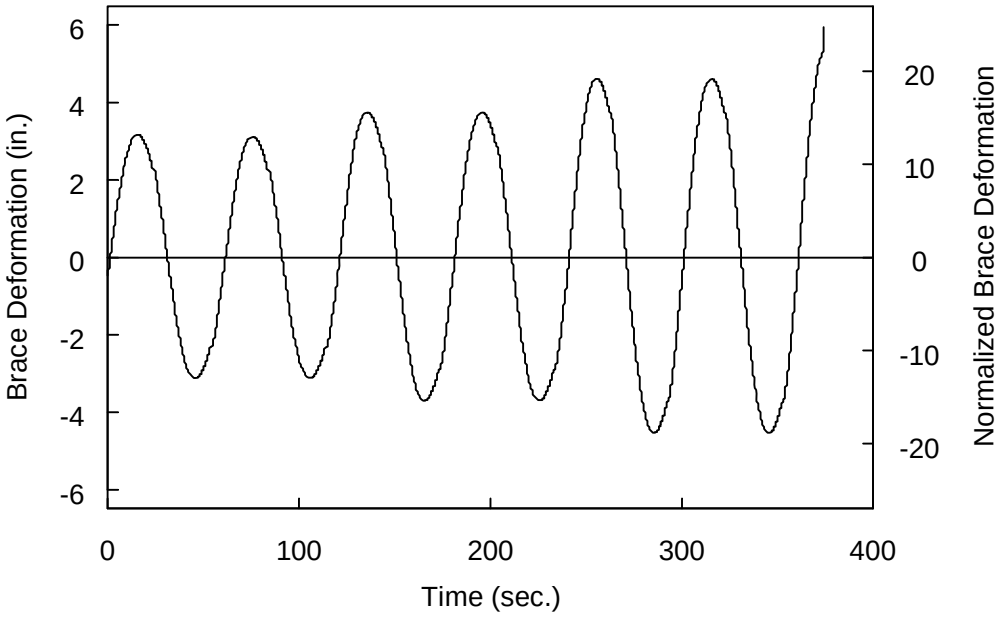

(a) Axial Direction

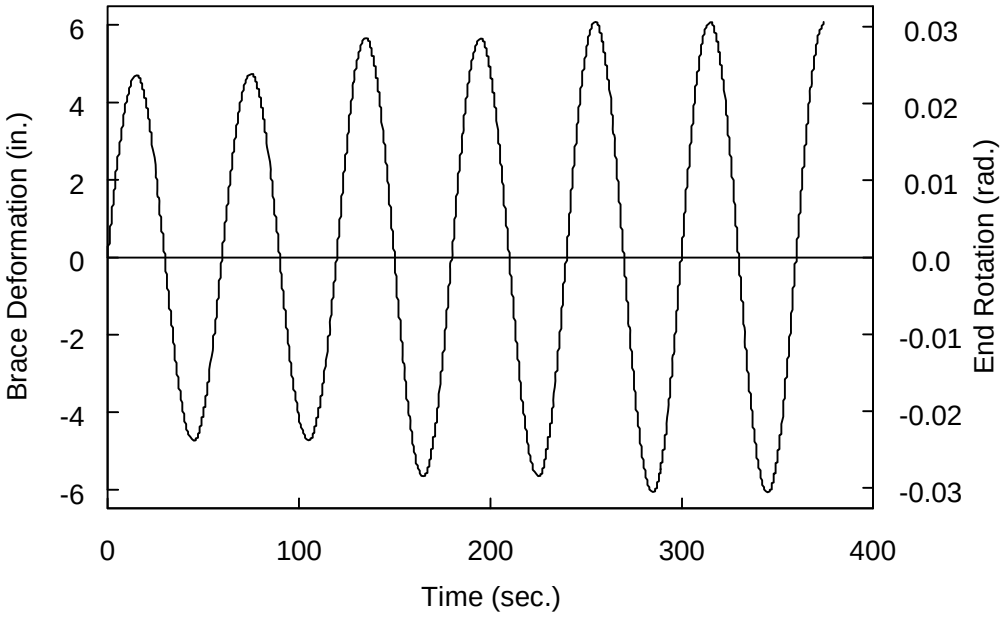

(b) Transverse Direction

Figure 3.50 Specimen 3G: Brace Deformation Time Histories (High-Amplitude Protocol)

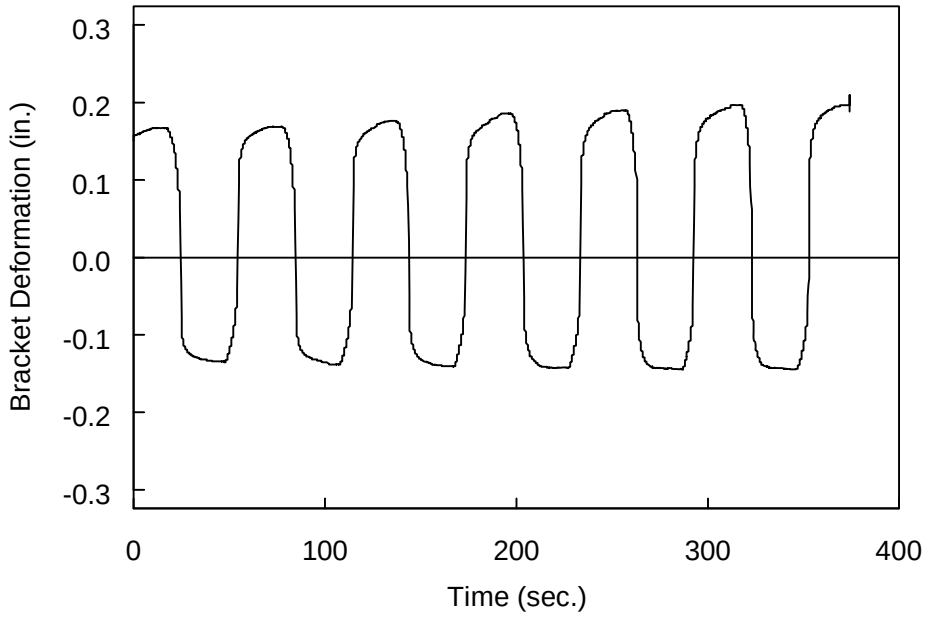

(a) Platen End Bracket

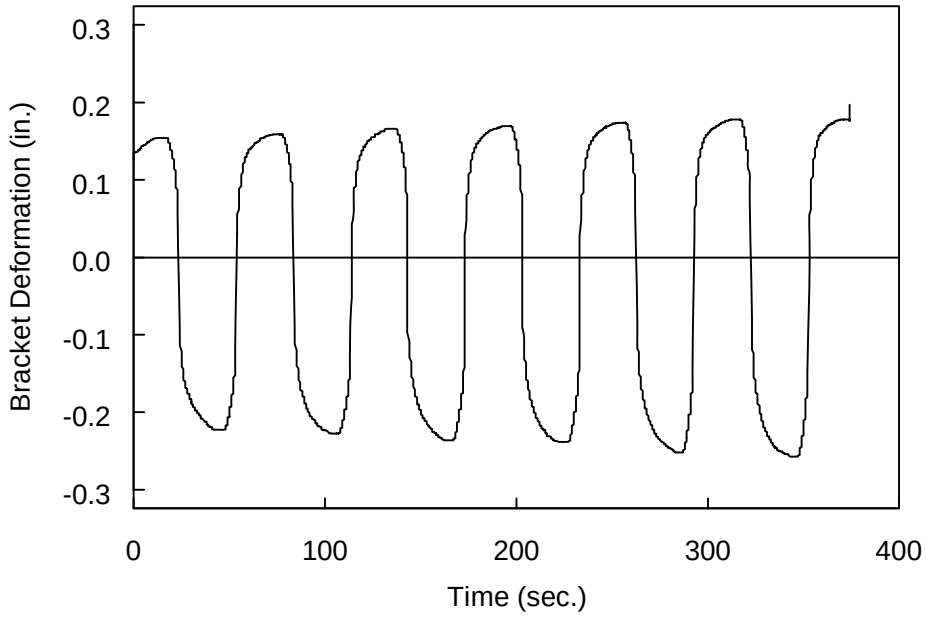

(b) Wall End Bracket

Figure 3.51 Specimen 3G: Bracket Deformation Time Histories (High-Amplitude Protocol)

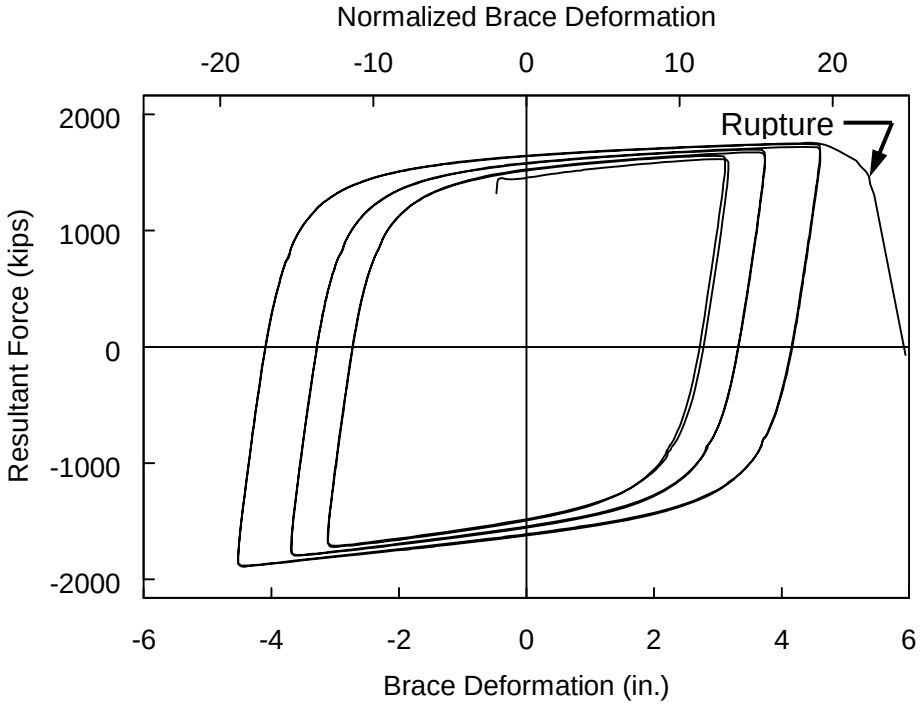

Figure 3.52 Specimen 3G: Brace Force versus Axial Deformation (High-Amplitude Protocol)

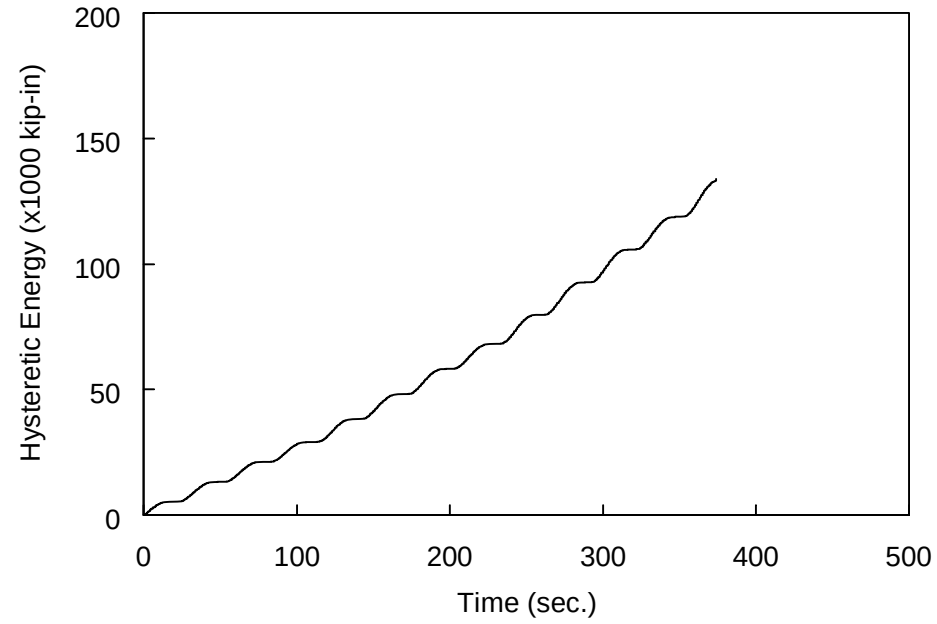

Figure 3.53 Specimen 3G: Hysteretic Energy Time History (High-Amplitude Protocol)

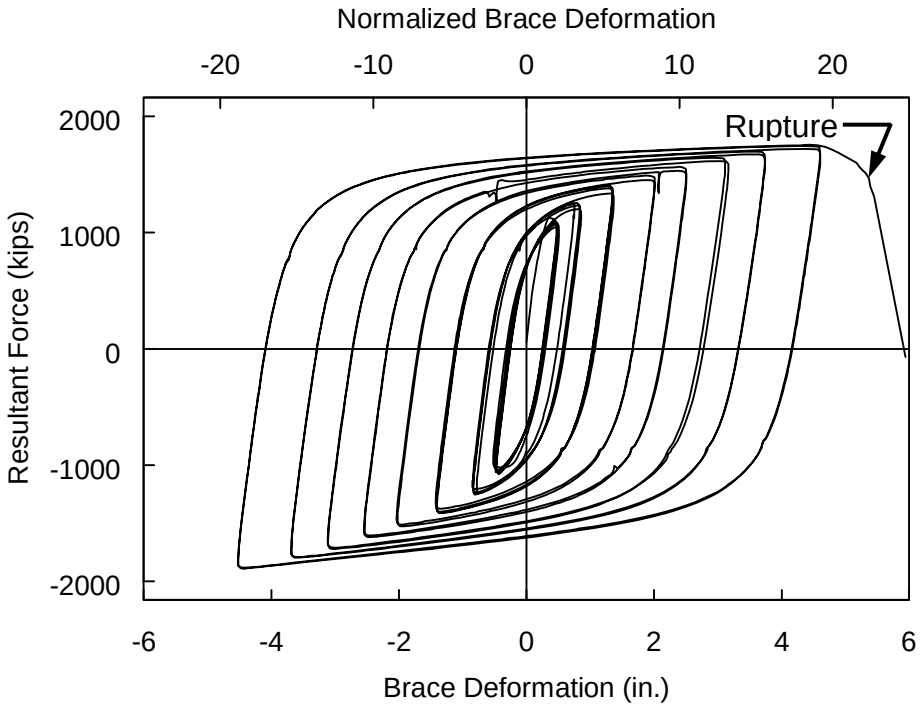

Figure 3.54 Specimen 3G: Brace Force versus Axial Deformation (All Cycles)

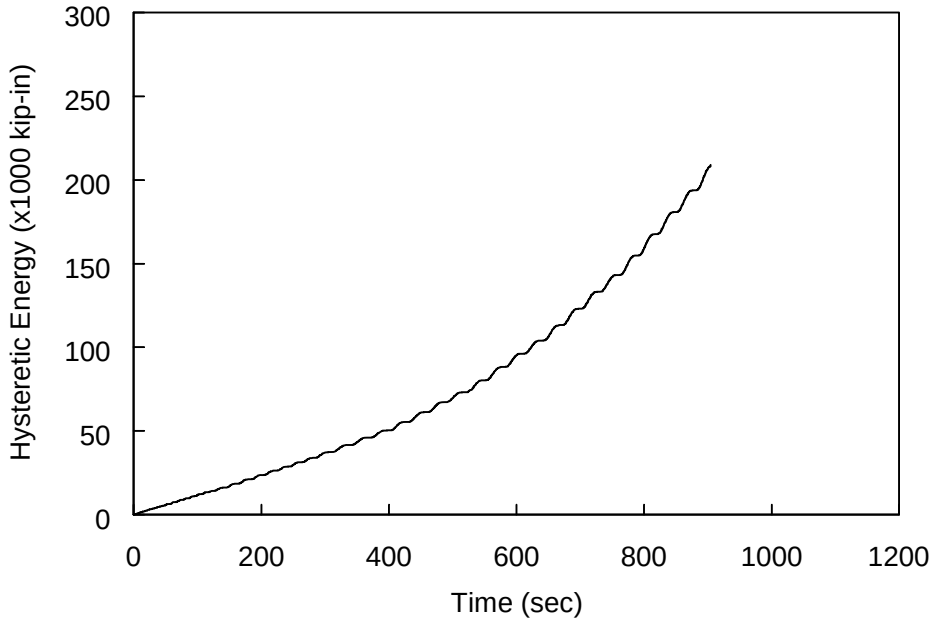

Figure 3.55 Specimen 3G: Hysteretic Energy Time History (All Cycles)

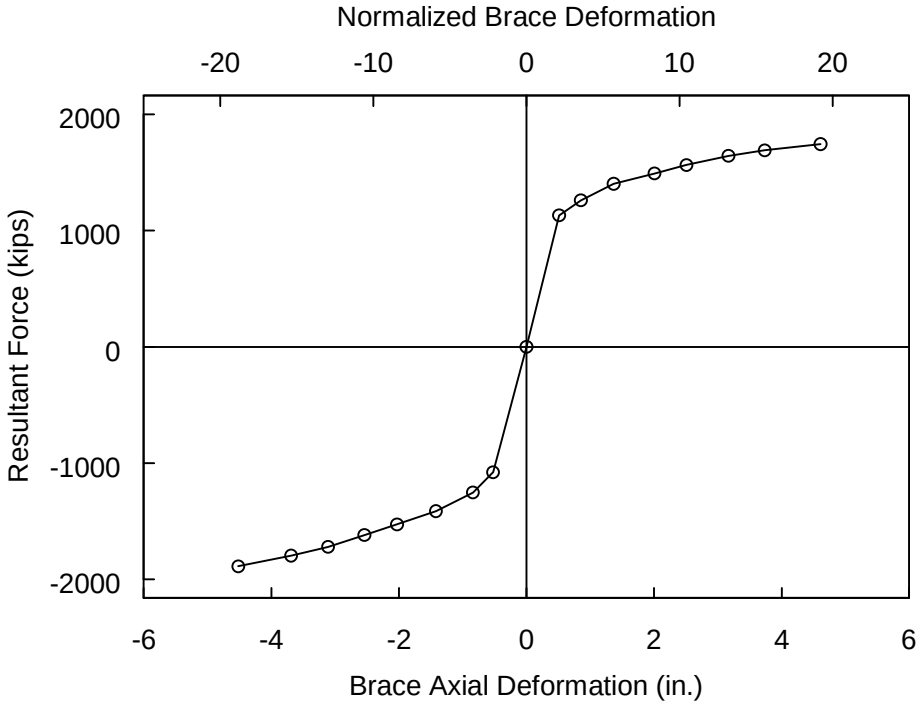

Figure 3.56 Specimen 3G: Brace Response Envelope

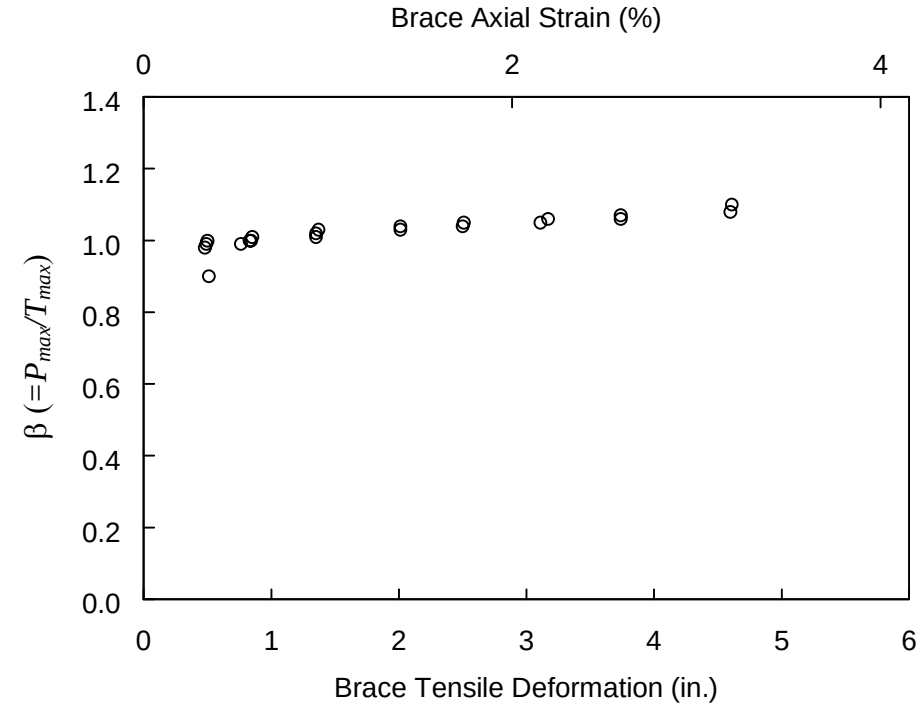

Figure 3.57 Specimen 3G: β versus Axial Deformation Level

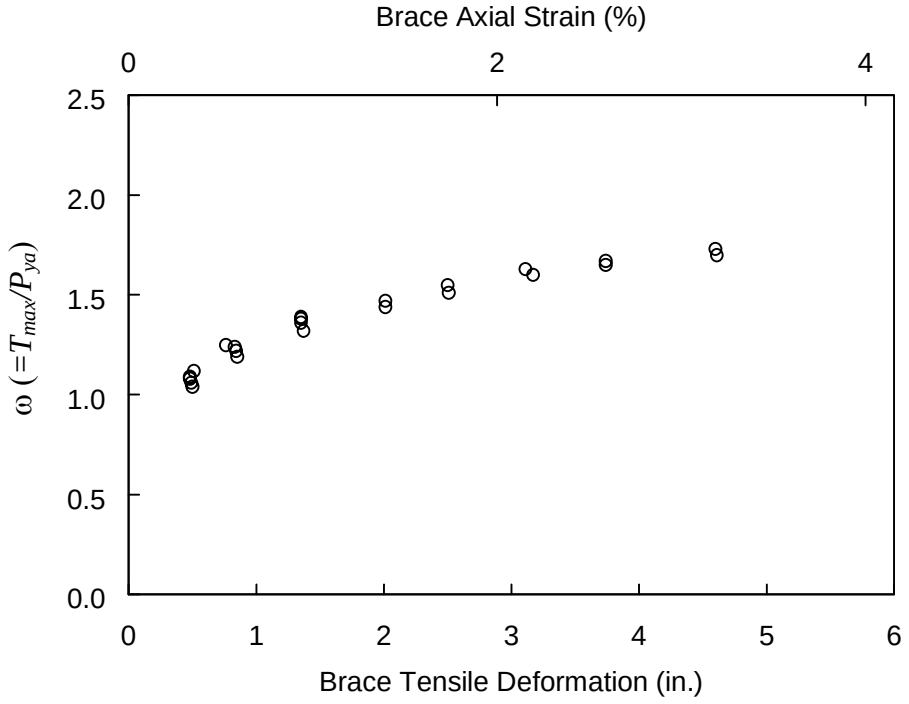

(a) Tension

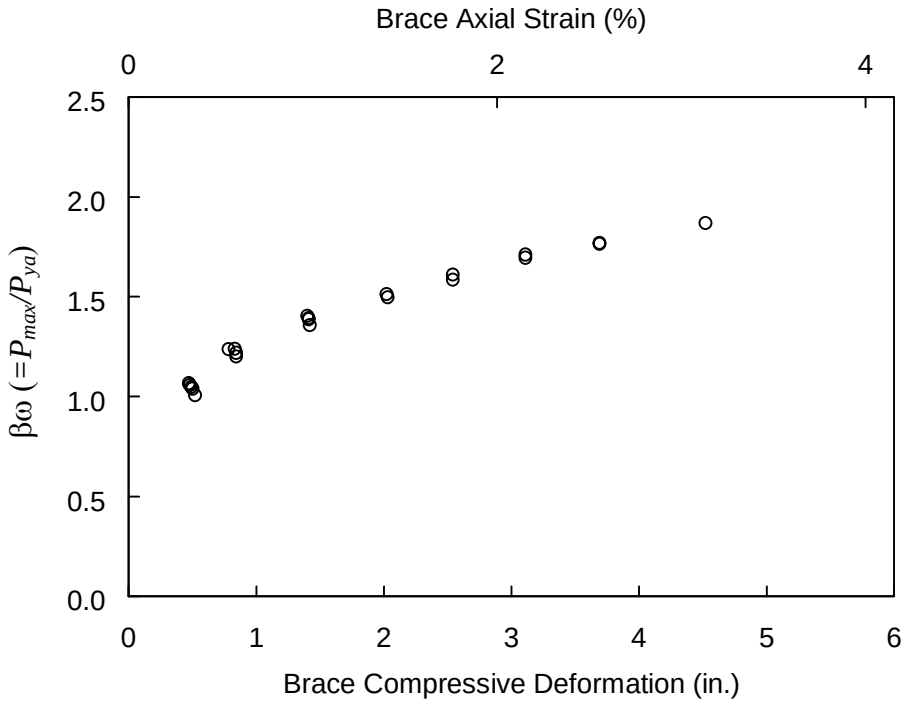

(b) Compression

Figure 3.58 Specimen 3G: ω and βω versus Axial Deformation Level

(a) Platen Bracket (East End)

(b) Wall Bracket (West End)

Figure 3.59 Specimen 4G: Gusset Bracket before Test

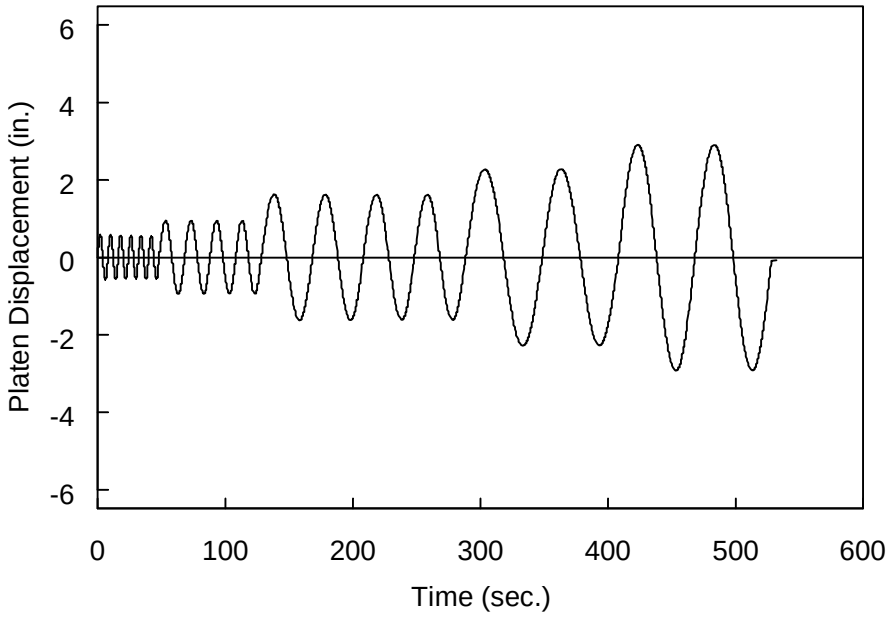

(a) Longitudinal Direction

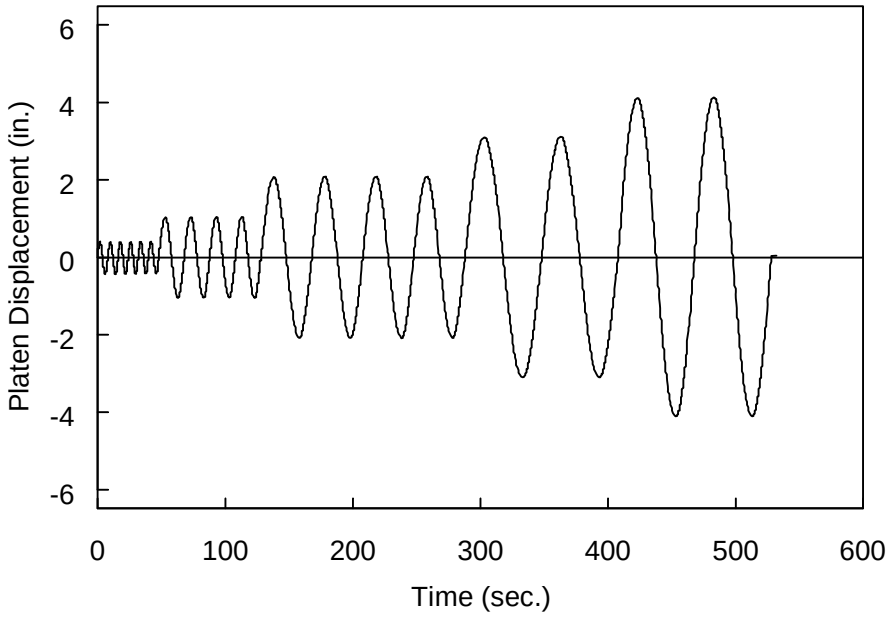

(b) Transverse Direction

Figure 3.60 Specimen 4G: Table Displacement Time Histories (Standard Protocol)

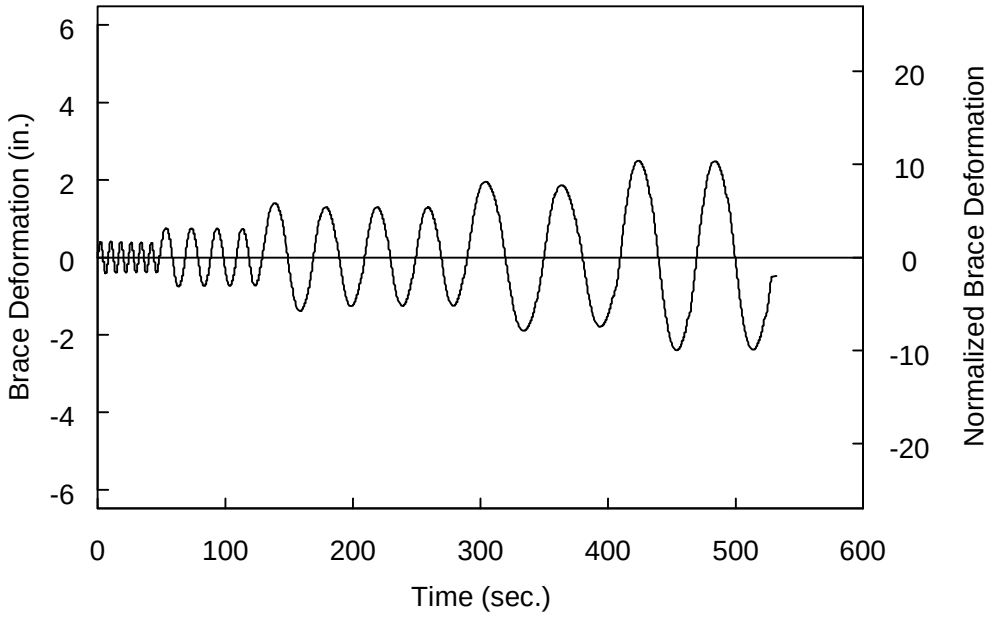

(a) Axial Direction

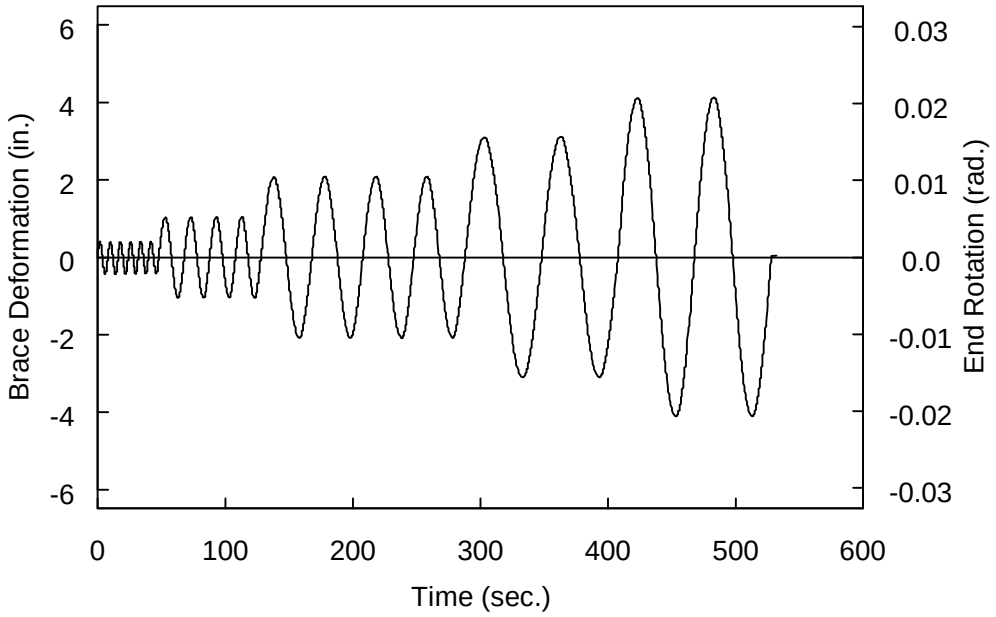

(b) Transverse Direction

Figure 3.61 Specimen 4G: Brace Deformation Time Histories (Standard Protocol)

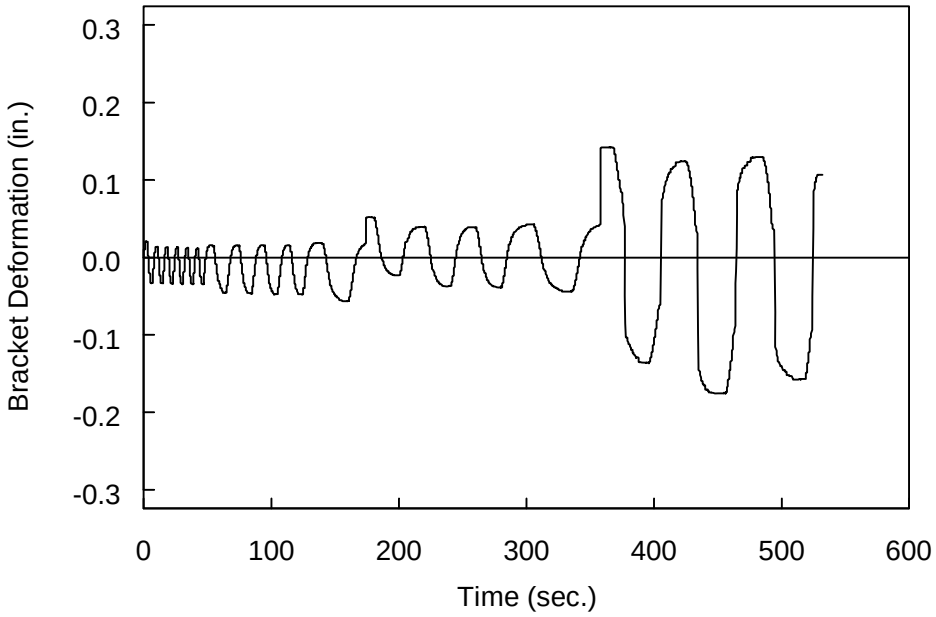

(a) Platen End Bracket

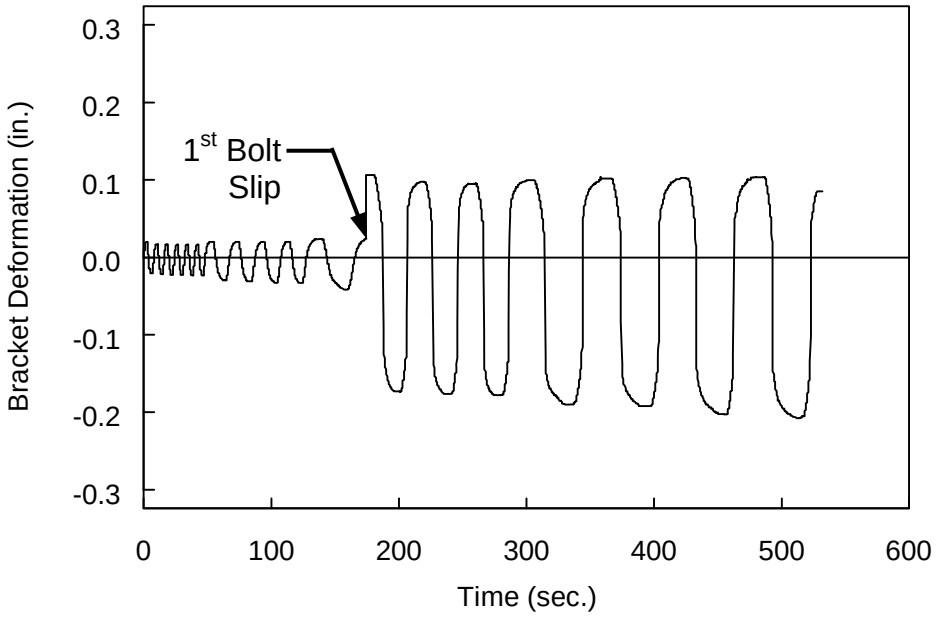

(b) Wall End Bracket

Figure 3.62 Specimen 4G: Bracket Deformation Time Histories (Standard Protocol)

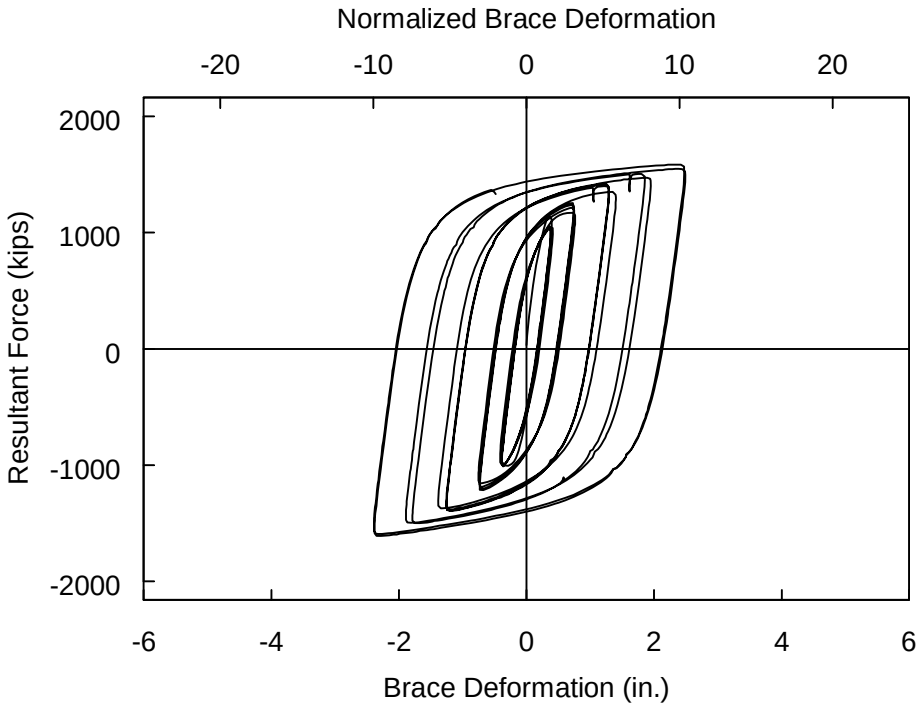

Figure 3.63 Specimen 4G: Brace Force versus Axial Deformation (Standard Protocol)

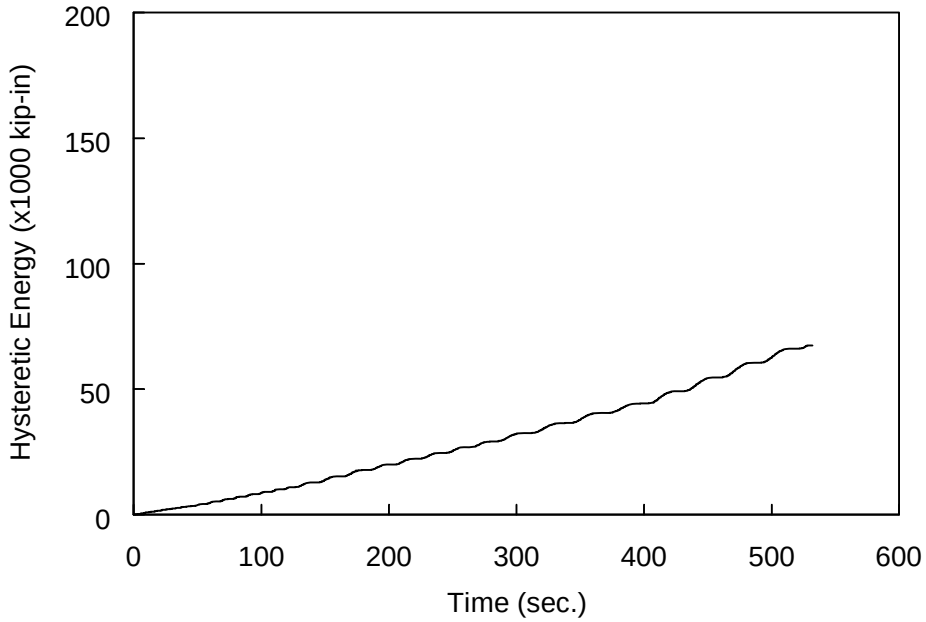

Figure 3.64 Specimen 4G: Hysteretic Energy Time History (Standard Protocol)

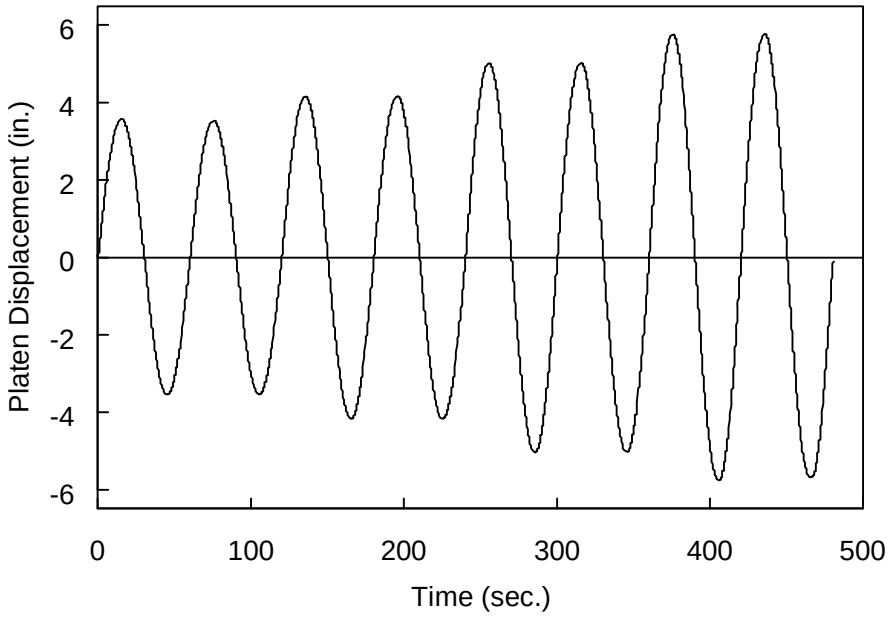

(a) Longitudinal Direction

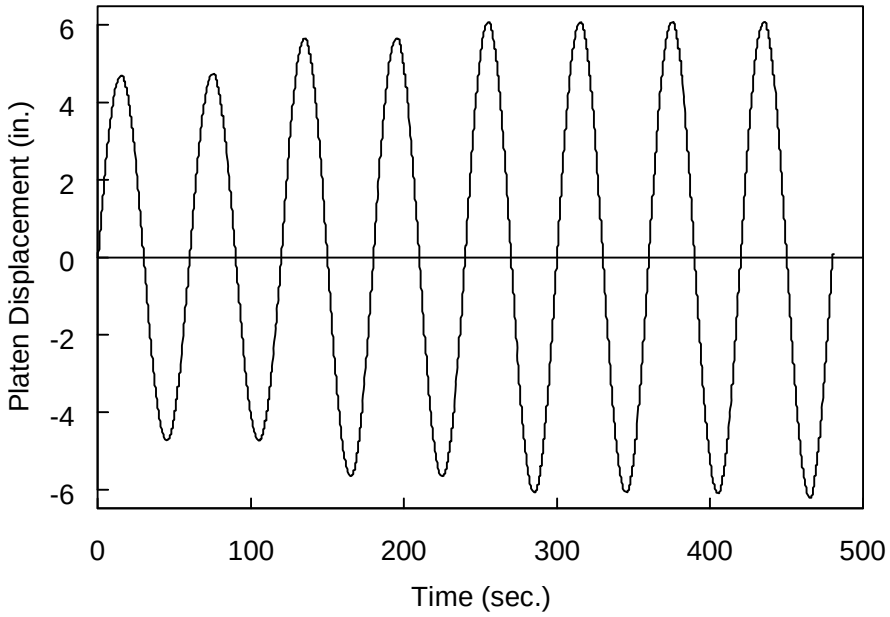

(b) Transverse Direction

Figure 3.65 Specimen 4G: Table Displacement Time Histories (High-Amplitude Protocol)

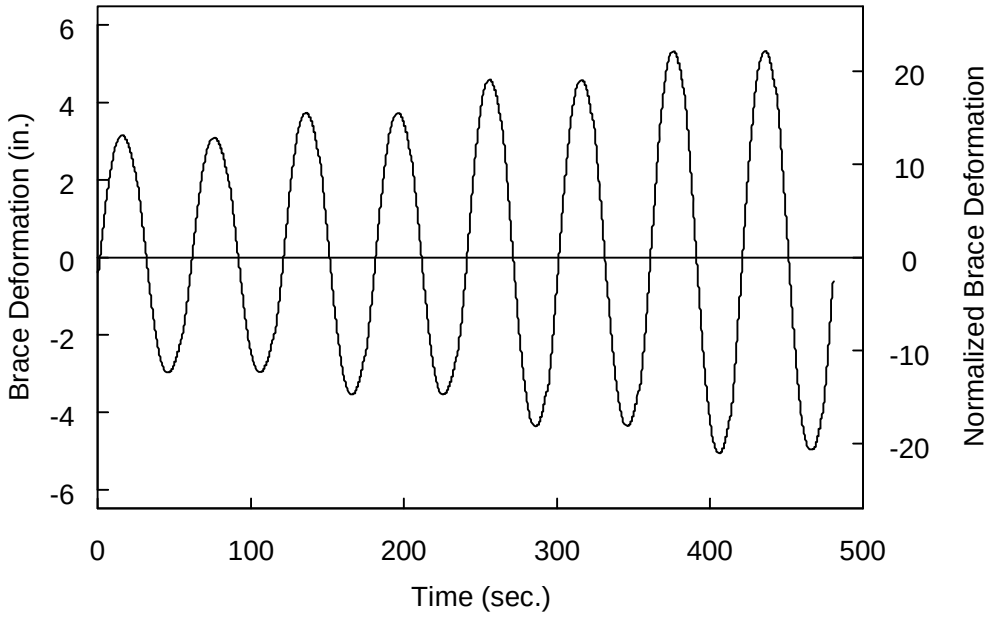

(a) Axial Direction

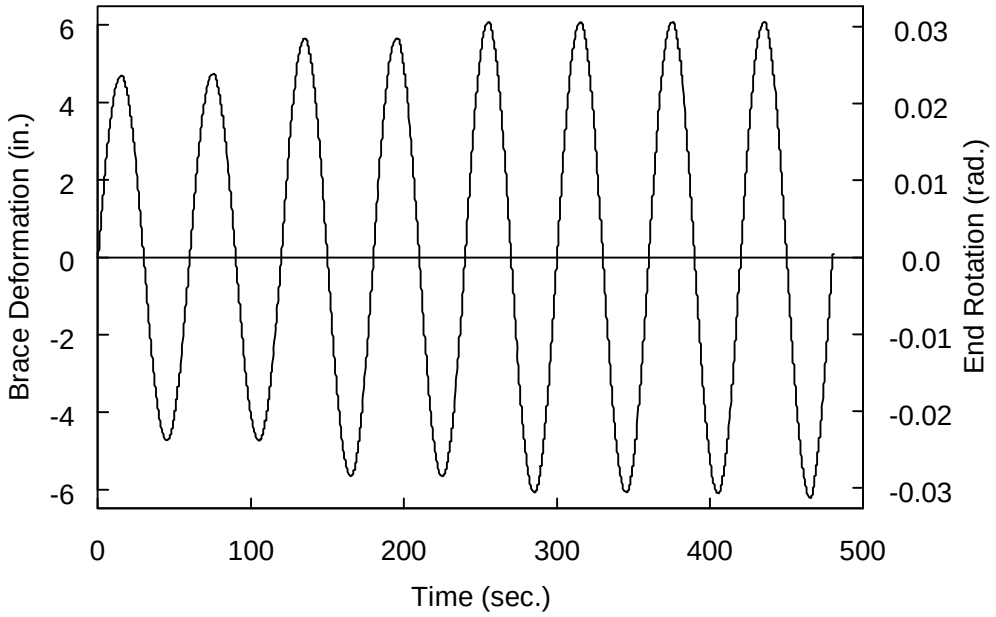

(b) Transverse Direction

Figure 3.66 Specimen 4G: Brace Deformation Time Histories (High-Amplitude Protocol)

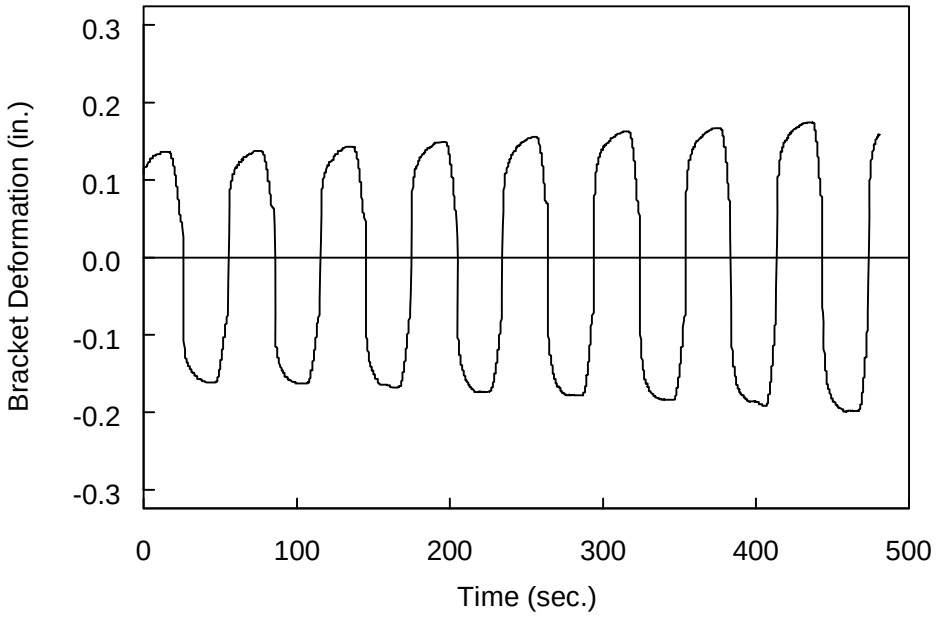

(a) Platen End Bracket

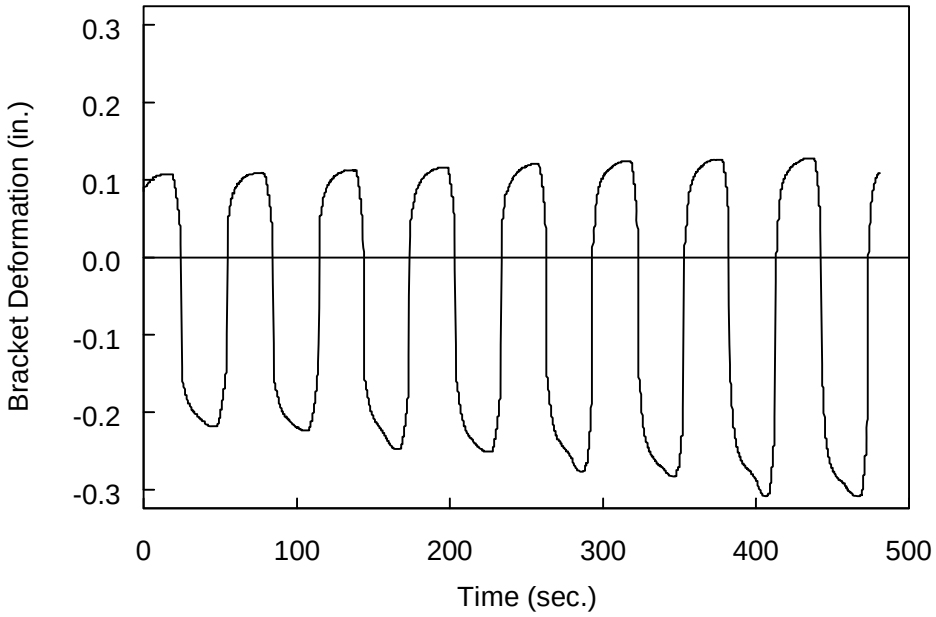

(b) Wall End Bracket

Figure 3.67 Specimen 4G: Bracket Deformation Time Histories (High-Amplitude Protocol)

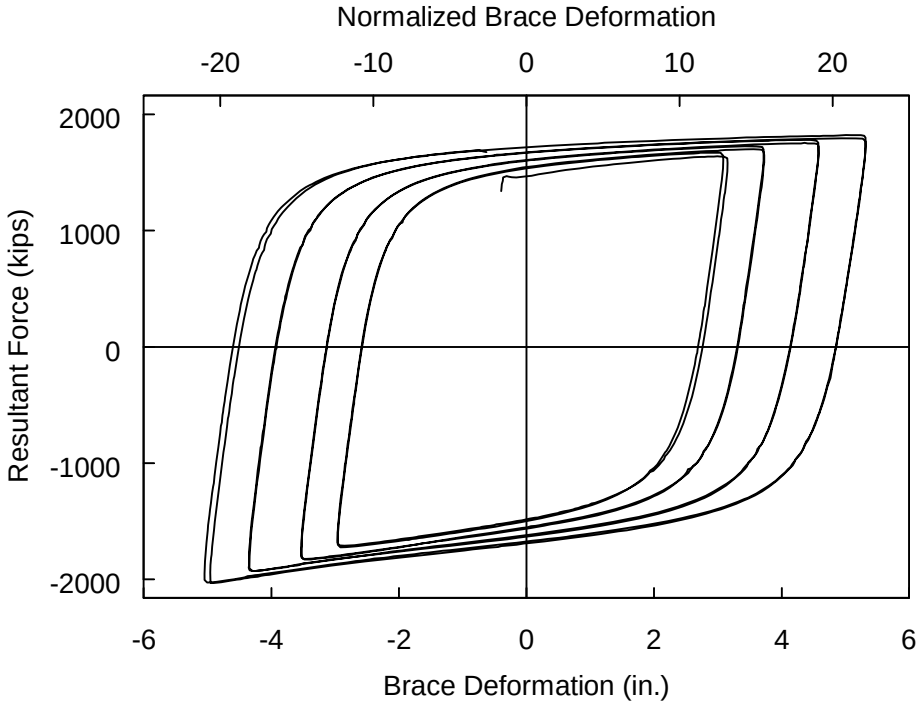

Figure 3.68 Specimen 4G: Brace Force versus Axial Deformation (High-Amplitude Protocol)

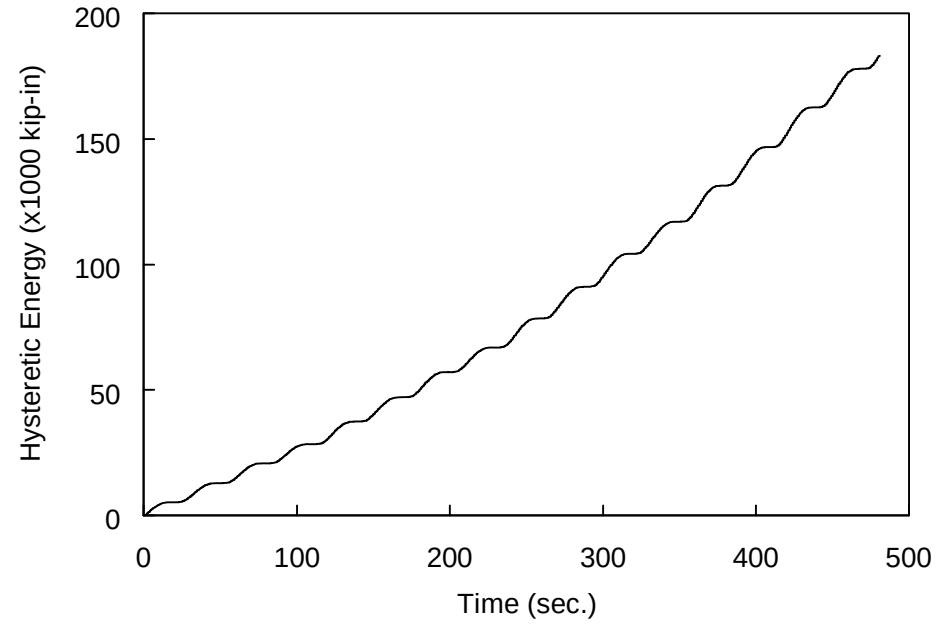

Figure 3.69 Specimen 4G: Hysteretic Energy Time History (High-Amplitude Protocol)

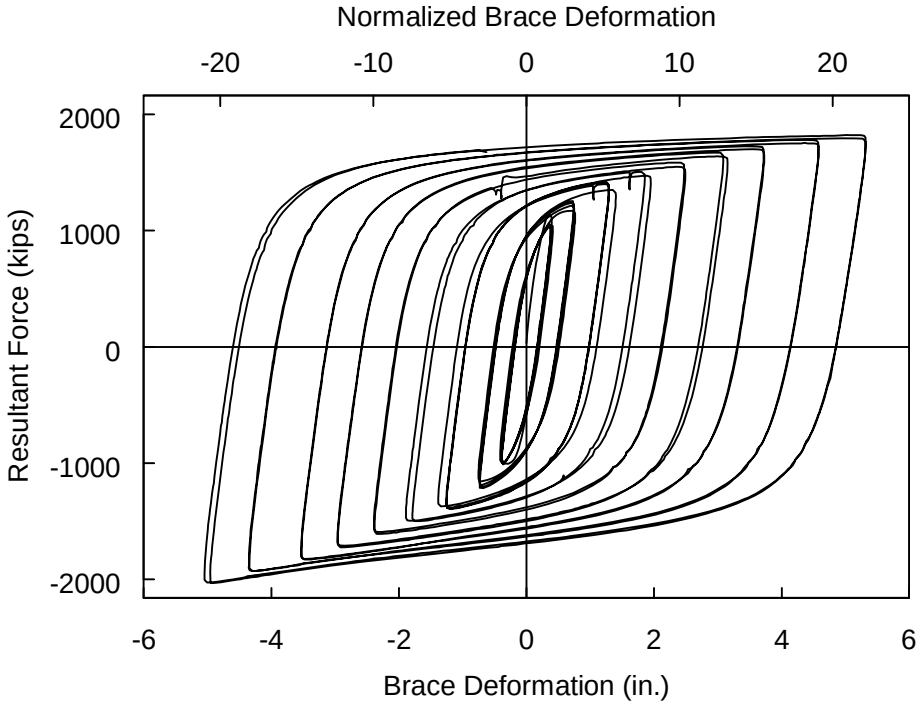

Figure 3.70 Specimen 4G: Brace Force versus Axial Deformation (All Cycles)

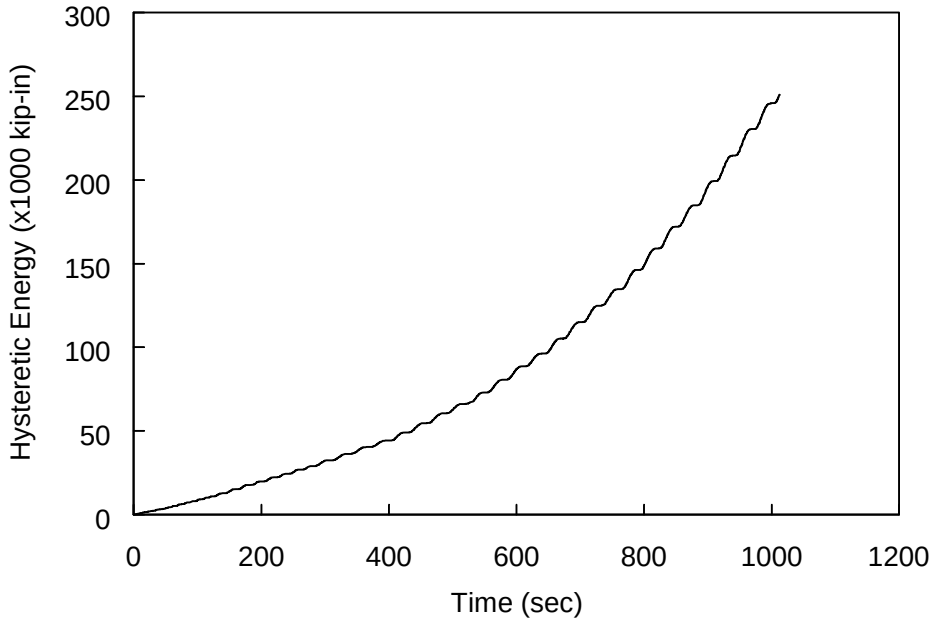

Figure 3.71 Specimen 4G: Hysteretic Energy Time History (All Cycles)

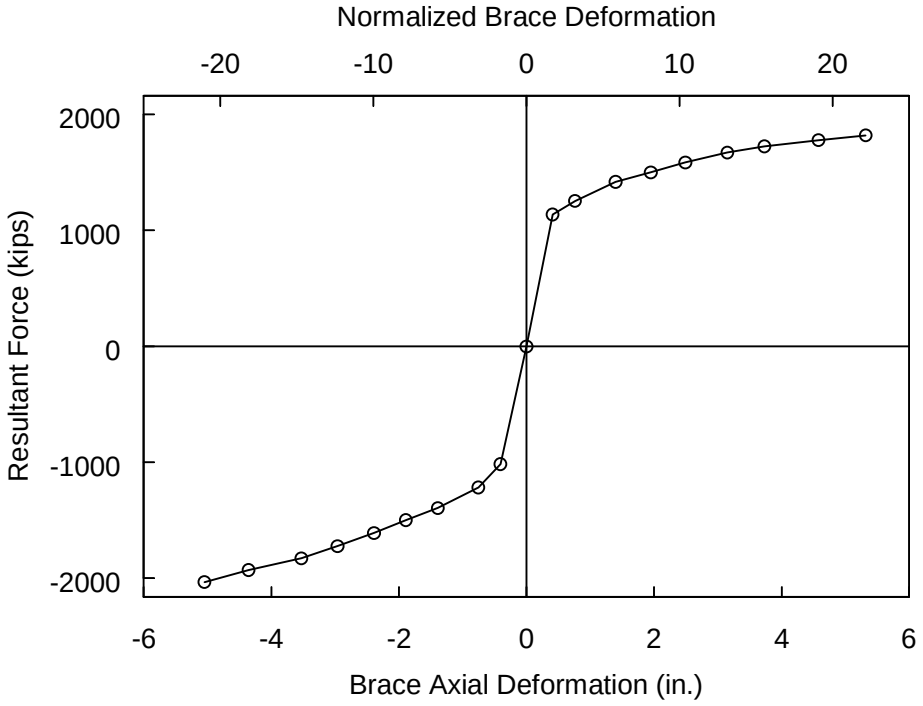

Figure 3.72 Specimen 4G: Brace Response Envelope

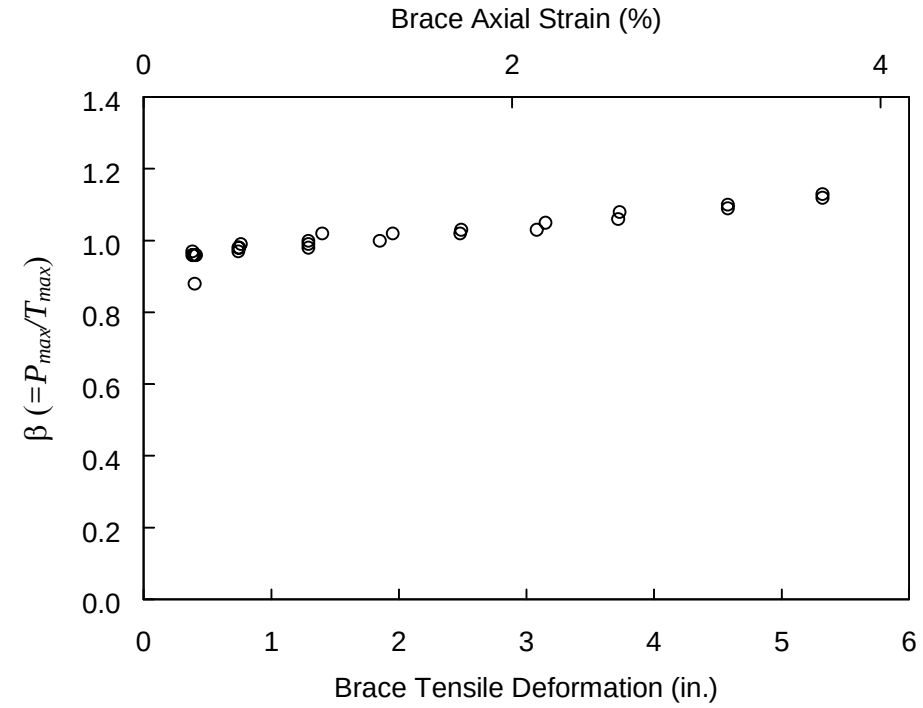

Figure 3.73 Specimen 4G: β versus Axial Deformation Level

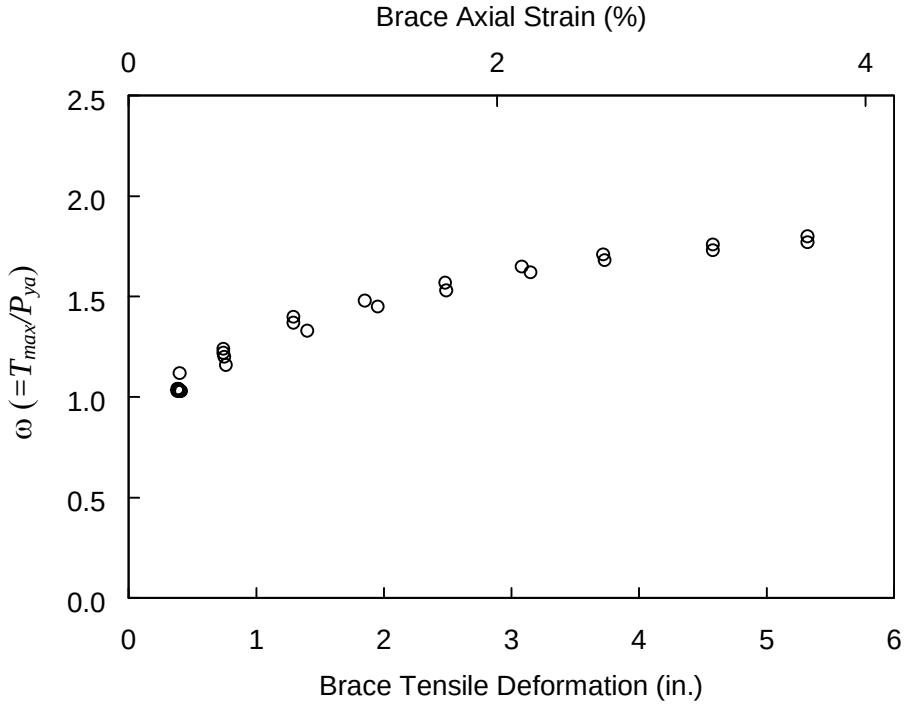

(a) Tension

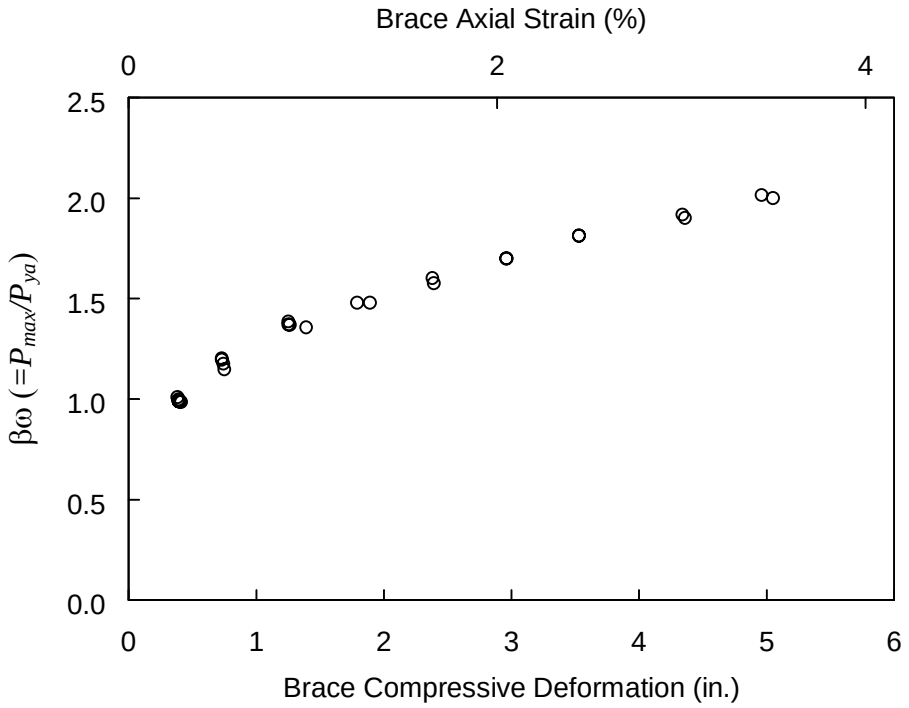

(b) Compression

Figure 3.74 Specimen 4G: ω and βω versus Axial Deformation Level

4. COMPARISON OF TEST RESULTS

4.1 Overall Performance

All four specimens performed very well in the Standard Loading Protocol. Figure 4.1 shows the brace force versus axial deformation and Figure 4.2 shows the brace response envelopes for the four specimens. The brace response envelopes show nominally identical response for the two specimen pairs. Table 4.1(a) provides peak response quantities for the Standard Loading Protocol and Table 4.1(b) provides these quantities for all cycles. Compared to Specimen 1G, Specimen 2G showed increased compressive strength at large deformations resulting from a problem with the confining HSS centering mechanism and the core plate bearing on one end of the confining HSS. The maximum β value of 1.28 for Specimen 2G resulted from this increased compressive strength. Each specimen experienced over 3% core plate axial strain and 0.031 radians of connection end rotation. The BRB end connection detail with plates that were welded to the BRB core plate and bolted to the gusset brackets performed well.

4.2 Hysteretic Energy, E_h, and Cumulative Inelastic Deformation, η

The total hysteretic energy and cumulative inelastic deformation achieved by each specimen is summarized in Table 4.1(c). Note that Specimen 3G experienced core plate fracture. The cumulative inelastic axial deformation achieved by all specimens was significantly greater than the $200\Delta_{by}$ required by the AISC *Seismic Provisions* for uniaxial brace test specimens.

4.3 Comparison with the AISC and FEMA 450 Acceptance Criteria

Section T10 of the AISC *Seismic Provisions* and Section 8.6.3.7.10 of FEMA 450 provide the following four acceptance criteria for buckling-restrained brace testing:

(1) The plot showing the applied load versus displacement history shall exhibit stable, repeatable behavior with positive incremental stiffness.

All specimens exhibited stable repeatable behavior with positive incremental stiffness.

(2) There shall be no fracture, brace instability or brace end connection failure.

None of the four specimens fractured during the Standard Loading Protocol. Specimen 1G, 2G, and 4G did not fracture during testing. Specimen 3G fractured near the end of the High-Amplitude Loading Protocol after undergoing cycles at deformation levels significantly higher than those prescribed by the AISC *Seismic Provisions* and FEMA 450. No brace instability or brace connection failures were observed during this testing program.

(3) For brace tests, each cycle to a deformation greater than Δ_{by} the maximum tension and compression forces shall not be less than $1.0P_{yn}$.

This criterion was met for all specimens (see Tables 3.1 to 3.4).

(4) For brace tests, each cycle to a deformation greater than Δ_{by} the ratio of the maximum compression force to the maximum tension force shall not exceed 1.3.

The maximum value of the ratio, β, of maximum compression force to maximum tension force for each specimen is summarized in Table 4.1(a and b). Maximum β values were less than 1.3 for all four specimens.

Table 4.1 Specimen Performance Summary

(a) Maximum Response Quantities (Standard Loading Protocol)

Specimen	β	ω	βω	Brace Strain		End Rotation (rad.)
				Tension ε (%)	Compression ε (%)	
1G	1.07	1.63	1.72	1.78	-1.74	0.021
2G	1.08	1.60	1.71	1.76	-1.72	0.021
3G	1.05	1.55	1.60	1.73	-1.76	0.021
4G	1.03	1.57	1.59	1.72	-1.65	0.021

(b) Maximum Response Quantities (All Cycles)

Specimen	β	ω	βω	Brace Strain		End Rotation (rad.)
				Tension ε (%)	Compression ε (%)	
1G	1.17	1.83	2.13	3.51	-3.46	0.031
2G	1.28	1.79	2.28	3.37	-3.37	0.031
3G	1.10	1.73	1.87	3.19	-3.13	0.031
4G	1.13	1.80	2.01	3.68	-3.50	0.031

(c) Hysteretic Energy and Cumulative Inelastic Deformation

Specimen	Cumulative Inelastic Deformation, η	Hysteretic Energy, E_h (kip-in)
1G	$1{,}143\Delta_{by}$	144,900
2G	$1{,}083\Delta_{by}$	134,300
3G	$631\Delta_{by}$	208,900
4G	$758\Delta_{by}$	250,900

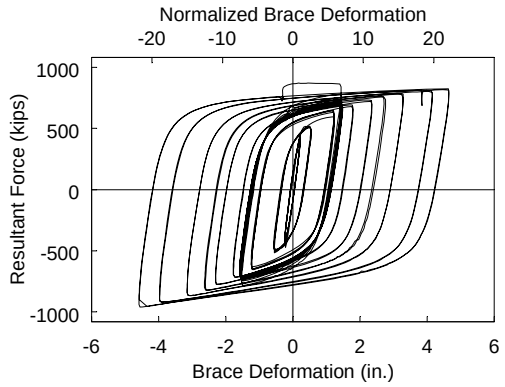

(a) Specimen 1G

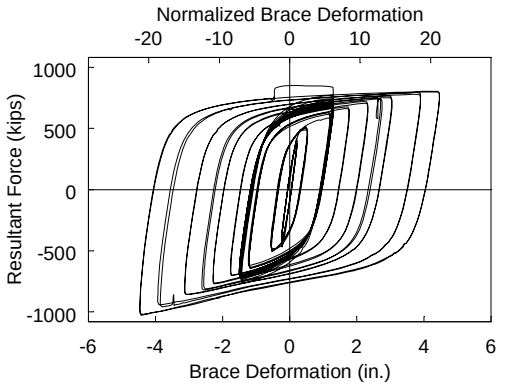

(b) Specimen 2G

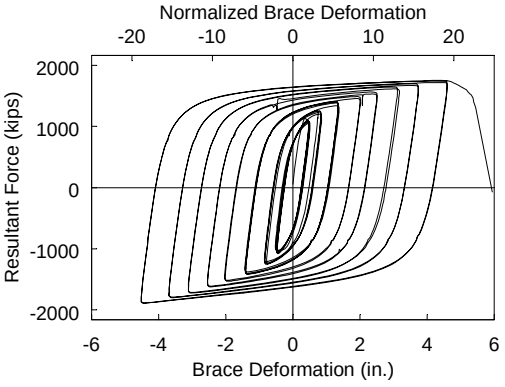

(c) Specimen 3G

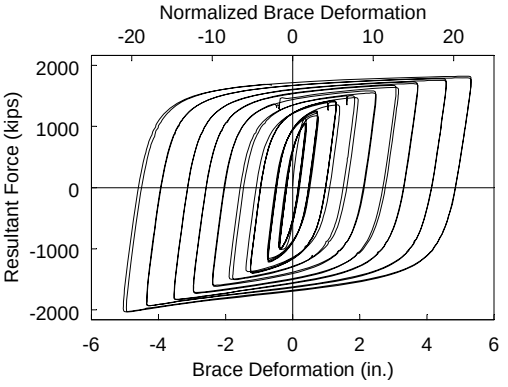

(d) Specimen 4G

Figure 4.1 Brace Force versus Axial Deformation (All Cycles)

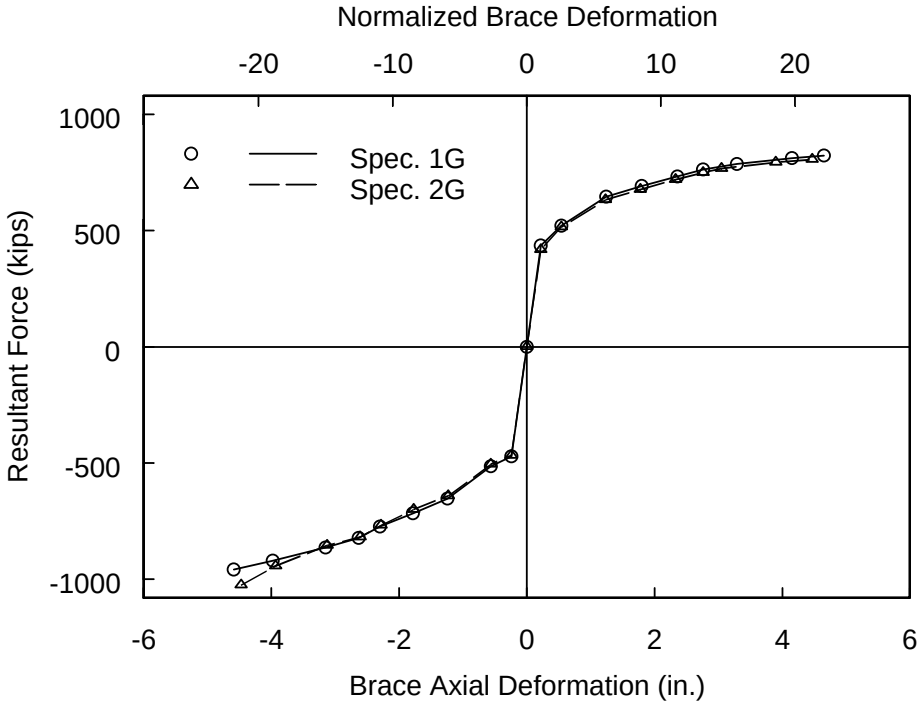

(a) Specimens 1G and 2G

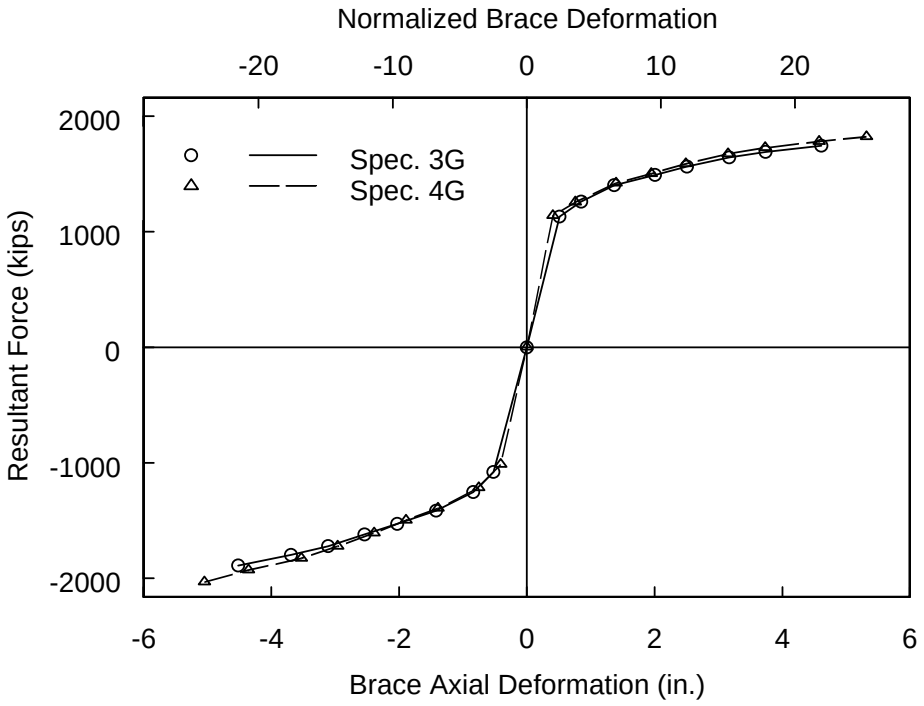

(b) Specimens 3G and 4G

Figure 4.2 Brace Response Envelopes

5. SUMMARY AND CONCLUSIONS

5.1 Summary

Two pairs of nominally identical buckling-restrained brace (BRB) specimens (four total) were tested in subassemblage configuration for CoreBrace. The Specimens 1G and 2G yielding core plates were flat in shape with a yielding cross-sectional area of 12 in^2. The Specimens 3G and 4G yielding core plates were cruciform in shape with a yielding cross-sectional area of 27 in^2. All core plates were specified to be fabricated from A36 steel. The actual yield strength for Specimens 1G and 2G was 450 kips and for Specimens 3G and 4G was 1013 kips. The core plates were encased in grout-filled A500 Grade B steel hollow structural sections.

The ends of each brace were spliced to gusset brackets with A572 Grade 50 steel connection plates that were welded to the BRB core plate and bolted to the gusset brackets with fully-tensioned high-strength A490 bolts. The bracket on one end of the brace was attached to a strong-wall and the other end to a shake table platen. Specimens were cyclically tested by imposing both longitudinal and transverse displacements to the end of the brace attached to the shake table.

All specimens were subjected to a Standard Loading Protocol, followed by a High-Amplitude Loading Protocol. Specimens 1G and 2G were additionally subjected to 15 cycles of a Low-Cycle Fatigue Loading Protocol. The Standard Loading Protocol was developed in accordance with the 2005 AISC *Seismic Provisions for Structural Steel Buildings* and 2003 *NEHRP Recommended Provisions for Seismic Regulations for New Buildings and Other Structures* (FEMA 450). An additional High-Amplitude Loading Protocol was developed to impose greater deformation demand on the BRB specimens. Transverse displacements applied to the test specimens were calculated from the prescribed axial displacements using the brace length, L_b, and an assumed brace angle of 60° from horizontal. Longitudinal and transverse displacements were in phase to simulate realistic frame action effects at the gusset connection.

Specimens 1G and 2G were subjected to the Standard, High-Amplitude, and Low-Cycle Fatigue Loading Protocols. The steel core plates of Specimens 1G and 2G did not fracture during testing. Specimen 3G was subjected to the Standard and High-Amplitude

Loading Protocols. The steel core plate fractured on the first $4.3\Delta_{bm}$ tension excursion during the High-Amplitude Loading Protocol. Specimen 4G was subjected to the Standard and High-Amplitude Loading Protocols without steel core plate fracture.

5.2 Conclusions

Based on the test results, the following conclusions and observations can be made.

(1) All specimens performed well under the Standard Loading Protocol, and no fracture, brace instability or brace end connection failures were observed.

(2) Prior to fracture, all specimens were able to accommodate a connection end rotation of up to 0.031 radians.

(3) Plots showing the applied load versus brace deformation showed stable, repeatable behavior with positive incremental stiffness.

(4) For all cycles to an axial deformation greater than the yield deformation, Δ_{by}, the maximum tension and compression forces were not less than 1.0 times the nominal brace yield force, P_{yn}.

(5) For all cycles to an axial deformation greater than the yield deformation, Δ_{by}, the ratio of the maximum compression force to the maximum tension force did not exceed 1.3.

(6) The cumulative inelastic axial deformation achieved by all specimens was significantly greater than the $200\Delta_{by}$ required by the AISC *Seismic Provisions for Structural Steel Buildings* for uniaxial brace test specimens.

REFERENCES

(1) AISC, *Manual of Steel Construction: Load & Resistance Factor Design*, American Institute of Steel Construction, Chicago, IL, 2001.

(2) AISC, *Seismic Provisions for Structural Steel Buildings*, American Institute of Steel Construction, Chicago, IL, 2005.

(3) Clark, P., Aiken, I., Kasai, K., Ko, E., and Kimura, I., "Design procedures for buildings incorporating hysteretic damping devices." *Proceedings*, 68th Annual Convention, SEAOC, Sacramento, CA, 1999.

(4) Federal Emergency Management Agency, *NEHRP Recommended Provisions for Seismic Regulations for New Buildings and Other Structures*, FEMA 450, Washington, D.C., 2003.

(5) Lopez, W.A., "Design of unbonded braced frames." *Proceedings*, 70th Annual Convention, SEAOC, Sacramento, CA, pp. 23-31, 2001.

(6) Merritt, S., Uang, C.M. and Benzoni, G., "Subassemblage testing of CoreBrace buckling-restrained braces." *Report No. TR-2003/01*, University of California, San Diego, La Jolla, CA, 2003.

(7) Newell, J., Uang, C.M. and Benzoni, G., "Subassemblage testing of CoreBrace buckling-restrained braces (F series)." *Report No. TR-2005/01*, University of California, San Diego, La Jolla, CA, 2005.

(8) Okahashi, Y., and Reavely, L.D., "Preliminary buckling-restrained brace results." University of Utah, Salt Lake City, UT, 2004.

(9) Reina, P. and Normile, D., "Fully braced for seismic survival." *Engineering News Record*, July 21, pp. 34-36, 1997.

(10) Sabelli, R. and Aiken, I., "Development of building code provisions for buckling-restrained braced frames." *Proceedings*, 72nd Annual Convention, SEAOC, Sacramento, CA, pp. 219-226, 2003.

(11) Shuhaibar, C., Lopez, W.A., and Sabelli, R., "Buckling-restrained braced frames." *Proceedings*, ATC-17-2, Seminar on Response Modification Technologies for Performance-Based Seismic Design, ATC and MCEER, pp. 321-328, 2002.

(12) Staker, R. and Reaveley, L.D., "Selected study on unbonded braces." *Proceedings*, ATC-17-2, Seminar on Response Modification Technologies for Performance-Based Seismic Design, ATC and MCEER, pp. 339-349, 2002.